



VALIDATION OF THE GALLAGHER  
PROTONOSPHERIC MODEL

THESIS

Kelly M. Law, Captain, USAF

AFIT/GAP/ENP/99M-04

19990402 008

DEPARTMENT OF THE AIR FORCE  
AIR UNIVERSITY  
**AIR FORCE INSTITUTE OF TECHNOLOGY**

Wright-Patterson Air Force Base, Ohio

Approved for public release; distribution unlimited

AFIT/GAP/ENP/99M-04

VALIDATION OF THE GALLAGHER  
PROTONOSPHERIC MODEL

THESIS

Presented to the Faculty of the Graduate School of Engineering

of the Air Force Institute of Technology

Air University

Air Education and Training Command

In Partial Fulfillment of the Requirements for the

Degree of Master of Science in Physics

Kelly M. Law, B. S.

Captain, USAF

March, 1999

Approved for public release; distribution unlimited.

The views expressed in this thesis are those of the author and do not reflect the official policy or position of the Department of Defense or the U.S. Government.


VALIDATION OF THE GALLAGHER PROTONOSPHERIC MODEL

Kelly M. Law, B.S.  
Captain, USAF

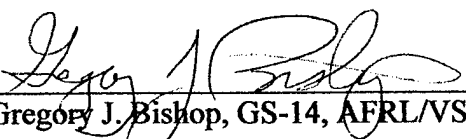
Approved:

  
Derrill T. Goldizen, Major, USAF (Chairman)

3 Mar 99  
date

  
Cecilia A. Miner, Lt Col, USAF

3 Mar 99  
date

  
Gregory J. Bishop, GS-14, AFRL/VSBP

11 Feb 99  
date

## Acknowledgments

I would be remiss if I failed to thank Jesus and all his Saints for getting me through this ordeal. I am especially indebted to the wonderful role models I found in Anthony, Thomas, Catherine, and Albert. Their example shed great light on the humbling lessons of patience, perseverance, and humility that I so needed to learn.

On the secular level, I would be equally remiss if I did not thank my advisor, Major Derrill Goldizen for injecting a healthy sense of reality into research problems, my sponsor Mr. Greg Bishop, for providing not only the impetus for the research but the tools with which to conduct it, and my great helper Dr. Andy Mazzella of NWRA, who tolerated reams of email questions and never tired of my “dope slaps”. I am also thankful for the assistance of Dr. Dennis Gallagher, Mr. Lincoln Brown, Mr. Rob Daniell, and Lt Col Cecilia Miner for their roles in turning this research adventure into a finished product.

While slightly out of place, all the professors who tolerated my presence in their classrooms must be thanked for *their* patience and guidance without which I would never have gotten to the research at all.

Kelly M. Law

## Table of Contents

Acknowledgments .....	ii
Table of Contents .....	iii
List of Figures .....	vi
List of Tables .....	vii
Acronym Guide.....	viii
Abstract.....	x
<b>1. Introduction.....</b>	<b>1</b>
1.1 Problem Statement .....	1
1.2 Beneficiaries.....	2
1.3 Scope of Research.....	4
<b>2. Background .....</b>	<b>5</b>
2.1 Ionospheric and Protonospheric Morphology.....	5
2.2 Protonospheric Measurement.....	8
2.2.1 The GPS Constellation and TEC Measurements Using GPS .....	9
2.2.1.1 Differential Group Delay.....	11
2.2.1.2 TEC Retrieval .....	12
2.2.2 SCORE: Self Calibration of pseudo-Range Errors .....	13
2.2.2.1 Premise .....	13
2.2.2.2 Assumptions .....	13
2.2.2.3 General Steps.....	14
2.2.2.4 Advantages .....	16
2.2.2.3 Disadvantages.....	16
2.2.2.6 Past SCORE Validation.....	16
2.3 Models.....	17
2.3.1 Parameterized Ionospheric Model Version 1.7 (PIM 1.7) .....	17
2.3.2 The Gallagher Model .....	21
2.3.2.1 Empirical Data Set.....	21
2.3.2.2 The Gallagher Electron Density Profile Equations .....	23
<b>3. Methodology .....</b>	<b>28</b>
3.1 Method Development and Modification .....	28
3.1.1 Groundtruth Protonospheric TEC .....	28
3.1.1.1 Dual Station Technique (DST).....	28
3.1.1.2 Site Selection .....	31

3.1.1.3 Retrieval Rates.....	31
3.1.1.4 Data Reduction .....	32
3.1.1.5 Pittsburgh Anti-Spoofing.....	32
3.1.1.6 SCORE Calibration Adjustment- Search For Low-Latitude Cutoffs.....	33
3.1.2 Modeled Protonospheric TEC.....	38
3.1.2.1 Using Pittsburgh Slant Path Comparison Configuration.....	38
3.1.2.2 PIM Slant Configuration .....	39
3.1.2.3 PIM Altitude Grid Configuration .....	40
3.1.2.4 Producing PIM Output Over Time .....	43
3.2 Comparison Configuration.....	44
3.2.1 The PTEC Comparison Process-General Data Manipulation .....	45
3.2.1.1 Groundtruth GPS Protonospheric TEC Data (MPTEC).....	45
3.2.1.2 Modeled Protonospheric TEC Data (PIMPTEC).....	47
<b>4. Data Description and Analysis.....</b>	<b>51</b>
4.1 Scope.....	51
4.1.1 Planned Scope .....	51
4.1.2 Resultant Scope.....	51
4.1.3 Groundtruth Data Set .....	52
4.2 Examinations.....	54
4.2.1 Initial Gallagher Examination .....	54
4.2.1.1 Expectations for the Gallagher Model.....	54
4.2.1.2 Devised Tests for the Gallagher Model.....	54
4.2.1.3 Gallagher Results.....	56
4.2.2 MPTEC vs. PIMPTEC Comparisons and Results .....	59
4.2.2.1 MPTEC Standard Deviation.....	66
4.2.2.2 Reduced Chi-Squared (RCS).....	66
4.2.2.3 Positive and Negative Bias (Model Residual).....	68
4.2.2.4 Optimum Gallagher Time Period .....	69
4.2.3 MPTEC Errors and Inaccuracies.....	69
4.2.3.1 Orphans and Wild Points.....	70
4.2.3.2 Common IPP Window.....	72
4.2.3.3 Geomagnetic Storm Influence.....	76
4.2.3.4 Protonospheric Influence / Poor Low-latitude Cutoffs .....	77
4.2.3.5 Multipath Impacts.....	79
4.2.3.6 Low Elevation Angle.....	79
<b>5. Summary, Conclusions, and Recommendations.....</b>	<b>81</b>
5.1 Summary .....	81
5.2 Conclusions.....	81
5.2.1 MPTEC Measurements Using Dual Station Technique.....	81
5.2.2 MPTEC Output Using The Gallagher Model .....	82
5.3 Recommendations.....	83
5.3.1 The Gallagher Model .....	83

5.3.2 The Dual Station Technique.....	83
Appendix A: Statistical Definitions.....	86
Appendix B: MPTEC Error Estimate .....	88
Appendix C: MPTEC Plots (Days 7074-7079, 7172-7177).....	94
Bibliography .....	106
Vita.....	109



## List of Figures

Figure	Page
Figure 1: Electron Density Profiles .....	6
Figure 2: Transition Region .....	7
Figure 3: The Earth, Ionosphere, and Protonosphere .....	8
Figure 4: Example of Typical PIM Input Stream File .....	19
Figure 5: PIM 1.7 Components.....	20
Figure 6: Coverage of RIMS Measurements Used In Gallagher Model .....	22
Figure 7: Temporal Applicability of the Gallagher Model ( $a_6$ Coefficient Plot).....	23
Figure 8: Gallagher Model Input of MLT Only.....	25
Figure 9: Example of Protonospheric TEC Output From Gallagher Model.....	26
Figure 10a: The Dual Station Technique .....	29
Figure 10b: The Dual Station Technique Geometry .....	30
Figure 11: Low-latitude Cutoffs .....	34
Figure 12a: Pittsburgh Calibration Using 40.75 ° Cutoff (Good Calibration).....	35
Figure 12b: Pittsburgh Calibration Using 41.55 ° Cutoff (Poor Calibration).....	36
Figure 13a: Charleston Low-latitude Cutoff Impact.....	38
Figure 13b: Pittsburgh Low-latitude Cutoff Impact .....	38
Figure 14: Pittsburgh's Raypath Into the Protonosphere.....	39
Figure 15: STEC and PIMPTEC Using 10 Point Altitude Grid .....	42
Figure 16: STEC and PIMPTEC Using CPI's 100 Point Altitude Grid .....	43
Figure 17: The Comparison Configuration.....	45
Figure 18a: Flowchart of the Comparison Method.....	48
Figure 18b: Example of MPTEC Measurement .....	49
Figure 18c: Example of PIMPTEC Calculation .....	50
Figure 19: Gallagher Day Comparison .....	57
Figure 20: Gallagher Solar 10.7 cm Flux Comparison .....	57
Figure 21: Gallagher $K_p$ Comparison .....	58
Figure 22: PTEC Comparison.....	60
Figure 23: MPTEC By The Hour .....	64
Figure 24: Point By Point Comparison.....	65
Figure 25: Hourly Reduced Chi-Squared .....	67
Figure 26: Model Residual .....	69
Figure 27: IPP Latitudes and Timing.....	73
Figure 28: IPP Longitudes and Timing.....	73
Appendix C Figures: MPTEC Plots (7074-7079,7172-7177) .....	95-105

## List of Tables

Table	Page
Table 1: CPI's 100 Point Altitude Grid .....	41
Table 2: Data Inventory .....	53
Table 3a: Spring MPTEC Data .....	62
Table 3b: Summer MPTEC Data .....	63
Table 3c: PIMPTEC Data .....	64
Table 4: Reduced Chi-Squared Results .....	66
Table 5: Satellites and Site Orphans .....	71
Table 6a: IPP Raypath Distances: Spring MPTEC Data .....	75
Table 6b: IPP Raypath Distances: Summer MPTEC Data .....	75
Table A1: Example: Pittsburgh Multipath Day 7078 .....	90
Table A2: Example: Charleston Multipath Day 7078 .....	91
Table A3: Multipath Results .....	92
Table C1: Date Conversion .....	94

### Acronym Guide

AIAA	American Institute of Aeronautics and Astronautics
AFRL/VS	Air Force Research Lab/Space Vehicles Directorate
ALTAIR	Tracking Radar on Kwajalein Atoll
ATS	Research Satellite
AZ-EL	Azimuth – Elevation
Bimf	Interplanetary Magnetic Field
B <sub>imf</sub>	Interplanetary Magnetic Field
B <sub>y</sub>	IMF Field Orientation
B <sub>z</sub>	IMF Field Orientation
CAA	Cumulative Phase Average Adjustment
CGM	Corrected Geomagnetic
CHA	Charleston
CHA1	Charleston
CORS	Continuous Observing Reference System
CumuPhAv Adj	Cumulative Phase Average Adjustment
DCP	Differential Carrier Phase Delay
DGD	Differential Group Delay
DOD	Department of Defense
DST	Dual Station Technique
EOF	Empirical Orthonormal Functions
F10.7	Solar Flux at 10.7 cm wavelength
f1	GPS Frequency 1575.42 MHz
f2	GPS Frequency 1227.6 MHz
GPS	Global Positioning System
HF	High Frequency
hmF1	Height of F1 Ionospheric Peak
hmF2	Height of F2 Ionospheric Peak
IMF	Interplanetary Magnetic Field
IPP	Ionospheric Penetration Point
IPPLAT	IPP Latitude
IPPLON	IPP Longitude
ITEC	Generic Ionospheric TEC
K <sub>p</sub>	Planetary Geomagnetic Activity Index
K <sub>p</sub>	Planetary Geomagnetic Activity Index
LAT	Latitude
LON	Longitude
LT	Local Time
MLT	Magnetic Local Time
MPTEC	Measured Slant Protonospheric TEC using GPS
NAVSTAR	GPS
NSAMP	Number of Samples
OGO	Research Satellite
PC	Personal Computer
PAA	Phase Averaging Adjustment

PhAvAdj	Phase Averaging Adjustment
PIM	Parameterized Ionospheric Model
PIMTEC(G)	Calculated STEC using PIM including the Gallagher Model
PIMTEC	Calculated STEC using PIM without the Gallagher Model
PIMPTEC	Calculated Slant Protonospheric TEC using PIM and Gallagher
PIT1	Pittsburgh
PIT	Pittsburgh
PLASPH	Plasmasphere Switch in PIM
PTEC	Generic Protonospheric TEC
RCS	Reduced Chi Squared
RF	Radio Frequency
RIMS	Retarding Ion Mass Spectrometer
RINEX	Receiver Independent Exchange Format Version 2
RINMTI	RINEX Conversion Program
SAT PRN	GPS Satellite Number Identifier
SCORE	Self Calibration of Pseudo-Range Errors
SSN	Sun Spot Number
StdDev	Standard Deviation
STEC	Slant Total Electron Content
STEC (G)	Slant Total Electron Content From PIM with Gallagher Model
SUPIM	Sheffield University Plasmasphere Ionosphere Model
TEC	Total Electron Content
TEQC	Quality Control Program for GPS Data Files
UNAVCO	University NAVSTAR Consortium
URSI	International Union of Radio Science
UT	Universal Time
VTEC	Vertical Total Electron Content

Abstract

Ionospheric models are used in many systems throughout the Department of Defense: for example, they are useful in correcting range errors in radio signals. However, correction models don't incorporate the protonosphere, the torus-shaped plasma volume above the ionosphere. The Gallagher Protonospheric Model, recently incorporated into the Parameterized Ionospheric Model 1.7 (PIM 1.7), was validated against protonospheric total electron content (PTEC) measurements made by the GPS system. Gallagher model calculations of slant PTEC for Pittsburgh ground station looking south with a raypath at an elevation of 26 degrees were compared against GPS PTEC measurements for the same configuration derived from the Dual Station Technique (DST). In the DST, 11 days of GPS TEC measurements were obtained from Charleston and Pittsburgh, taking advantage of the latitudinal asymmetry of the protonosphere to obtain PTEC. The Gallagher model results were in general agreement with measured PTEC, indicating a slight diurnal change in PTEC ( $< 2$  PTEC). Groundtruth PTEC accuracy was estimated at 2-3.5 PTEC, masking any trend measurement, yet good enough to validate the potential of Self Calibration Of Pseudorange Errors (SCORE) and DST to measure PTEC using GPS. PIM 1.7 users should be aware of Gallagher's limits: empirical, limited to 00-10 Magnetic Local Time, and  $\pm 40$  degrees geomagnetic latitude.

# **1. Introduction**

## **1.1 Problem Statement**

While extensive progress has been made in modeling the total electron content (TEC) of the ionosphere, the same is not true for the protonosphere. The Gallagher model, an empirical protonospheric model, has recently been incorporated into the Parameterized Ionospheric Model Version 1.7 (PIM 1.7). The question now is: how well does the Gallagher model represent the protonosphere? This thesis seeks to answer part of that question by comparing the Gallagher model output (PIMPTEC) to results of a new technique for measuring protonospheric TEC that will function as groundtruth TEC (MPTEC).

Bishop [1997] has developed a simple, geometrical “dual-station” technique, which uses the Global Positioning System (GPS) constellation to measure protonospheric TEC (MPTEC). TEC is a height-integrated measurement of the number density of electrons in a column of base area  $1 \text{ m}^2$  (one TEC unit is equal to  $1 \times 10^{16}$  electrons/ $\text{m}^2$ ). Ionospheric TEC (ITEC) measurements are used in model development and space forecasting and analysis. Accurate estimates of both ionospheric TEC (ITEC) and protonospheric TEC (PTEC) are crucial to the development of ionospheric models such as the Parameterized Real-time Ionospheric Specification Model (PRISM). Good models are necessary in forecasting ionospheric impacts on Department of Defense (DOD) High Frequency (HF) and satellite communications and in post-event analysis. Accurate knowledge and modeling of TEC allows for better calibration of GPS bias and correction estimates for transmitter and receiver biases.

## 1.2 Beneficiaries

Air Force Research Lab/Space Vehicles Directorate (AFRL/VS), the 55<sup>th</sup> Space Weather Squadron, and others could benefit from improved models. Anybody who uses a space based system that can be impacted by the ionosphere/space environment would like an accurate, timely forecast of the event before it happens. In the least, they would want an analysis of the impact afterwards, and the forecaster/analyst would need to have the best possible ionospheric model. Proper incorporation of the protonosphere into that model would help.

Why do we care about ionospheric and protonospheric models? One reason is that we are becoming increasingly dependent upon GPS, especially in precision weapons and navigation aids. One of the largest sources of error in GPS measurement is ionospheric impact. Without any correction, ionospheric errors could account for up to 100-200 meters of pseudo-range error [Bishop, 1999]. Dual frequency receivers can measure and compensate for ionospheric impacts and decrease the pseudo-range error to about 1.2 meters [American Institute of Aeronautics and Astronautics (AIAA), 1996]. Dual-frequency GPS receivers have now become the primary means of monitoring ionospheric TEC, globally. As such, the error in GPS measurements of ionospheric TEC feeds directly into global ionospheric maps and models. Single frequency receivers can use ionospheric models to accommodate the ionospheric impact and compensate for errors as well. However, while these models allow for error reduction, they do not yet account for the protonosphere. This can detract from proper error reduction. While PTEC is often much less than ITEC, it has been found, during certain conditions, particularly winter nighttime, to contribute over 50% of total TEC measured

by GPS [Lunt et al., 1998 a]. In such cases, ionospheric correction models would not be accurate. Their “correction” of pseudo-range error could underestimate the inaccuracies. For an extreme example, if a GPS TEC measurement, assumed to be purely ionospheric, actually included 15 TEC from the protonosphere, the extra PTEC would result in about 2.4 meters of range error. Even if range estimates are only off by a meter or so, this error cannot be ignored. A few meters may not sound like much... unless you are trying to drop a GPS precision guided munition down an air conditioning shaft or land an airliner at an airport in bad weather using GPS guided navigation and landing aids.

A second reason for concern is that ignoring protonospheric contribution in measurements and models could have an impact on radar systems as well. Local measurements of GPS TEC are used as a driver in PRISM to correct errors in the U.S. Army’s ALTAIR radar on Kwajalein Atoll [Bishop, 1999]. In this function, the model output (driven by local GPS TEC measurements) is used to determine purely ionospheric TEC, used as a diagnostic yet, at near equatorial latitudes, the measurements would be contaminated by the protonosphere which the model can only treat as purely ionospheric TEC.

A further illustration of the concern for ionospheric accuracy (by thoroughly measuring and modeling the protonospheric contribution to TEC measurements) is the current work in delivering real-time space weather support products to the theater warfighter. A prime diagnostic of the real-time accuracy of such products would be comparing slant GPS TEC measurements in theater against model output, like PRISM [Bishop, 1999].



As such, it is critical that we expand our knowledge of the protonosphere and the role it might play in contributing to TEC errors in measurements and models. Building and testing new models is as important as designing and recording new measurements. The Gallagher model is the first protonospheric model to be incorporated into the Parameterized Ionospheric Model 1.7 (PIM 1.7). While limited in scope, it is the first step towards incorporating protonospheric influence in space environment models.

If a model shows merit, its development and eventual adoption by the scientific community will provide a stepping stone for future improvement and application of the model. Ionospheric modelers, model users, GPS users, and remote sensing (RS) users will benefit by increased knowledge of how well we can model ITEC and PTEC.

### **1.3 Scope of Research**

In this initial research, PIMPTEC is compared against groundtruth MPTEC as measured from GPS. The comparison configuration is limited to comparing TEC values measured and modeled along one raypath between a site and a specific Ionospheric Penetration Point (IPP). As a result, conclusions are valid for a narrow set of conditions. PIMPTEC will be calculated for a set of seasonally representative days (spring, summer, fall, winter). For selected days from each of those four seasons, GPS TEC measurements will be taken for two sites, calibrated, and then applied to the Dual Station Technique (DST) to calculate MPTEC. Then PIMPTEC and MPTEC will be analyzed to see how the Gallagher model performed against real measurements.

## 2. Background

### 2.1 Ionospheric and Protonospheric Morphology

The ionosphere can be defined as a body of weakly ionized plasma surrounding the earth from an altitude of 90 km to approximately 1000 km. The ionosphere can be broken up into four layers differentiated by their photochemical and plasma transport mechanisms. These are the D, E, F<sub>1</sub>, and F<sub>2</sub> layers. A typical mid-latitude ionospheric electron density profile can be seen in Figure 1.

The D region electron density peaks near 90 km, and its major ions are NO<sup>+</sup> and O<sub>2</sub><sup>+</sup>. The E region electron density peaks near 100 km with major ions NO<sup>+</sup> and O<sub>2</sub><sup>+</sup>. The F<sub>1</sub> region peaks (hm F<sub>1</sub>) between 180 and 220 km with major ions NO<sup>+</sup>, O<sup>+</sup>, O<sub>2</sub><sup>+</sup>. The F<sub>2</sub> region peak (hm F<sub>2</sub>) ranges from 250 to 400 km with the major ions O<sup>+</sup>, H<sup>+</sup>, and He<sup>+</sup>. An electron is associated with each singly ionized atom, and ions and free electrons are created and destroyed in pairs, maintaining electrical neutrality. Therefore, physical and chemical modeling of ion density profiles will determine TEC profiles [Johnson, 1961].

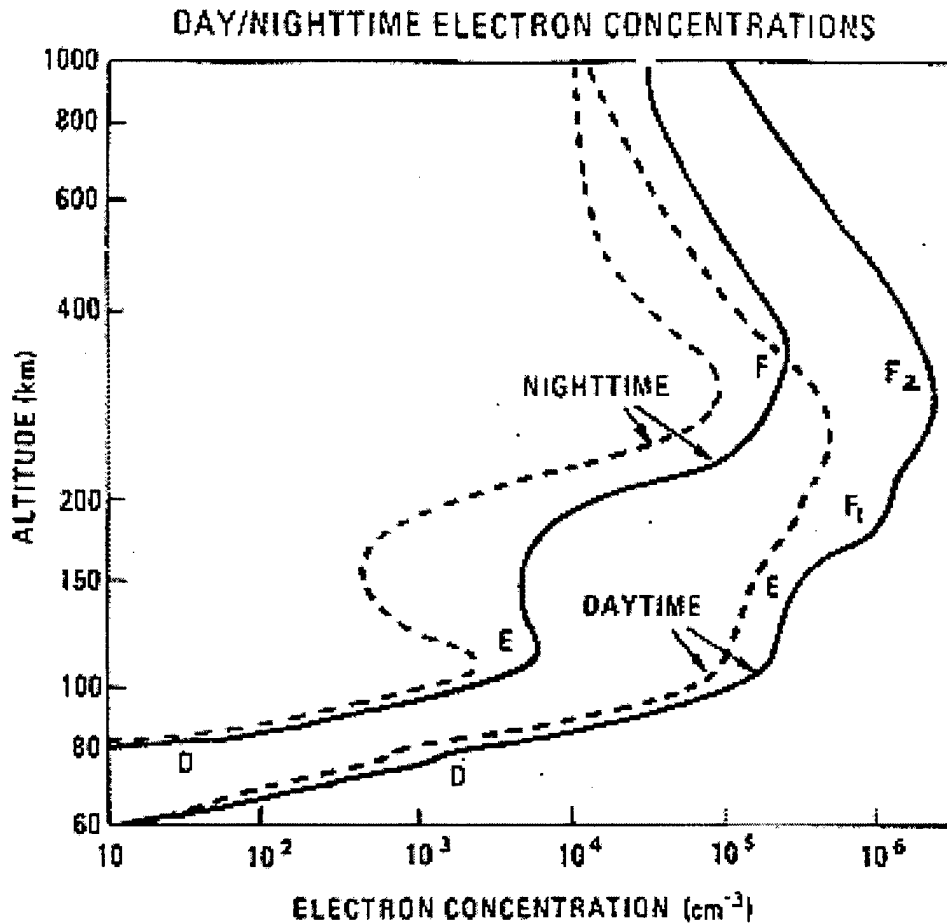


Figure 1. The Ionosphere. Solid lines are profiles at solar maximum. Dashed lines are profiles at solar minimum. [Tascione, 1994]

At what altitude are we no longer in the ionosphere? Where does the protonosphere begin? The answer is not definite. While the topside ionosphere is defined (using electron density) as the region above the  $F_2$  peak, the “base” of the protonosphere is considered the region where the dominant ion changes from  $O^+$  to  $H^+$  [Johnson]. Around 800 km,  $O^+$  and  $H$  undergo charge exchange reactions whereby  $H^+$  gradually becomes the dominant ion. This transition from ionosphere to protonosphere occurs between 800 and 2000 km, but it is not a well-defined boundary. See Figure 2.

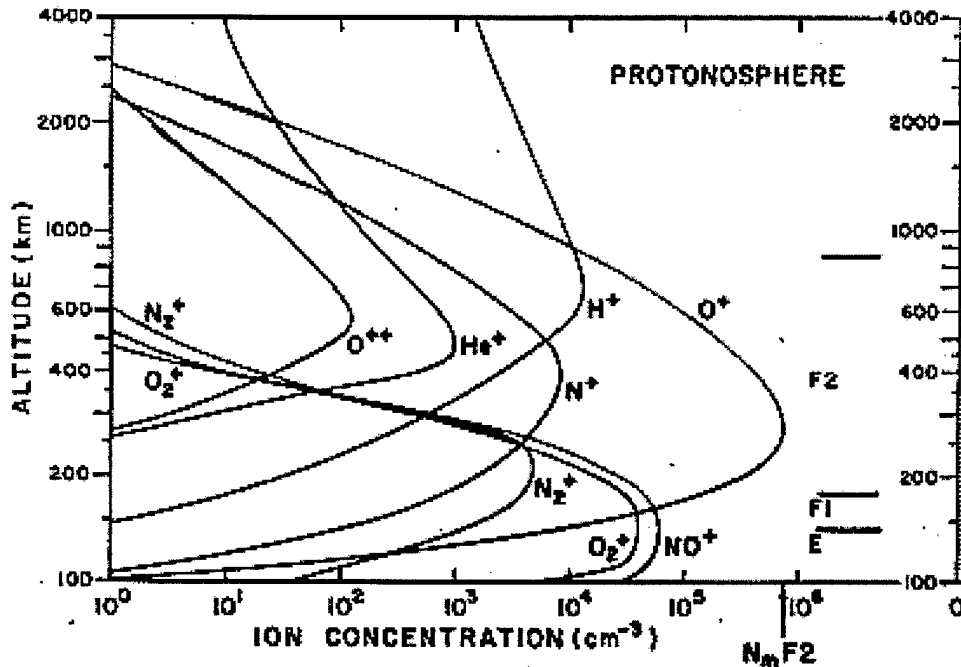


Figure 2. Transition Region. Above the F2 peak, O<sup>+</sup> decreases with altitude. Near 1000 km, H<sup>+</sup> becomes the dominant ion. [National Academy of Sciences, 1977]

The protonosphere (or plasmasphere) is the co-rotating, torus-shaped, low density, cold plasma region extending from the topside ionosphere (~ 300-400 km) out to an altitude of approximately 20000 – 30000 km and ranging from approximately – 60 to + 60 ° magnetic latitude. See Figure 3. Bishop's Dual Station Technique makes use of this latitudinal boundary to measure groundtruth PTEC (MPTEC).

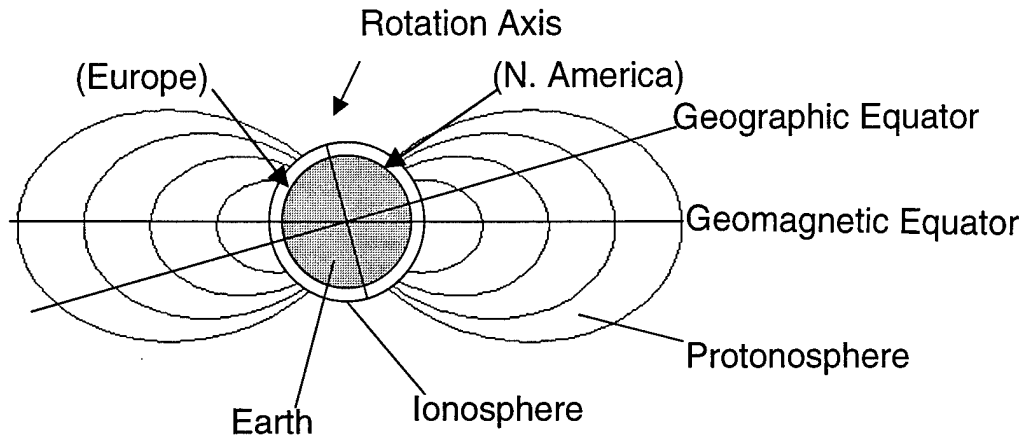


Figure 3. The Earth, Ionosphere, and Protonosphere. [NOT to scale]. Note that the protonosphere has greater influence in Europe (left side) than it does in North America (right side.)

A sound understanding of the structure and dynamics of the protonosphere is a goal yet to be realized. Steps towards it include properly measuring various aspects of the protonosphere and building better models. Using GPS for PTEC measurement is another advance in the history of protonosphere exploration. Data recovered will help explore the applicability of new models and aid in their development.

## 2.2 Protonospheric Measurement

Early measurements of the protonosphere were obtained during ground based studies of the phenomena of “whistlers.” These studies determined the average shape of the protonosphere and the general location of the plasmapause between 3 and 5 earth radii, and suggested the protonosphere consisted of low density, cold ( $\sim 1$  eV) plasma [Kivelson, 1995]. The advent of the space age provided some measurements via satellite, such as the OGO-5 that confirmed the general location of the plasmapause. Geostationary satellites were used to send radio transmissions to ground stations, which then employed Faraday rotation techniques to measure electron density profiles below

2000 km [Kivelson]. In the 1970's, the ATS-6 geostationary satellite used an ionospheric beacon to measure electron profiles in the protonosphere [Kersley et al., 1977]. The Dynamics Explorer used the retarding ion measurement spectrometer (RIMS) in the 1980's to explore a wider region of the protonosphere [Gallagher et al., 1988]. By the late 1980's, the GPS constellation was in place and has since expanded our ability to measure ITEC. Now, that platform could do the same for PTEC.

However, with an indistinct boundary between the ionosphere and protonosphere, it becomes difficult to specify exactly what fraction of the GPS measured TEC consists of ionospheric rather than protonospheric electrons. Early PTEC measurements found the PTEC contribution to total TEC had a diurnal variation ranging from 10% during the day to 40% at night [Kersley et al.]. More recent measurements estimate that PTEC contribution during solar minimum could well be over 50% at night [Lunt et al., 1998 a]. Therefore, understanding the protonosphere's influence in TEC measurements is important in modeling efforts as it can, at times, account for over half the measured GPS TEC. But, how does GPS actually measure TEC?

### **2.2.1 The GPS Constellation and TEC Measurements Using GPS**

GPS has far exceeded its original purpose as a navigation platform. TEC and PTEC measurement is another addition to the versatile application of GPS technology. GPS consists of a constellation of at least 24 geostationary satellites orbiting the planet at approximately 20,330 km altitude [AIAA]. A worldwide network of receiving stations is used to measure TEC from the satellites.

The passage of a radio signal through the atmosphere is directly affected by electron density along the raypath. Radio signals are retarded in the presence of free electrons such that the group velocity,  $v_g$  equals the index of refraction,  $n$  (a function of electron density), times the speed of light,  $c$ . This effect is used to calculate TEC by measuring the resulting time delay of the signal.

Radio waves sent from GPS satellites to ground receivers must travel through the atmosphere, ionosphere, and possibly the protonosphere as well. These media, particularly the ionosphere, contain electrons that alter the radio waves and thus allow us to extract information about the electrons along the radiowave paths.

In a vacuum, radio waves travel at the “speed of light.” Group velocity is the speed at which energy and information travel through the medium as a finite wave packet. Phase velocity is the speed at which the wave phase planes appear to move within the packet. The group and phase velocities of a wave are altered in different ways as the wave transits through a region of higher electron density: group velocity decreases, and phase velocity increases. The group velocity changes are measured at the receiver as time delays in the received signal. The time delays can also be thought of as errors in distance, called range errors. Pseudo-range refers to the conversion of the apparent signal transit time to a distance, using a constant speed of light, without accounting for the TEC delays. These pseudo-range errors can be many meters at their extremes [AIAA].

Fortunately, our understanding of how the radio waves are altered and how the index of refraction is dependent upon the radio frequency itself, provides a tool for measuring and correcting these errors. The index of refraction for a plasma is less than

one and is inversely dependent on electron density. As electron density increases, the index of refraction gets smaller. As the frequency of the radio signal increases, the index of refraction gets larger for a given electron density. Different radio frequencies will be altered by the electrons in different ways. By using two radio frequencies, rather than one, we can take advantage of the refraction index–frequency relationship and isolate the errors.

### 2.2.1.1 Differential Group Delay

Dual frequency GPS receivers are designed to receive signals at two phase coherent frequencies,  $f_1$  and  $f_2$ .  $f_1$  is 1575.42 MHz and  $f_2$  is 1227.6 MHz. The time delay of the wave groups at each frequency is measured. The difference between the two ionospheric time delays allows us to directly measure the absolute range error or the absolute TEC between the ground and satellite [AIAA].

$$\delta (\Delta t) = \frac{40.3}{c} TEC \left( \frac{1}{f_2^2} - \frac{1}{f_1^2} \right) \quad [1]$$

Where  $\delta (\Delta t)$  is the difference between the ionospheric time delays for each frequency [Hz]. TEC here is the number of electrons per square meter. Even with noisy pseudo-range measurements, many measurements of the time delays can be made over a pass, providing subnanosecond accuracies for the time delays. Multipath effects can limit the effectiveness of the DGD measurements of TEC; but generally, TEC measurements can be considered accurate. Errors caused by multipath will be discussed in Chapter 4, Data Description and Analysis.



### 2.2.1.2 TEC Retrieval

Differential Group Delay provides a way to measure TEC. We now have a simple relationship between TEC and delay time. A dual-frequency station receiving signals from the GPS satellite will measure a delay time (D) in nanoseconds as the signals pass through the ionosphere and protonosphere. A system-specific constant is used to calculate TEC from the delay: for GPS, a value of 2.85 is used [Handbook of Geophysics, 1985] to calculate slant TEC (in TEC units), the total column density of electrons along the slant path between satellite and ground receiver. The time delay, D, is in nanoseconds. This slant TEC (STEC) is then converted into equivalent vertical TEC (VTEC).

$$\text{STEC} = 2.85 D \quad [ 2 ]$$

$$\text{VTEC} = \text{STEC} / \text{Sec}[\chi] \quad [ 3 ]$$

This is limited to values of zenith angle  $\chi$  less than or equal to 40 degrees [Filby, 1997], where  $\chi$  is the angle between the ray path and the vertical taken at a designated ionospheric height, normally 350 to 400 km [AIAA].

Accuracy of GPS TEC is a function of biases in the transmitter and receiver, averaged correction factors for the biases, and environmental influences such as horizontal density gradients and ionospheric disturbances. Generally, accuracy is given

as 2 – 3 TEC units [Bishop et al., 1998]. However, Bishop [1997] has achieved accuracies of less than 2 TEC units using techniques similar to the technique described in this thesis. The research discussed here, however, achieved MPTEC accuracies of approximately 2 to 3.5 TEC units, which will be addressed later in Chapter 4, Data Description and Analysis.

## **2.2.2 SCORE: Self Calibration of pseudo-Range Errors**

“Of course, the ideal situation is one in which the GPS user can directly make dual-frequency group delay and differential carrier phase measurements to correct automatically for the first-order ionospheric time delay.”

--J.A. Klobuchar  
[AIAA]

The SCORE method was recently shown to produce accuracy to within a fraction of a TEC unit for ionospheric measurements and to within 1 TEC for protonospheric measurements [Lunt et al., 1998 b ].

### **2.2.2.1 Premise**

If the raypaths to two different receivers pass through the same point in the ionosphere (IPP), we can (neglecting the protonosphere) assume the ionospheric TEC measured for each is identical: that is, since the receivers are taking measurements through the same IPP, they measure the same ionosphere, assuming no horizontal TEC gradients exist in the region of the two stations. Ionospheric TEC differences between the two receivers can be attributed largely to satellite or receiver biases. The errors are minimized in the SCORE calibration process.

### **2.2.2.2 Assumptions**

The usefulness of this concept is expanded when we assume the ionosphere is stationary in local time and latitude and can be modeled as an infinitely thin shell.

These assumptions allow measurements taken at different times through the same IPP (defined by latitude, local time, and altitude) to be regarded as having seen the same ionosphere. With the thin shell assumption, we are treating the electrons in the ionosphere as if they existed only at 350 km in altitude. If seen as an infinitely thin shell, conversion from slant TEC units (STEC) to vertical TEC units at the IPP (VTEC) is done with simple geometry, as suggested by equation 3 in section 2.2.1.2.

### 2.2.2.3 General Steps

TEC measurements include not only actual TEC, but also biases from the satellite and receiver, as well as some unknown error. The SCORE process given below takes these measured TEC values and converts them to a vertical TEC in a way that accounts for bias and measurement error [Mazzella, Private Communication, 1998].

#### SCORE

**Step 1)** Convert Slant TEC to equivalent Vertical TEC at the IPP.  $\cos [\chi]$  equals  $f(\epsilon)$  so long as the zenith angle is equal to or less than 40 degrees. The impact of having too large a zenith angle will be addressed in section 4.2.3.6, Low Elevation Angle at Pittsburgh (Slant Factor Function Assumptions) and in Appendix B, MPTEC Error Estimate.

$$\text{VTEC} = \text{STEC} * f(\epsilon) \quad [4]$$

where

$$f(\epsilon) = \cos \left( \sin^{-1} \left( \frac{R}{R+h} \cos(\epsilon) \right) \right) \quad [5]$$

and is called the Slant Factor Function.  $R$  is the radius of the Earth,  $\epsilon$  is the elevation angle, and  $h$  is the altitude of the ionosphere. Here,  $h$  is 350 km.

**Step 2)** Relate actual measurement of TEC to measured STEC, bias, and errors.

$$STEC_{\alpha i}(\theta, \tau) = MSTEC_{\alpha i}(\theta, \tau) - (B_{\alpha} + B_R) + \Delta_{\alpha i} \quad [6]$$

$\theta$  is latitude.

$\tau$  is local time (LT).

$\alpha, \beta$  refer to satellite numbers.  $R$  is the receiver.

$\Delta$  is the measurement error (unknown).

$B$  refers to the biases in the satellites ( $\alpha, \beta$ ) and receiver ( $R$ ).

**Step 3)** Minimize the measurement error.

$$E = \sum_{\alpha} \sum_{\beta \neq \alpha} \sum_j W_{\alpha i \beta j} [(M_{\alpha i}(\theta, \tau) - (B_{\alpha} + B_R)) f(\epsilon_{\alpha i}) - (M_{\beta j}(\theta, \tau) - (B_{\beta} + B_R)) f(\epsilon_{\beta j})]^2 \quad [7]$$

Where the weighting function is defined as:

$$W_{\alpha i \beta j} = \exp\left(-\left(\frac{\theta_{\alpha i} - \theta_{\beta j}}{\Delta \theta}\right)^2\right) \exp\left(-\left(\frac{\tau_{\alpha i} - \tau_{\beta j}}{\Delta \tau}\right)^2\right) \exp\left(-\left(\frac{T_{\alpha i} - T_{\beta j}}{\Delta T}\right)^2\right) \quad [8]$$

Where

$\Delta \theta = 1.0$ . This is the latitudinal scaling denominator in degrees.

$\Delta \tau = 0.1$ . This is the local time scaling denominator in hours.

and  $\Delta T = 3.0$ . This is the associated scaling value for universal time in hours.

#### **2.2.2.4 Advantages**

Because the method is self-consistent, relying on only the satellite signals and data, calibration can be done by anyone. There is no need for test signals or an array of observing receivers.

#### **2.2.2.5 Disadvantages**

SCORE is generally only applicable to two-frequency GPS receivers. The given assumptions (stationary, thin-shell ionosphere) are not realistic but can be considered reasonable. The low-latitude cutoff adjustment (discussed below) for the protonospheric influence must be determined for each site.

#### **2.2.2.6 Past SCORE Validation**

As seen in the assumptions upon which SCORE is based, SCORE has no parameters that include the influence of the protonosphere. It is most accurate when applied solely to the ionosphere or to regions where protonospheric influence can be neglected, such as at high latitudes. A validation study concluded that SCORE was highly accurate, to within a fraction of a TEC unit, when compared to models wherein the assumption was made that all the plasma was concentrated below 1100 km. When compared to models incorporating the protonosphere out to GPS orbit altitudes, SCORE was consistently high by about 2 TEC units. In seeking to remedy this discrepancy, it was postulated that excluding regions in the calibration where the measurements were influenced by the protonosphere would increase accuracy. As such, low-latitude cutoffs were built into the SCORE process, and an accuracy of less than 2 TEC for all measurements was achieved. Incorporation of low-latitude cutoffs into the current study is discussed later but the key point made here is that the cutoffs increase the

accuracy of the calibration by excluding the protonosphere. Although the protonosphere is excluded in calibration, it is included in the measurements. The measurements can be taken through a full range of latitudes if desired, but are calibrated based only on the restricted data defined by the cutoffs. See Figure 11, cited in Chapter 3, Methodology.

## **2.3 Models**

### **2.3.1 Parameterized Ionospheric Model Version 1.7 (PIM 1.7)**

Unlike many empirical models in use today, PIM 1.7 is a physics based, theoretical climatological ionosphere model. PIM has two distinct advantages over empirical models that uniquely suit it to the problem at hand. First, empirical models, based on actual data, tend to average out spatial and temporal variability. Empirical models are appropriate for large-scale, general features. Theoretical models, based on physics and chemistry, provide more representative results. Second, whereas empirical models are limited by the available data, PIM's accuracy is only limited by the completeness of the physics and chemistry inherent in its model components and the computer resources available to carry out the calculations. PIM provides more realistic results that can be specified for particular geophysical conditions. While not accurate in the sense that they can be proven as such, they are the "potentially realizable" features that might be observed for the given conditions [Daniell et al., 1995].

Another advantage in using PIM is its recent upgrade incorporating the user-selectable Gallagher protonospheric TEC model. This feature allows PIM 1.7 to be used as an ideal test bed for the Gallagher validation.

The advantage of PIM's theoretical climatological model is offset somewhat by compromises made to ensure PIM's ease of use, particularly its speed in calculating the output on a desktop PC. First, seven of the eleven models within PIM are empirical, but the empirical models are used as input to the theoretical models. Second, PIM assumes a tilted dipole magnetic field for the earth. Third, the output database is approximated by semi-analytical functions in order to save storage space and reduce computing time [Daniell et al.].

PIM takes as input several discrete geophysical variables as specified by the user. See Input Stream File, Figure 4. Inputs include the orientation of the interplanetary magnetic field ( $B_{imf}$ ), the averaged 27 day solar flux ( $F_{10.7}$ ), the sun spot number (SSN), the  $K_p$  index (planetary geomagnetic activity), as well as the date, local time, and desired grid system for the output. This information is used by PIM to calculate desired outputs as approximated by semi-analytical functions; in particular, altitude profiles are approximated by empirical orthonormal functions (EOFs). Longitude variations are modeled using tabulated coefficients and Fourier series and latitudinal variations by grid specific orthogonal polynomials [Daniell, et al.]. See Figure 5.

The output can be presented as electron density profile parameters (peak electron densities and altitudes), full electron density profiles, or TEC along user specified paths.

1998	YEAR (1800-2100)
274	DAY (1-366)
0023	UT (0000-2359)
0	OUTPUT TYPE (0:frq,hghts,tec 1:edps 2:edps,frq,hghts,tec)
0	OUTPUT GRID TYPE (0:rect latlon 1:latlonprs 2:azel (grnd))
27423pim.out	OUTPUT FILE NAME (CHAR*32)
+	By IMF (- neg, + pos)
+	Bz IMF (- neg, 0 zero, + pos)
0	SSN TREATMENT (0:f107/SSN decoup 1:SSNfromf107 2:f107fromSSN)
135	F 10.7 cm Solar Instantaneous (Ignored if 2 above) (0-300)
150	SSN (0-300) Ignored if treat = 1
7	Magnetic Kp Index (0-9) Ignored if 1
1	foF2 Normalization Integer (0:URSI-88 1:NONE)
1	foE Normalization Integer (0:CCIR 1:NONE)
4	LLF Sector Use Integer (0:all 1:Brazil 2:India 3:Pacific 4:USA)
G	COORDINATE SYSTEM TYPE (G:geographic M:magnetic)
10	NUMBER OF LATITUDE POINTS (GT 0)
35	STARTING LATITUDE (degrees north -90 - 90)
1	LATITUDE INCREMENT (degrees north -180 - 180; NONZERO)
1	NUMBER OF LONGITUDE POINTS (GT 0)
-70	STARTING LONGITUDE (degrees east -360 - 360)
1	LONGITUDE INCREMENT (degrees east -360 - 360; NONZERO)
1	NUMBER OF LATLON PAIRS (1-1000)
35,-70	SITELAT/SITELON (north/east (ie west is neg)
35	SITE LATITUDE
-70	SITE LONGITUDE
1	NUMBER OF AZIMUTH POINTS (GT 0)
1	STARTING AZIMUTH (degrees -360 - 360)
1	AZIMUTH INCREMENT (degrees -360 - 360; NONZERO)
1	NUMBER OF ELEVATION POINTS (GT 0)
1	STARTING ELEVATION (degrees 0-90)
1	ELEVATION INCREMENT (degrees -90 - 90; NONZERO)
10	NUMBER OF ALTITUDE POINTS (1-100)
1600	ALTITUDE GRID (km 90-25000)
90	260 430 600 770 940 1110 1280
1450	1600
Y	PLASMASPHERE INCLUSION (Y yes N no)

Figure 4. Example of typical PIM Input Stream File. This sets the configuration of PIM, specifies geophysical and solar conditions, and specifies the desired output.



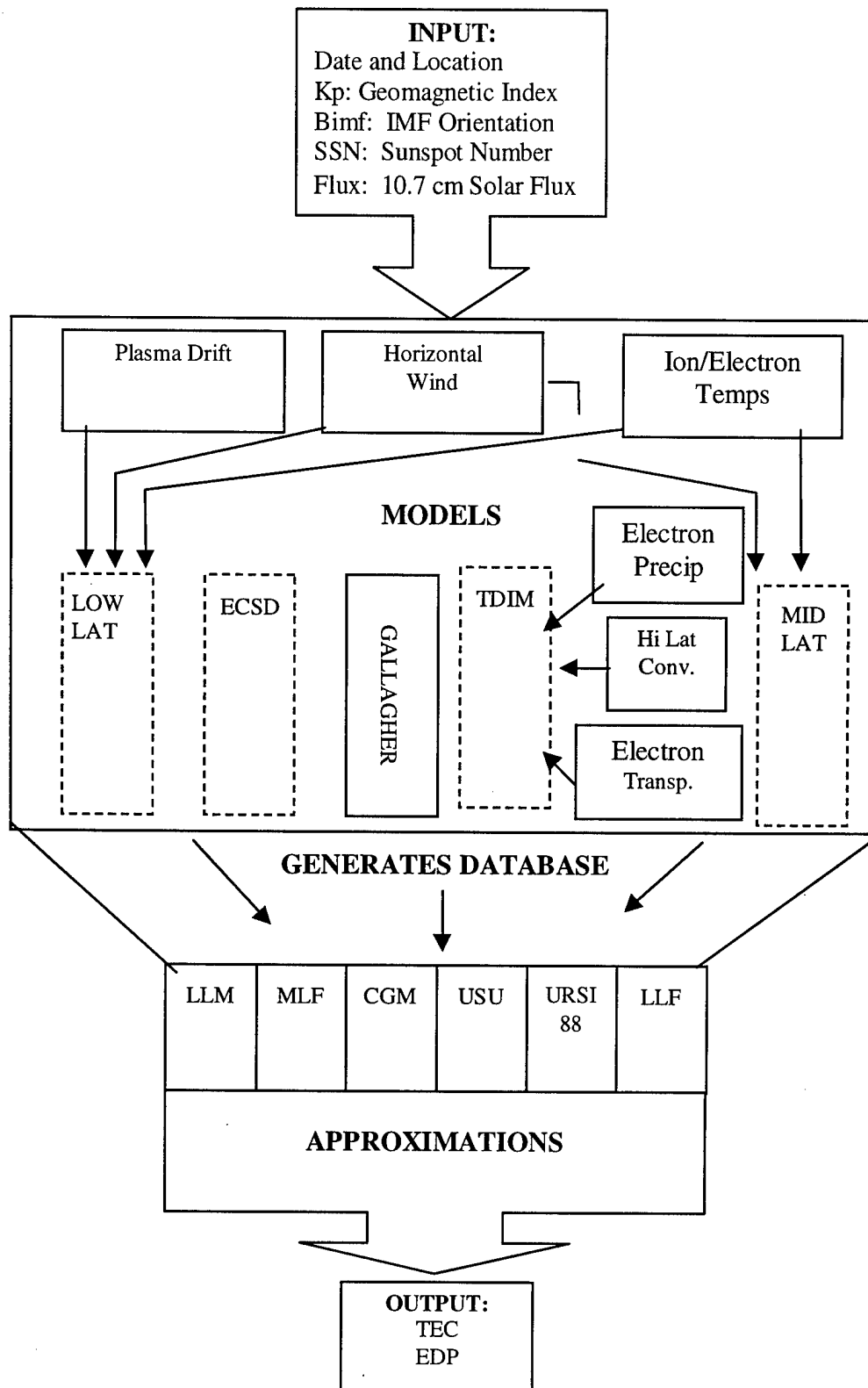


Figure 5. PIM 1.7 Components. For more detail refer to the PIM 1.7 User's Guide [Computational Physics, Inc., 1998]

## **2.3.2 The Gallagher Model**

### **2.3.2.1 Empirical Data Set**

The Gallagher model is an empirical model based on protonospheric retarding ion measurement spectrometer (RIMS) data collected by the Dynamics Explorer 1 spacecraft from 1981 to 1986. The measurements were grouped according to similarity, then fit to analytical expressions using the thin sheath approximation. The version currently in use is based on data from 1981 and 1986. See Figure 6. Note that this figure encompasses the data set over all 24 hours. Yet, the model best represents the protonosphere only from 00 – 12 Magnetic Local Time (MLT) and between +/- 40 degrees geomagnetic latitude, as all the data has not been reduced and successfully fit (Figure 7). The model provides  $H^+$  vertical density profiles as well as plasmapause location and shape for the steady state protonosphere [Gallagher, 1988]. With the Gallagher switch in PIM, one can specify an output producing results for just the ionosphere or for both the ionosphere and the protonosphere [Daniell et al.]. Differencing the results of the two model executions provides the Gallagher protonospheric profile.

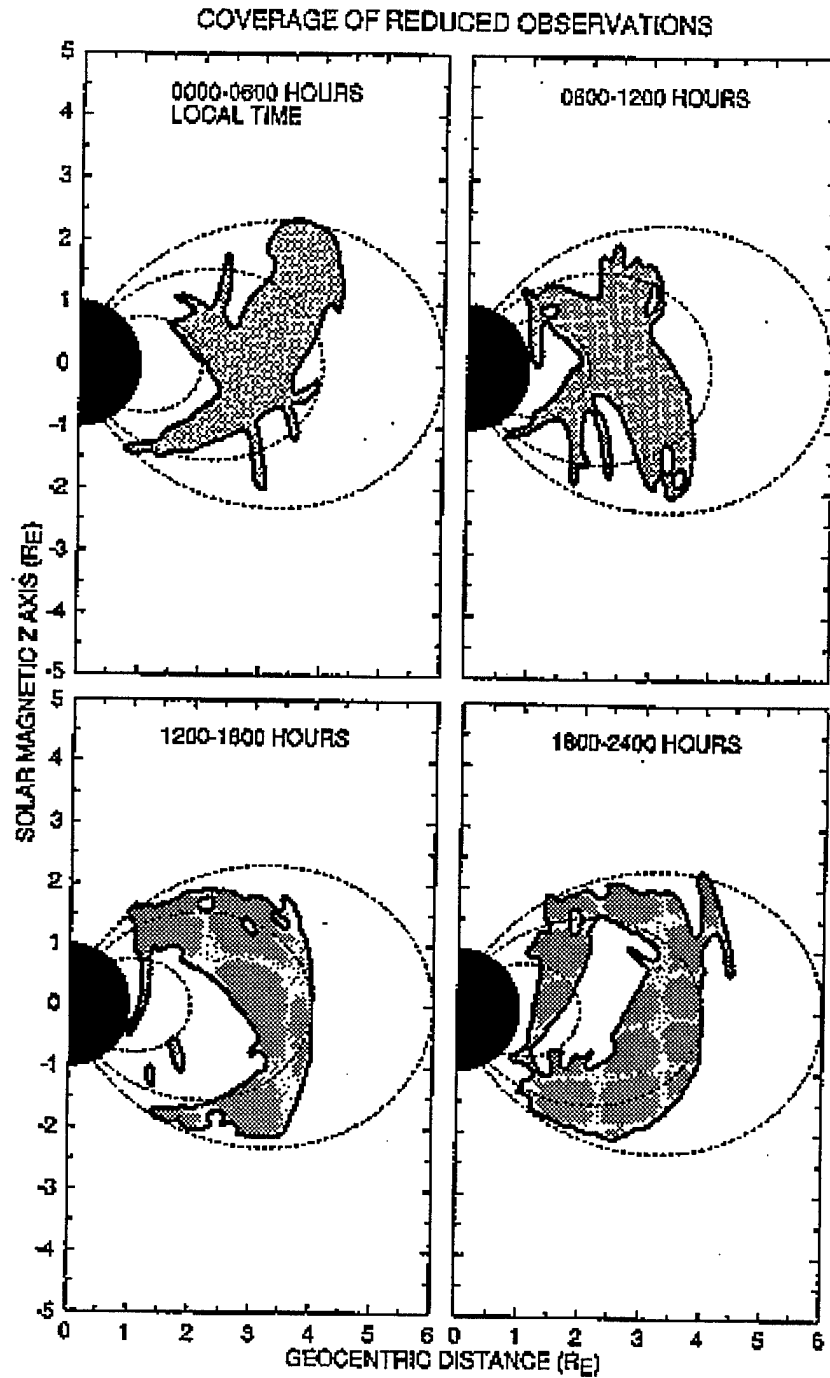


Figure 6. Coverage of Reduced RIMS measurements making up the empirical database of the Gallagher model. Shaded areas are locations represented by reduced data.

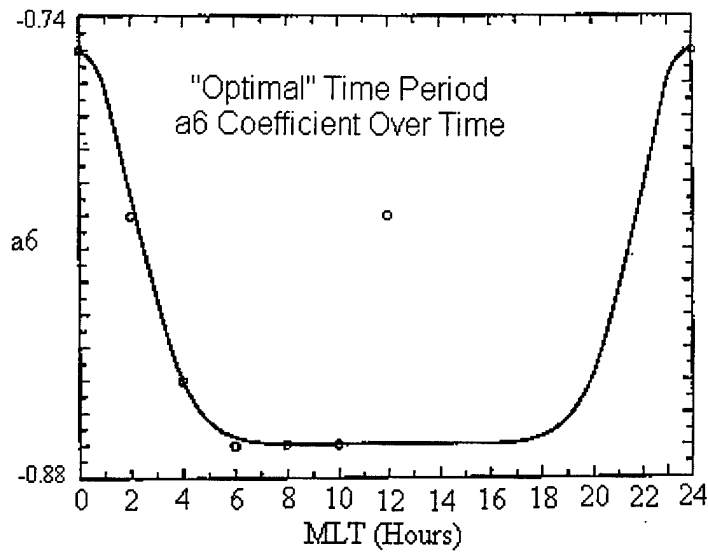


Figure 7. Temporal Applicability of the Gallagher Model. Plotted above is the coefficient  $a_6$ . 8 points are fit to the solid curve. In actuality, the anomalous point at 12 MLT has been ignored in the fit. Hours 00 – 10 MLT appear to have the best fit.

### 2.3.2.2 The Gallagher Electron Density Profile Equations

The model consists of several equations and coefficients from which we can calculate a protonospheric electron density profile. TEC is calculated from the profile. In this section, I will present the equations, identify parameters that affect output, and review some concerns with the model.

Below are the equations, as presented in Gallagher's 1988 paper:  $n$  is the electron density.

$$\text{Log}_{10}(n) = a_1 \cdot F(L) \cdot G(L) \cdot H(L) \quad [9]$$

where

$$F(L) = a_2 - \exp(a_3 \cdot (1 - a_4 \cdot \exp(-h/a_5))) \quad [10]$$

$$G(L) = a_6 \bullet L + a_7 \quad [11]$$

$$H = (1 + (L / a_8)^{[2(a_9-1)]})^{[-(a_9/(a_9-1))]} \quad [12]$$

In the paper, n is given as:

$$n \propto 10^{(-a_2 a_6 L)} \quad [13]$$

F, G, H are all dependent on L, the McIlwain parameter that describes the distance of the magnetic field lines above the surface of the earth in units of earth radius. L is given as:  $L = [(R+h)/R] / (\cos^2[\theta])$  where R is the radius of the earth, h is the altitude of a given field line in the equatorial plane, and  $\theta$  is the geomagnetic latitude. For example,  $L = 1$  is 6370 km at the equatorial surface ( $h = 0$ ).

The Gallagher coefficients, obtained by reducing and fitting the RIMS data, are as follows:

$$a_1 = 1.4$$

$$a_2 = 1.53$$

$$a_3 = -.036$$

$$a_4 = 30.76$$

$$a_5 = 159.9$$

$$a_6 = -.87 + .12 \bullet \exp[-(x^2)/9]$$

$$a_7 = 6.27$$

$$a_8 = .7 \cos [ 2 \pi ( \text{MLT} - 21 ) / 24 ] + 4.4$$

$$a_9 = 15.3 \cos [ 2 \pi \text{MLT} / 24 ] + 19.7$$

where  $x$  and MLT are Magnetic Local Time. The variable  $x = \text{MLT}$  between 00-12 MLT and  $x = \text{MLT} - 24$  between 12-24 MLT. For the sites chosen in this research, MLT and LT differ by only 15 minutes. For example, 24:00 LT is equal to 23:45 MLT.

Inspection of the equations and coefficients reveals that only changes in MLT will alter the output of the model. Changes in  $K_p$ , SSN, 10.7 cm Flux, IMF orientation, date, and season (all parameters that will alter PIM ionospheric output) will not impact protonospheric output. Refer to Figure 8, which highlights this fact that the Gallagher model ignores most input parameters entered into PIM.

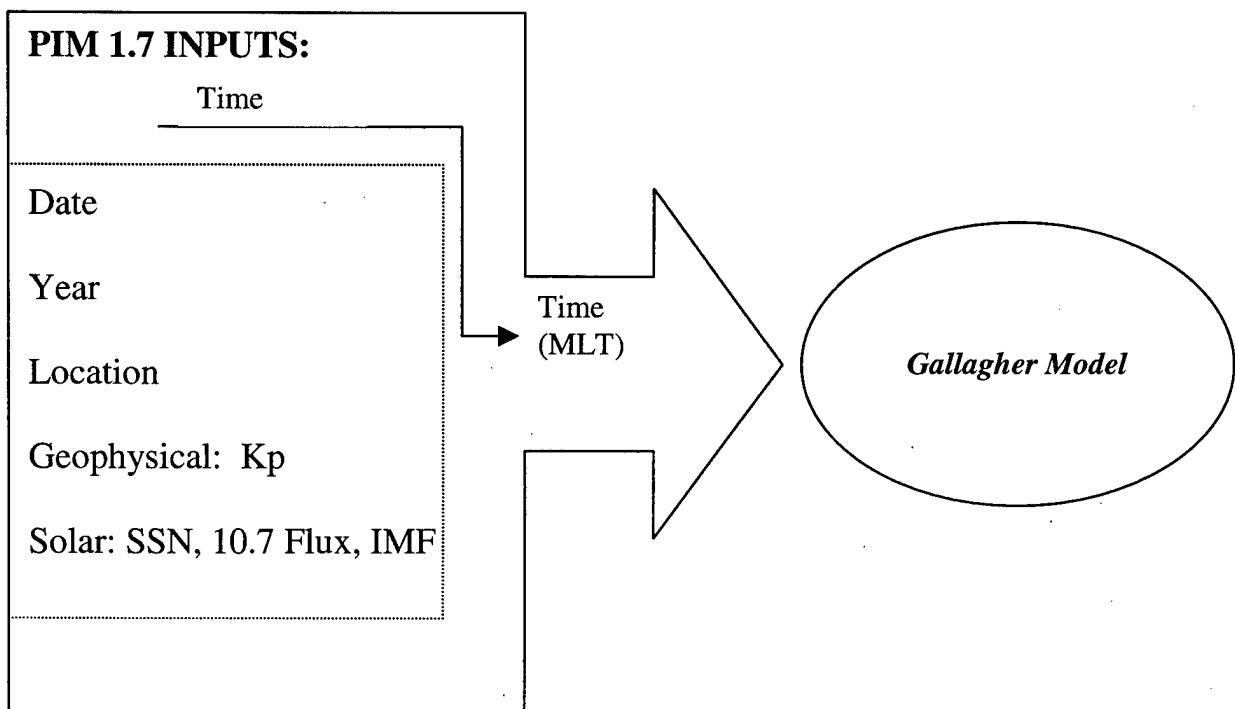


Figure 8. Though the Gallagher model is run within PIM, it is affected by changes in MLT alone and effectively ignores all other parameters in the input stream.

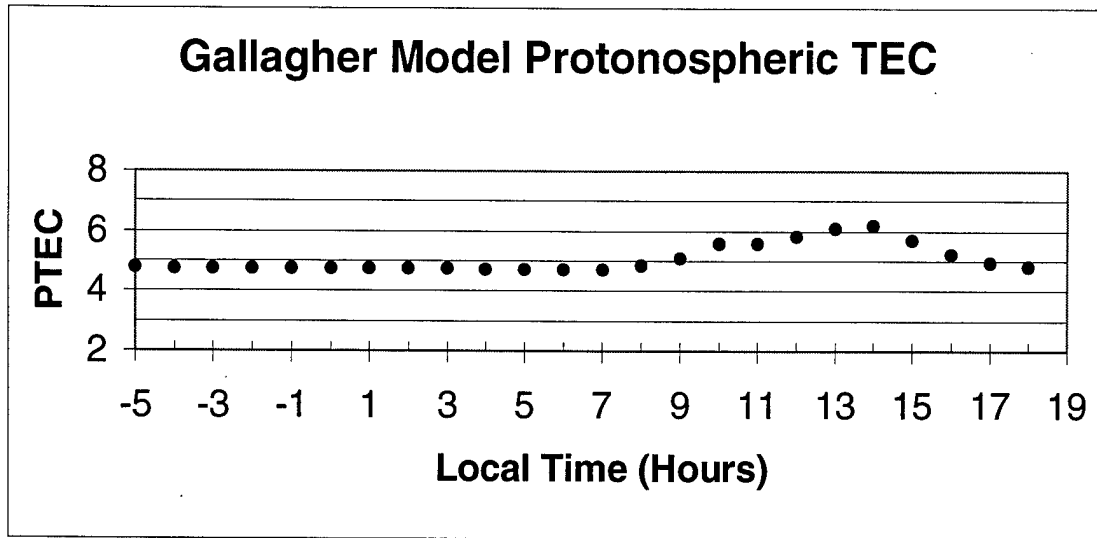


Figure 9. Example of output from the Gallagher Model.

Figure 9 shows diurnal PIMPTEC output obtained from the PIM 1.7 model using the Gallagher model. PIMPTEC results will be discussed in more detail later. While latitude ( $\theta$ ) is in the equation for the McIlwain parameter, the data used to create the model displayed no latitudinal protonospheric TEC variation along constant L-values [Gallagher, Private Communication, 1998]. The protonospheric output is not expected to vary with site latitude.

Two concerns arose in examining the Gallagher model as presented in the 1988 paper. First, the assumptions made in arriving at equation [13] for  $n$  were not stated. Second, the time period in which the model is representative is limited.

This author arrived at a different equation for  $n$  when assuming conditions for the plasmasphere. If we assume a value for the coefficient as representative of altitudes in the region of the plasmasphere (which are well above  $a_5 = 159.9$  km),  $F$  reduces to

$a_2 - \exp[a_3]$ .  $H$  simply reduces to values of 1 or just under 1 when considering  $L$  shells between 1.5 and 3. This gives:

$$n = 10^{[a_1 (a_2 - \exp(a_3) a_6 L)]} \quad [14]$$

While this equation is different from the equation published in the paper, the model studied did use the equation from the Gallagher paper. Implications, if any, of the differences in these equations were not examined and merit further study.

As stated in the paper, the model best represents the protonosphere from 00 to 12 MLT. Although Figure 7 shows that data covering all 24 hours, only the hours prior to 12 MLT could be successfully fit. In fact, it may be more correct to state that Gallagher is best applied between 00 – 10 MLT when one examines Figure 7. Here we can see the fit line for  $a_6$ , a function of magnetic local time, and the seven points the fit is based on. The eighth point for 12 MLT was anomalous and ignored in the fitting process [Gallagher, Private Communication, 1998]. Henceforth, the best representative time period for the model will be understood to be 00 – 10 MLT.

Now that we have some understanding of the GPS TEC measurement process that will lead to MPTEC and some background of the PIM and Gallagher models that produce PIMPTEC, we need to consider how to calculate and properly compare MPTEC and PIMPTEC.



### **3. Methodology**

The ultimate goal of this thesis is to compare GPS-measured groundtruth protonospheric TEC (MPTEC) with that produced from the PIM model (PIMPTEC); therefore, methodology can be discussed as two aspects: generating real measurements and model “measurements.” The methodology will render each set of data (groundtruth vs. modeled) into a comparable format. This section will address the development of both methods followed by the general steps in reaching the comparative protonospheric TEC (PTEC) values.

#### **3.1 Method Development and Modification**

While the steps outlined in section 3.2, Comparison Configuration, cover the general process, it’s important to understand that these explain the everyday calculations, not their development. Several major questions had to be addressed in development to ensure the best possible comparison and will be covered in this section. These issues will be discussed for both the ground truth measurements (MPTEC) and the model output (PIMPTEC).

##### **3.1.1 Groundtruth Protonospheric TEC (MPTEC)**

###### **3.1.1.1 The Dual Station Technique [Bishop et al, Private Communication, 1998]**

This section will outline the Dual Station Technique that uses calibrated GPS TEC data from Pittsburgh (PIT1) and Charleston (CHA1) to produce slant PTEC as seen from PIT1. This presupposes that the raw data has already been calibrated and the resulting TEC is as accurate as possible. The last section in this chapter (Section 3.2.1 The PTEC Comparison Process – General Data Manipulation), will address the steps in the calibration process. Because the two stations can view a common Ionospheric

Penetration Point (IPP), for appropriately chosen raypaths, the ionosphere seen from both sites is considered identical and allows the conversion of CHA1 slant Ionospheric TEC (ITEC) into an equivalent PIT1 slant ITEC. CHA1, looking northward through the axis of the torus-shaped protonosphere, will only measure ionospheric TEC. PIT1, looking southward into the side of the torus-shaped protonosphere, will measure both ionospheric and protonospheric TEC. From these measurements, the protonospheric TEC can be calculated.

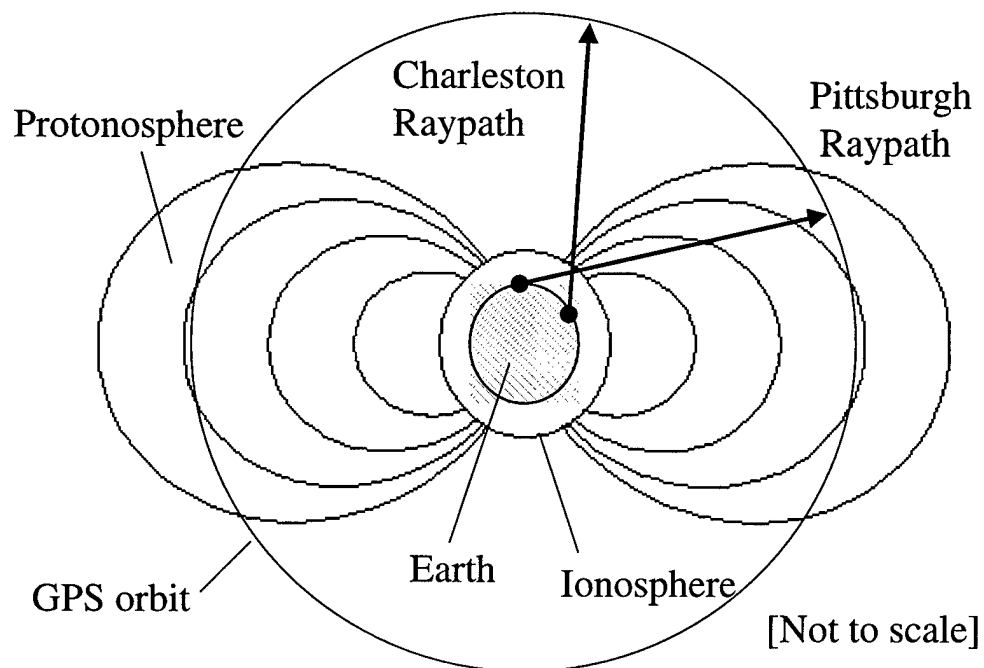


Figure 10a. The Dual Station Technique.

For each pair of STEC measurements the following tasks are performed:

**Step 1)** Convert CHA1 STEC, which is a measure of the ionosphere only as the raypath does not look into the protonosphere, to an equivalent VTEC at the IPP.

**Step 2)** Convert this CHA1 VTEC to STEC corresponding to the elevation angle of the IPP as it would be seen from PIT1. (A derived ionospheric TEC from PIT1)

**Step 3)** Subtract this derived “PIT1 STEC” from the total STEC actually measured from PIT1 (TEC including the ionosphere and protonosphere) at that elevation. This is the slant protonospheric TEC (PTEC) as seen from PIT1 or MPTEC.

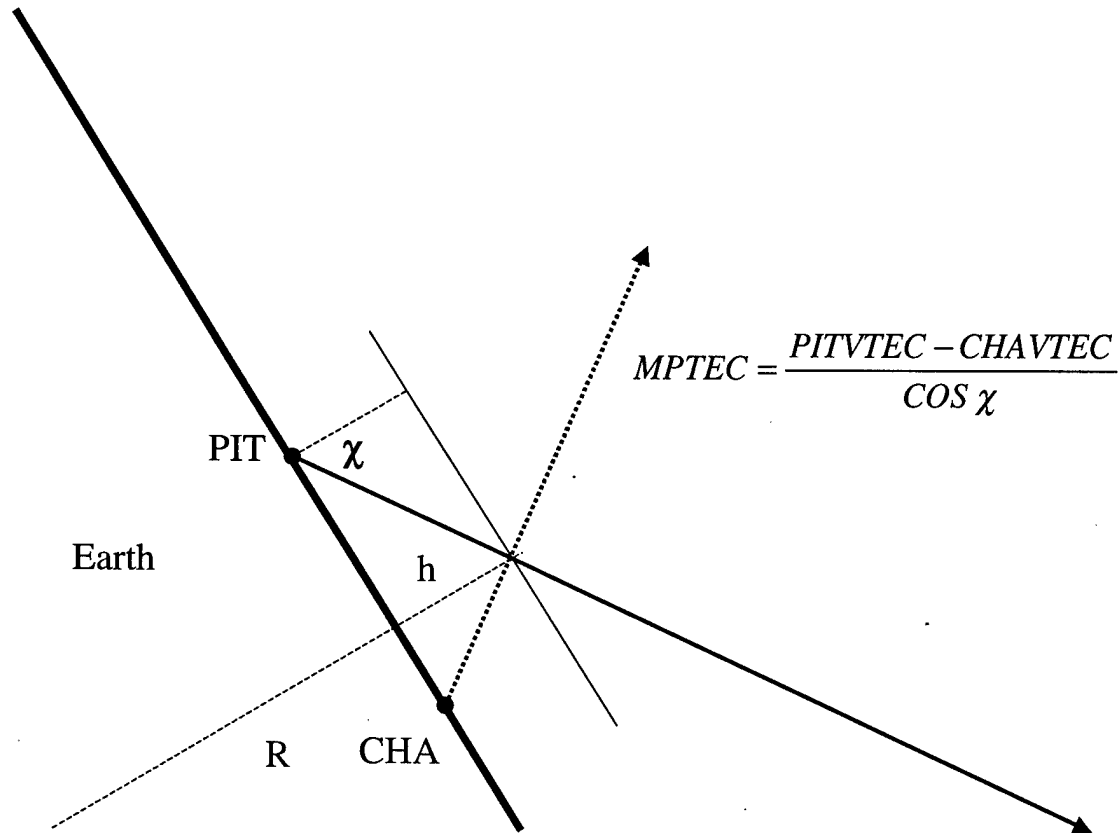


Figure 10b. The Dual Station Technique Geometry.

Essentially, the MPTEC is given by [Mazzella, Private Communication, 1998]:

$$MPTEC = \frac{(PIT1VTEC - CHA1VTEC)}{\cos \left[ \sin^{-1} \left( \frac{R}{R+h} \right) \cos \left( \frac{PIT1 ELEV}{180} \right) \right]} \quad [15]$$

Where  $R$  is the radius of the earth in km,  $h$  is the IPP altitude (350 km), and PIT1 ELEV is the raypath elevation from PIT1 to the IPP.

### **3.1.1.2 Site Selection**

Pittsburgh (40.55°N, 79.69° W geographic / 51.84° N, 5.51° W Corrected Geomagnetic (CGM)) and Charleston (32.75° N, 79.84° W geographic / 44.23° N, 6.37° W CGM) were chosen because they share nearly the same longitude and are close enough in latitude to satisfy the basic premise of the DST. They share the same ionosphere when viewing the same IPP at latitude 35° N at an altitude of  $h = 350$  km. Further, their data retrieval rates allow for comparable amounts of data to be processed for each site.

### **3.1.1.3 Retrieval Rates**

CHA1 retrieves GPS data at a collection rate of 30 seconds. PIT1 retrieves data at a 5-second rate. All the data retrieved from each site is used to create IPP database files with the exception of individual points removed as wild points. It is not until the bias calibrations are performed that a decimation factor is required to limit the processing time of vast amounts of data. For CHA1 a decimation rate of five was used: every fifth IPP database sample is pulled for use in calibration. Likewise, PIT1 uses a decimation factor of 30, also calibrating data every 150 seconds. Even though the calibration process is limiting the number of samples pulled in the process, when finished, data is available at the original retrieval rates: CHA1 every 30 seconds and PIT1 every 5 seconds.

Continuously Operating Reference System (CORS) archives for PIT1 were altered after Julian day 241 in 1997 (7241) to store data at a 30-second collection rate

requiring the decimation rate to be lowered to 5 for those dates. With this archival change, the raw data for PIT1 changed from 24 hourly files to a single file per day. Processing for each type of data was altered accordingly. For hourly files, an additional step to join 24 hourly files into one large daily file was done prior to the first step of Differential Group Delay/Differential Carrier Phase Delay (DGD/DCP) pass file generation.

#### **3.1.1.4 Data Reduction**

Large amounts of data were processed for each station's calibration, occasionally exceeding 2000 data points per day. In order to render this vast amount of data into comparable form against 24 hourly points from PIM, the groundtruth data was averaged into bins  $\pm 1800$  seconds from each hour. This produced 25 averaged TEC points per day. Due to the data collection restrictions at each site, the averaged TEC values for 00 UT bin only contain data from 0 to 1800 sec, and for the 24 UT bin, only from 84600 to 86400 sec. Therefore, there is no overlap in data from one day to the next.

#### **3.1.1.5 Pittsburgh Anti-Spoofing**

Unlike Charleston, Pittsburgh collected data under an "anti-spoofing" condition. The GPS receiver exchanges two pseudo-range variables and, if the processing does not adjust for this column swap, the GPS data will not produce TEC values [Gurtner, 1995]. Appending the file generation command line with "as" ensures that the proper columns are read during retrieval and processing. The anti-spoofing condition also produces Pittsburgh group delay data that is slightly more noisy than that of Charleston; however, it can still be used in the Dual Station Technique.

### **3.1.1.6 SCORE Calibration Adjustment – Search For Low-latitude Cutoffs**

As discussed in the section on the SCORE calibration process, a great deal of progress has been made in improving GPS TEC accuracy [Lunt et al, 1998 b]. This increase in accuracy was the result of adjusting the SCORE process by limiting the calibration data to certain IPP latitudes (or raypath elevation angles) such that SCORE calibration is based on almost purely ionospheric data (a negligible protonospheric component). See Figure 11. Lunt was able to adjust his SCORE process for single station GPS data in Aberystwyth, England, but the earth's tilted magnetic dipole renders the protonosphere geometry different for North America. See Figure 3. Appropriate low-latitude cutoffs had to be found for both Pittsburgh and Charleston that did not seriously limit the Dual Station Technique. Again, one must keep in mind that low-latitude cutoffs, restricting the latitudinal range of the data used in calibration, are not restricting the latitudinal range of the actual measurements. The cutoffs increase calibration accuracy while allowing measurements through an unrestricted latitude range.

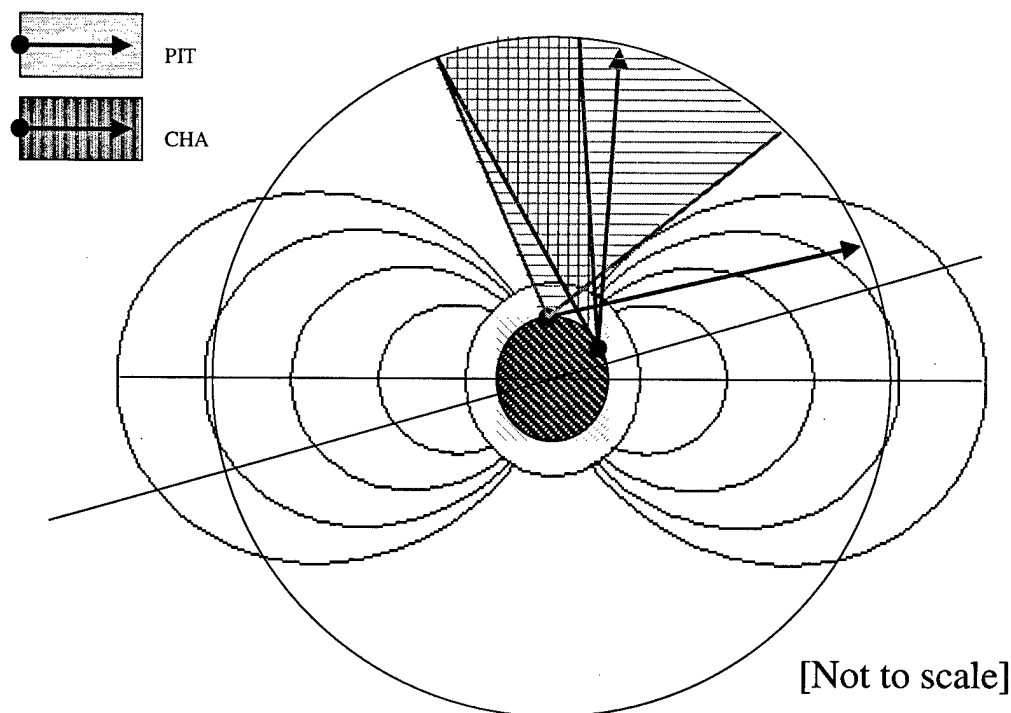


Figure 11. For a given site, the low-latitude cutoff is the IPP latitude below which the protonosphere begins to contaminate the TEC measurement calibration. Only data above the cutoff is used for calibration. The calibration is then applied to data from all latitudes.

The search for the best low-latitude cutoff was made difficult by several factors. The precise latitude at which the protonosphere begins to influence GPS TEC measurements is difficult to find and is likely not fixed. The protonosphere, due to asymmetry in the geomagnetic field, plays a less significant role in North American measurements and may be difficult to detect for purposes of a cutoff. Lastly, only the best possible cutoff, not the best cutoff, can be found given that protonosphere exclusion must be balanced with adequate data retrieval and processing. Selecting a low-latitude cutoff too far south or north simply results in an increase in “orphan”

satellites that fail to calibrate. (The term orphan refers to a satellite that fails to produce proper bias calculations [Mazzella, Private Communication, 1998].) Orphan impacts can best be demonstrated in Figure 12. Plots 12a and b are examples of a final bias calibration plot in the SCORE process. Good calibration is seen in Figure 12a, Pittsburgh using its low-latitude cutoff of 40.75 degrees.

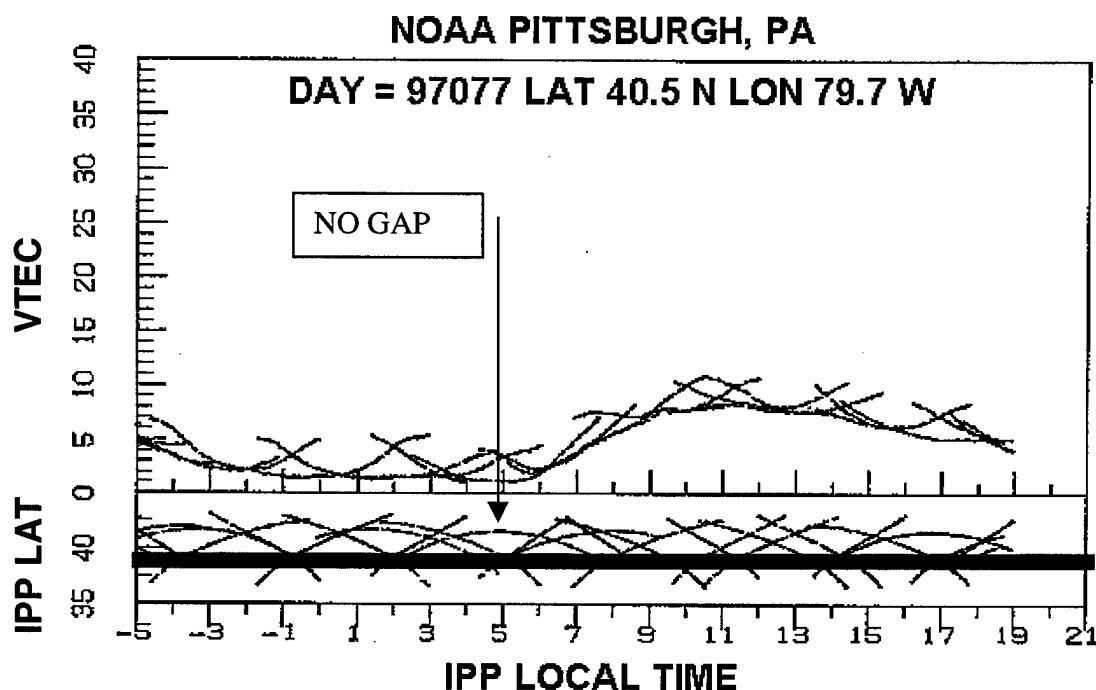


Figure 12a. Example of Pittsburgh site output using the cutoff of 40.75 degrees. (Note: Drawn line is not exactly 40.75 degrees.)

Figure 12b, with a 41.55 degree cutoff, experienced several orphan satellites that create wild points. If one took a ruler and set it perpendicular to the IPP LAT axis at the bottom of the graph for a particular low-latitude cutoff, you could examine the satellite passes available above the cutoff latitude (that is, above the ruler). Although the program plots all the satellite pass latitudes, the upper portion of plot is the resulting calibration from only the passes above the low-latitude cutoff. Lay a ruler across the



40.75 degree cutoff in Figure 12a, such that the VTEC was derived from pass data above the ruler only, and you can see that all the passes “connect” at 40.75 degrees. But, in plot b, doing the same at 41.55, you can see that small gaps appear between the satellite latitude passes. Those satellite passes do not “connect” with the others and, as such, are called orphans. Notice that while that “orphaned” satellites’ VTEC values are drastically changed, that other VTEC values are altered slightly as well. Another problem with a low-latitude cutoff is that it can also cut needed data out of the sample. If too many satellite passes are cut off or fail to properly calibrate, bias calibration fails for the entire day.

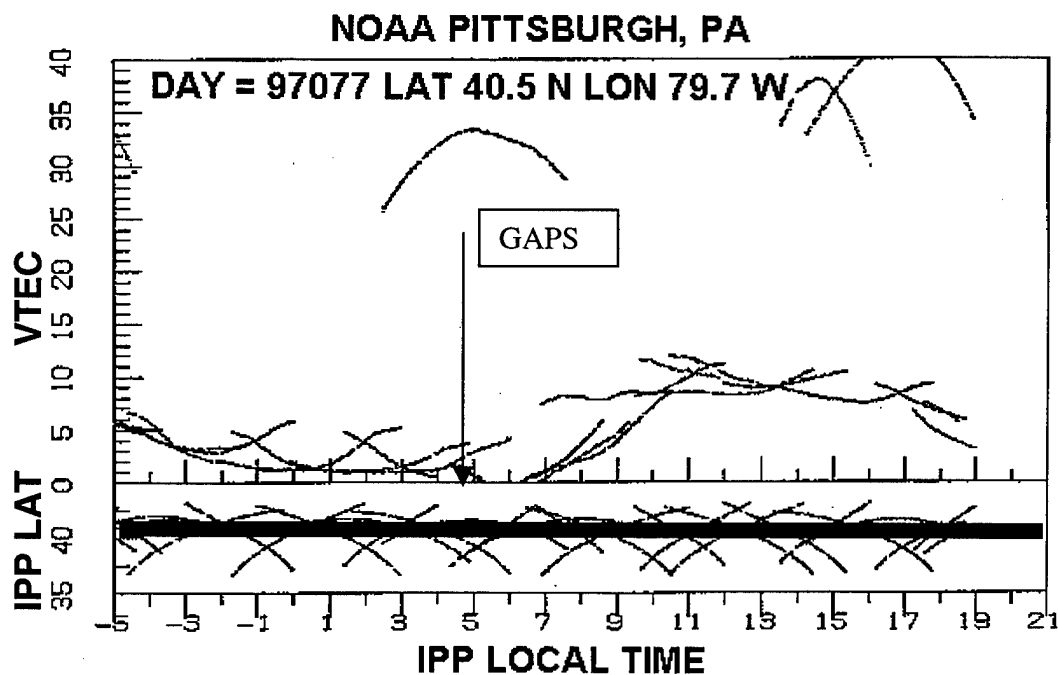


Figure 12b. The same results but with a poor cutoff of 41.55 degrees. (Note: Drawn line not exactly at 41.55 degrees.)

The search method followed the main calibration steps listed in section 3.2.1.1 Groundtruth GPS TEC Data (MPTEC). Initially, for one day in the data set, a bias calibration for a site was run without a cutoff. Unless specified, the bias calibration program defaults to an unrestricted latitude range of -90 to +90 degrees geographic. In actuality, the horizon limits the range of IPP latitudes a site can view to within about 18 degrees north and south of the site. This unrestricted calibration was done and a plot of VTEC vs. IPP Latitude was examined. The plot was used to gain a sense of the general raypath from station to satellite that begins to track through the high protonosphere and which must be excluded from the SCORE process. Detecting any protonosphere influence in addition to normal geometrical ionospheric TEC increase, as the raypath tracks through 'thicker' views of the ionosphere, is difficult. Once a potential cutoff latitude is found, a further series of SCORE calibrations for that day were made with varying low latitude cutoffs within 5 to 10 degrees of the suspected cutoff latitude and the results examined. One day of data was used to search for cutoffs. 24 suspected cutoffs (36.00 – 41.55 degrees geographic) were examined for Pittsburgh and 18 (30-40 degrees geographic) for Charleston. Cutoffs consistently producing the minimum TEC with the least orphans were selected as the site low-latitude cutoff. Refer to Figure 13. For Charleston, the low-latitude cutoff used was 33.1 ° N geographic. For Pittsburgh, it was 40.75 ° N geographic. These same cutoffs were used throughout the research. Low latitude cutoff impacts are discussed in Chapter 4, Data Description and Analysis.

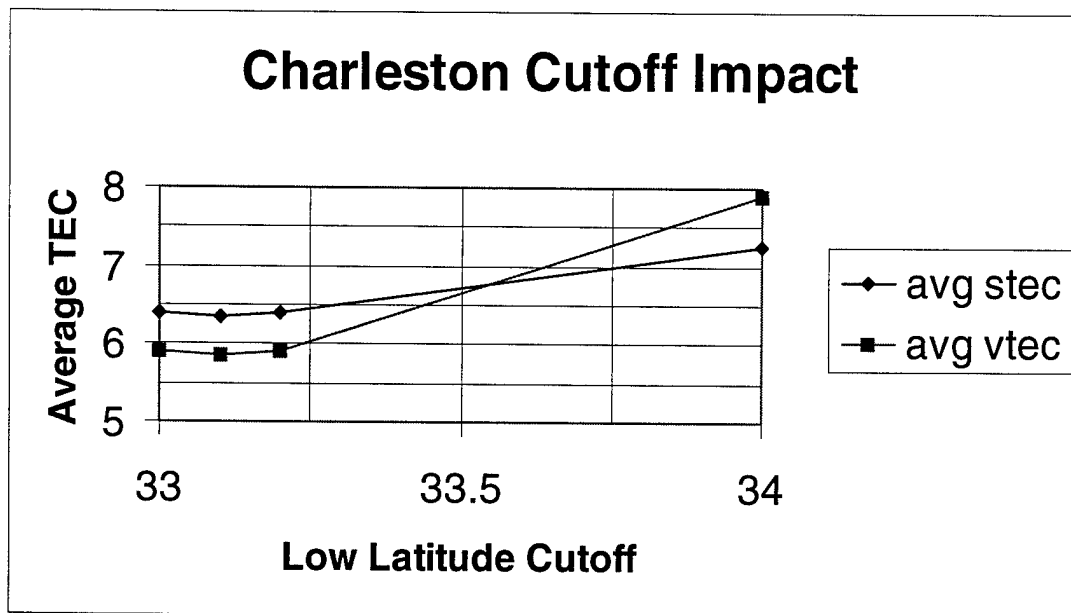


Figure 13a. Low-latitude cutoff impact on TEC.

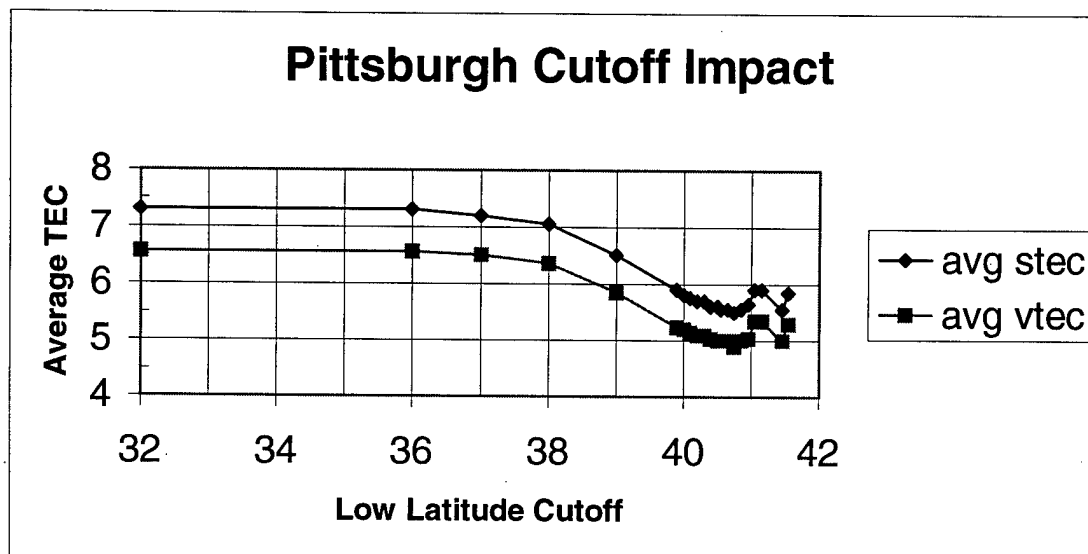


Figure 13b. Low-latitude cutoff impact on TEC.

### 3.1.2 Modeled Protonospheric TEC

#### 3.1.2.1 Using Pittsburgh Slant Path Comparison Configuration

As discussed in the background section, the Gallagher model best represents the protonosphere between  $-40^\circ$  and  $+40^\circ$  geomagnetic latitude. Since the final

comparison is STEC along a raypath from Pittsburgh, we ought to be concerned that Pittsburgh, located at nearly  $52^\circ$  geomagnetic, falls outside this range. But this does not invalidate the use of the Gallagher model: Pittsburgh raypaths to the IPP are looking into the heart of the protonosphere between  $-40^\circ$  and  $+40^\circ$ . See Figure 14.

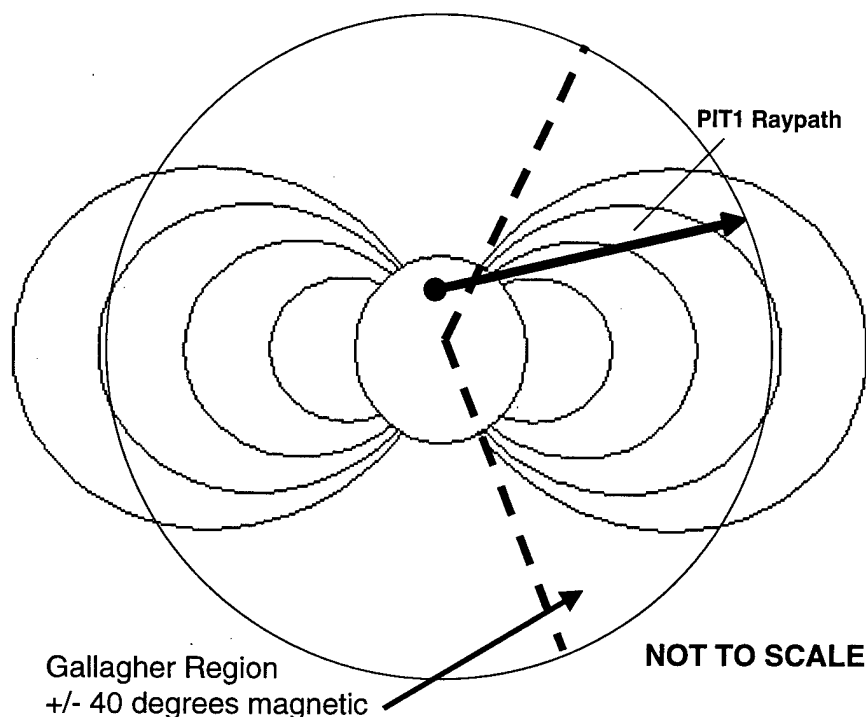


Figure 14. Site PIT1, at a latitude “outside” the latitudinal range of the Gallagher model, has a ray path looking into the protonosphere in that range.

### 3.1.2.2 PIM Slant Configuration

The azimuth/elevation output configuration of PIM was used, as it best replicates the groundtruth geometry. Pittsburgh was entered as the ground site with a raypath looking due south at an elevation range of  $26^\circ$ . This elevation best represents the ray path through an IPP latitude of  $35^\circ$  geographic and is used to derive PIMPTEC. Selection of IPP is discussed in Section 3.2, Comparison Configuration.

### 3.1.2.3 PIM Altitude Grid Configuration

PIM was used to produce STEC as seen from Pittsburgh. The azimuth/elevation configuration of PIM requires the input of an altitude grid. The PIM output TEC is actually more sensitive to the specification of altitude grid points than to the activation of the Gallagher model that incorporates the protonosphere. Compare Figure 15, PIMPTEC output using a 10 point altitude grid, with Figure 16, PIMPTEC output using a 100 point altitude grid. Consultation with the developers of PIM led to the use of this higher resolution altitude grid consisting of 100 variably-spaced altitude points, from 90 to 25,000 km, matching the interior default grid [Daniell, Private Communication, 1998]. This grid provides the most representative TEC possible. The same grid, ranging from 90 km to 25000 km, was used for both PIM execution modes (Gallagher ON/OFF) as described in section 3.2.1.2 Modeled Protonospheric TEC Data (PIMPTEC). See Table 1 on page 41.

90	95	100	105	110	115	120	125	130	135
140	145	150	160	170	180	190	200	210	220
230	240	250	260	270	280	290	300	310	320
330	340	350	360	370	380	390	400	410	420
430	440	450	460	470	480	490	500	525	550
575	600	625	650	675	700	800	825	850	875
900	1000	1050	1100	1150	1200	1300	1400	1500	1600
1700	1800	1900	2000	2100	2200	2300	2400	2500	3000
3500	4000	4500	5000	5500	6000	6500	7000	7500	8000
8500	9000	9500	10000	12500	15000	17500	20000	22500	25000

Table 1. Computational Physics Inc.'s 100 Point Altitude Grid for the STEC configuration of PIM 1.7. These are increments of altitude, along a specified slant path, in kilometers.

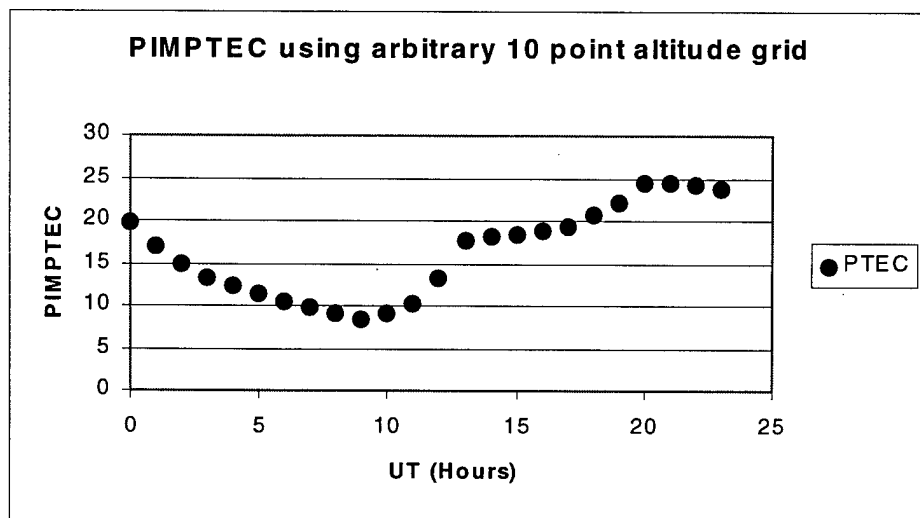
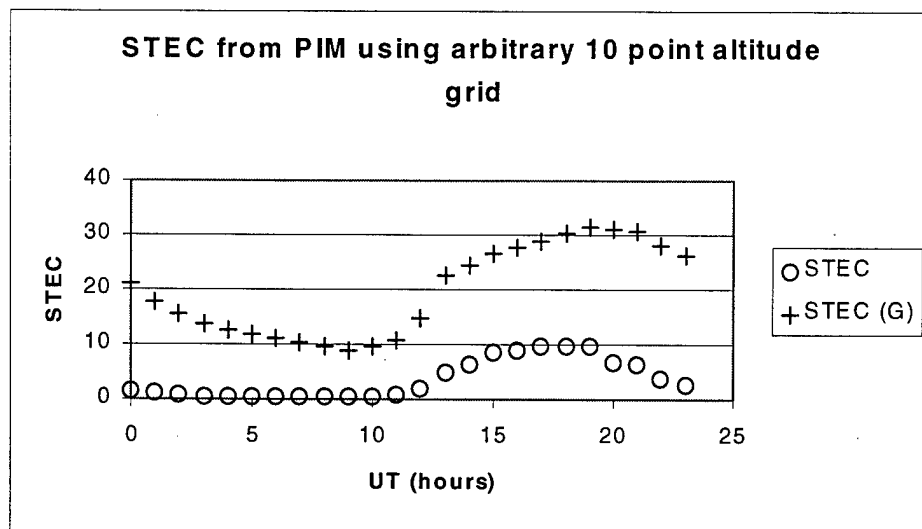


Figure 15. An example of PIM produced PIMPTEC using an arbitrary 10 point altitude grid instead of CPI's 100 point grid. Notice the drastic change in STEC (Open Circles) between Figure 15 and 16. As a result, PIMPTEC is altered simply due to the changes in altitude grid.

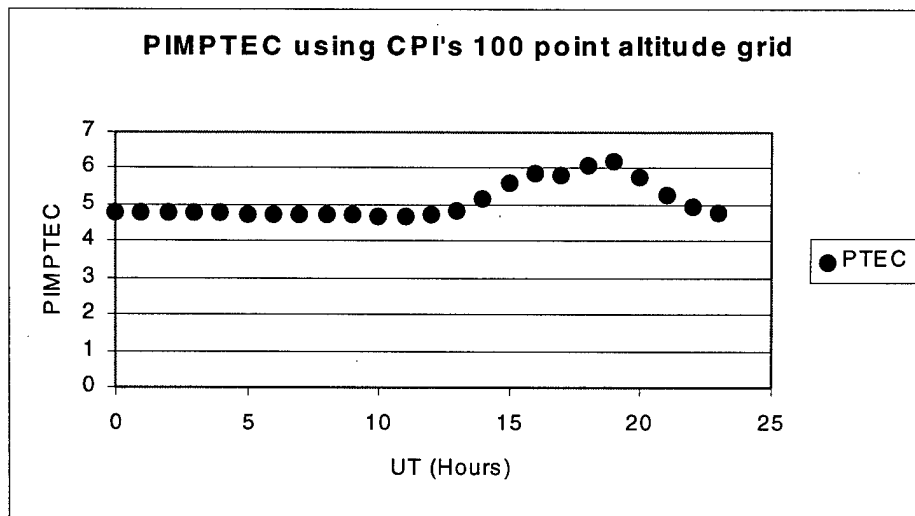
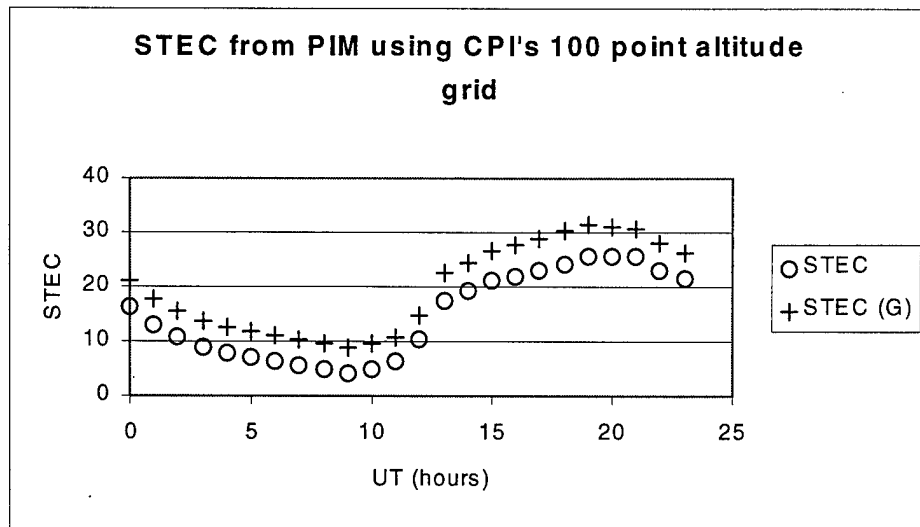


Figure 16. PIMPTEC using the default 100 point altitude grid.

#### 3.1.2.4 Producing PIM Output Over Time

One drawback of PIM is that it does not have an option for automatically producing output over a user-selected time period. While each execution allows for selection of altitude grids, site coordinates, and output type, each produces output only for one instant in magnetic local time (MLT). On the other hand, the groundtruth measurements are obtained at 5-second intervals at Pittsburgh and 30-second intervals at Charleston, implying a tremendous quantity of data. To keep computation times and



memory requirements reasonable, it was decided to create a 24-hour PIM run using 24 individual hourly executions.

### **3.2 Comparison Configuration**

As discussed in the background section, one of the premises of the Dual Station Technique is a common IPP at 350 km. The IPP latitude representing the best common IPP with the most TEC data points for both CHA1 and PIT1 was approximately 35 °. This required the calculation of MPTEC as seen from Pittsburgh looking through the 35-degree latitude IPP. As such, PIM was set to run from Pittsburgh with a southern azimuth at an elevation of 26 °. (Charleston's corresponding elevation angle was approximately 52 °.) This configuration produces PIMPTEC as geometrically close as possible to the MPTEC obtained from the GPS data. See Figure 17. The IPP Window, through which measurements of MPTEC are made, runs from 34.5 ° to 35.5 ° N geographic latitude and 74 ° to 86 ° W geographic longitude. The IPP Point, through which calculations of PIMPTEC using PIM are made, is at 35 ° N latitude and 79 ° W longitude.

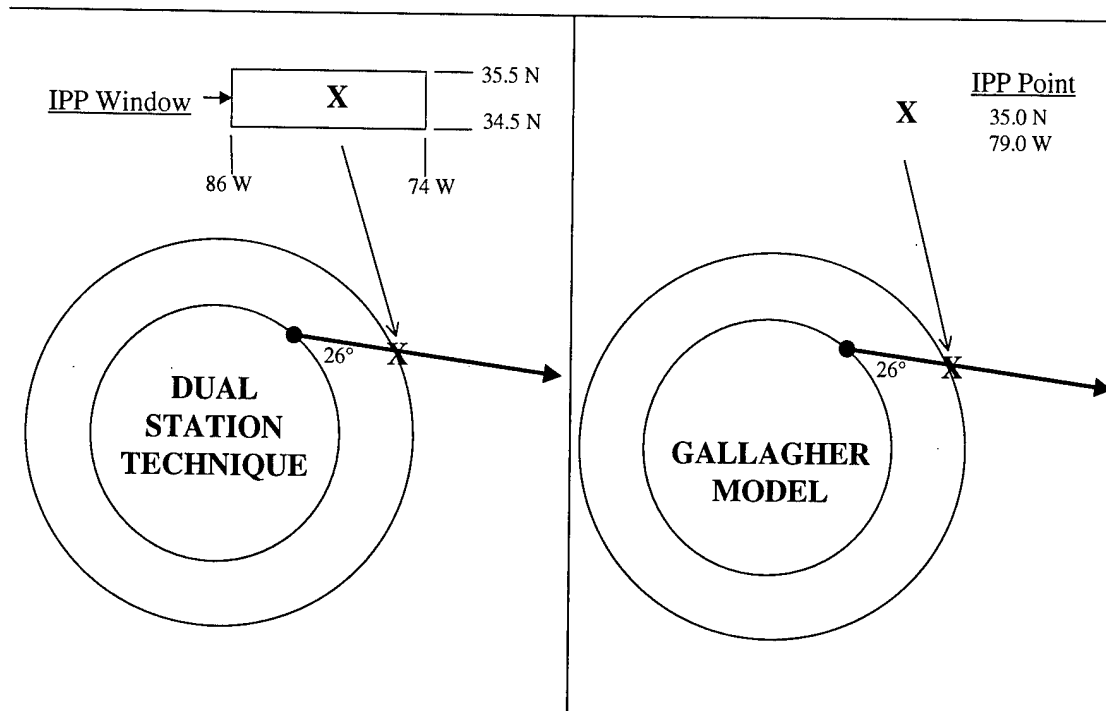


Figure 17. The Comparison Configuration. PIMPTec is calculated through an IPP point while measurements of MPTEC are calculated through an IPP Window.

### 3.2.1 The PTEC Comparison Process – General Data Manipulation

See flowchart and accompanying graphs, Figure 18a, b, and c. These provide a visual reference to the steps outlined in the next sections that describe how MPTEC and PIMPTec were produced.

#### 3.2.1.1 Groundtruth GPS TEC Data (MPTEC)

**Step 1)** Raw data for the day in question is retrieved from the National Geodetic Survey's CORS archives for both PIT1 and CHA1 and downloaded to the computer. Each site has its calibration (described below) done separately.

**Step 2)** Unzip and check each data file for the correct file type that will be recognized by the processing program. A data inventory is conducted to ensure all files are in place. Search is made for abnormally small files that may indicate faulty passes or missing data. Errant days are discarded from the data set.

**Step 3)** Place files in the calibration directory built for each site and then execute the processing batch files. The first batch file generates standard DGD/DCP pass files from the daily/hourly CORS data using the Receiver Independent Exchange Format Version 2 (RINEX) conversion program RINMTI V. 3.0.

**Step 4)** Perform wild point checks (using various batch files) that eliminate data points out of a preset range. Typically, DGD data points outside three standard deviations from the mean are removed.

**Step 5)** Perform fix jump. This program fixes DCP data discontinuities (jumps) by adjusting TEC levels for discrete data segments.

**Step 6)** Perform manual pass examination. View a plot of each pass (DGD vs. UT) and check for missed wild points or large gaps. Any satellite pass of less than 45 minutes or containing corrupted data (garbled, unusable) is deleted. Remaining wild points or gaps in other passes are eliminated.

**Step 7)** Generate azimuth/elevation files needed to plot output.

**Step 8)** Enter the correct low latitude cutoff parameter for the site in the bias calibration batch file. Run the bias calibration using the generated azimuth/elevation file. Check the resulting bias table for values of zero that indicate “orphans”: poor passes, faulty satellite calibration, wild points, etc. (Recall an orphan is defined as a satellite that fails to calibrate properly.) Data from these satellites will be disregarded in the comparison. (Although not done in this research, it is possible to use bias calibrations from successful days on adjacent days.) This completes the SCORE process. The following steps are data manipulation for the comparison.

**Step 9)** Convert the generated IPP data base files into a text table consisting of YEAR, MONTH, DAY, UT, AZIMUTH, ELEVATION, IPP Latitude (IPPLAT), IPP Longitude (IPPLON), STEC, and VTEC.

**Step 10)** Ingest data into spreadsheet for analysis. Data from 34.5 ° to 35.5 ° N latitude and 74 ° to 86 ° W longitude are ingested into the spreadsheets. MPTEC is calculated from the hourly averaged VTEC values from CHA1 and PIT1 as described in section 3.1.1.1 The Dual Station Technique.

### **3.2.1.2 Modeled Protonospheric TEC Data (PIMPTEC)**

**Step 1)** Obtain the following geophysical and solar information for the day in question:  $B_y$  and  $B_z$  IMF orientation, 10.7 cm Solar Flux (27 day mean), Sunspot number, and Planetary  $K_p$ .

**Step 2)** Update the geophysical and solar information in the input stream file. Ensure the plasmasphere function is set to Y. (This includes the protonosphere in the output STEC.)

**Step 3)** Run the batch file that calls PIM to execute 24 times in succession. This creates a text file as output that can be ingested into the spreadsheet.

**Step 4)** Ingest the text data. It is parsed automatically into a prepared worksheet and plotted as STEC vs. UT for a 24-hour period.

**Step 5)** Re-edit the original input stream file to set the plasmasphere function to N. (This does not include the protonosphere in the output STEC.) Execute PIM again.

**Step 6)** Ingest the non-plasmasphere PIM results into a separate worksheet.

**Step 7)** Take the difference of the two STEC results to obtain PIMPTEC for each of the 24 cardinal hours.

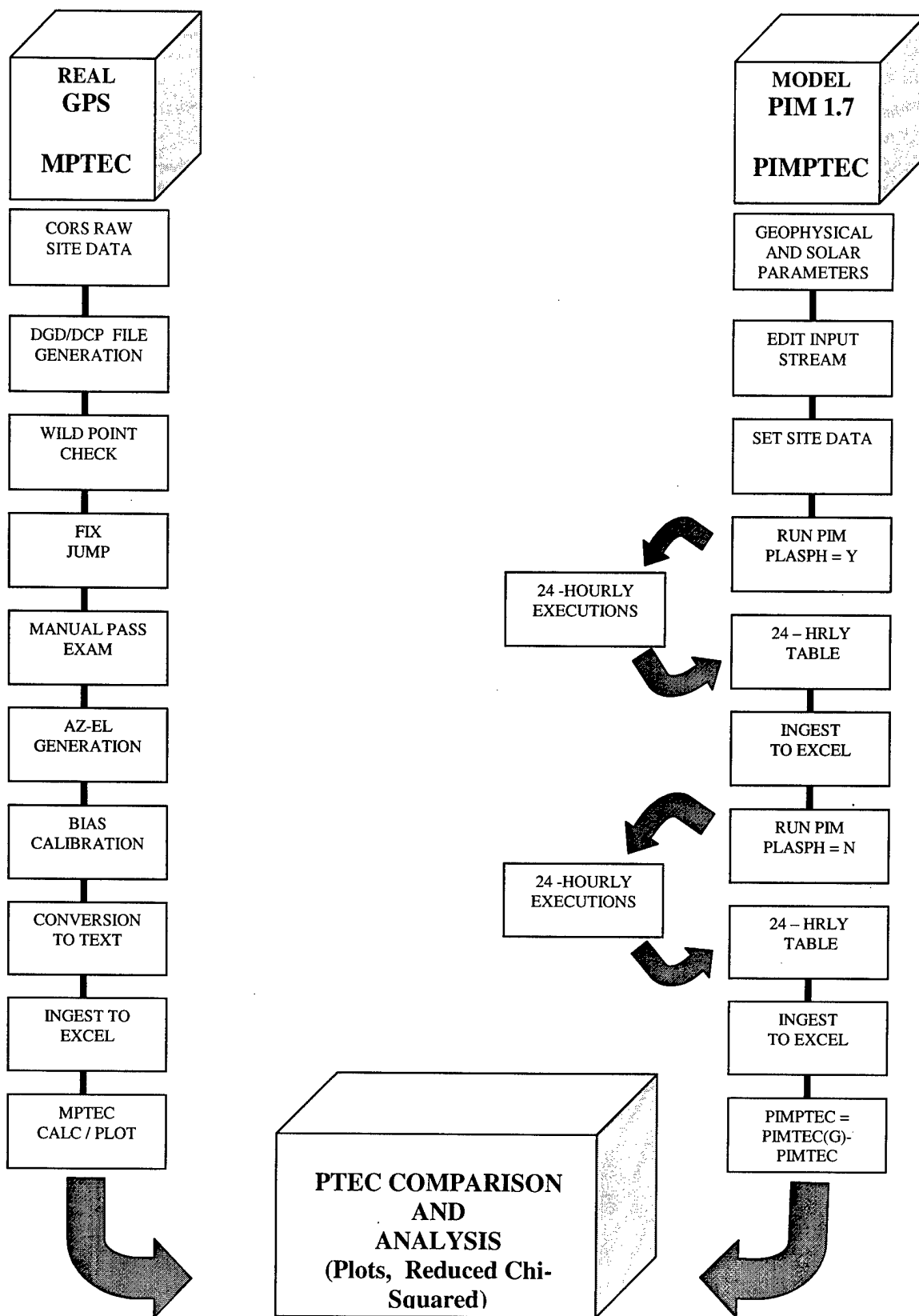


Figure 18a. Flowchart of the Comparison Method

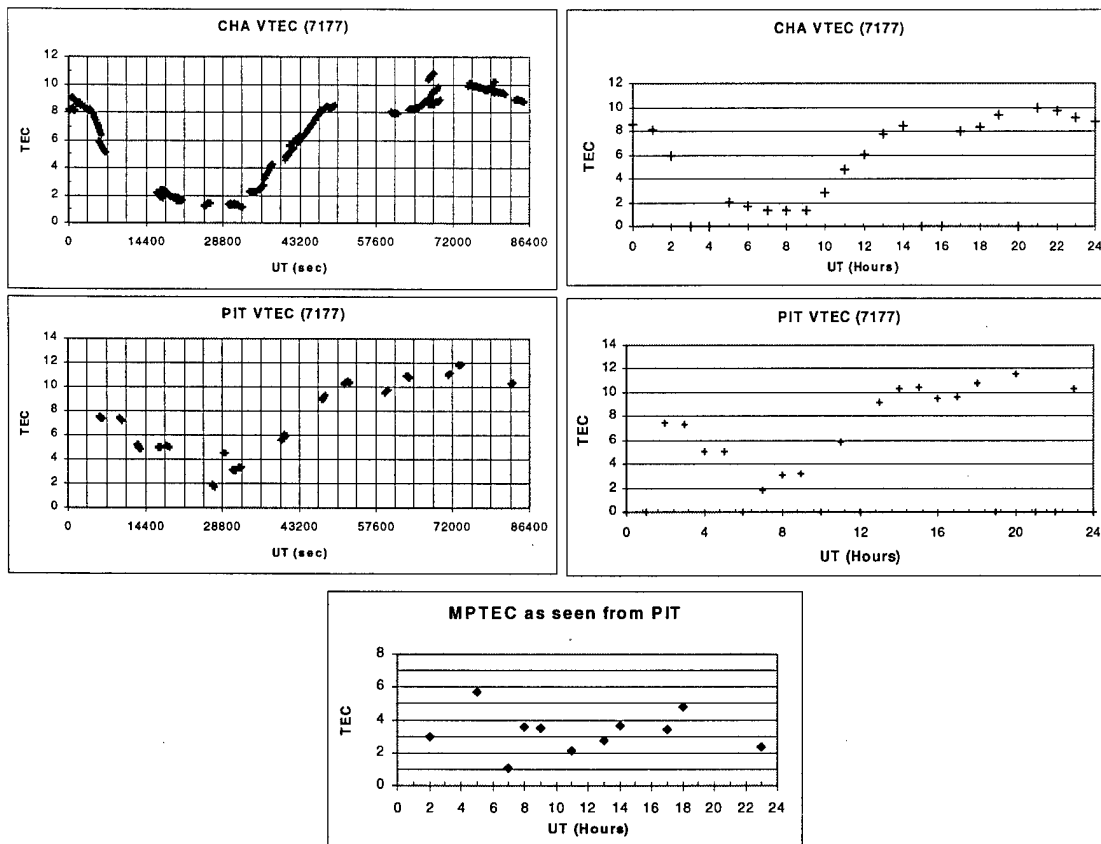


Figure 18b. Example of MPTEC measurement. Raw calibrated GPS VTEC for CHA and PIT is on the left. These thousands of data points are averaged into hourly bins on the right. From these averaged hourly VTEC points, MPTEC is calculated and plotted at the bottom.

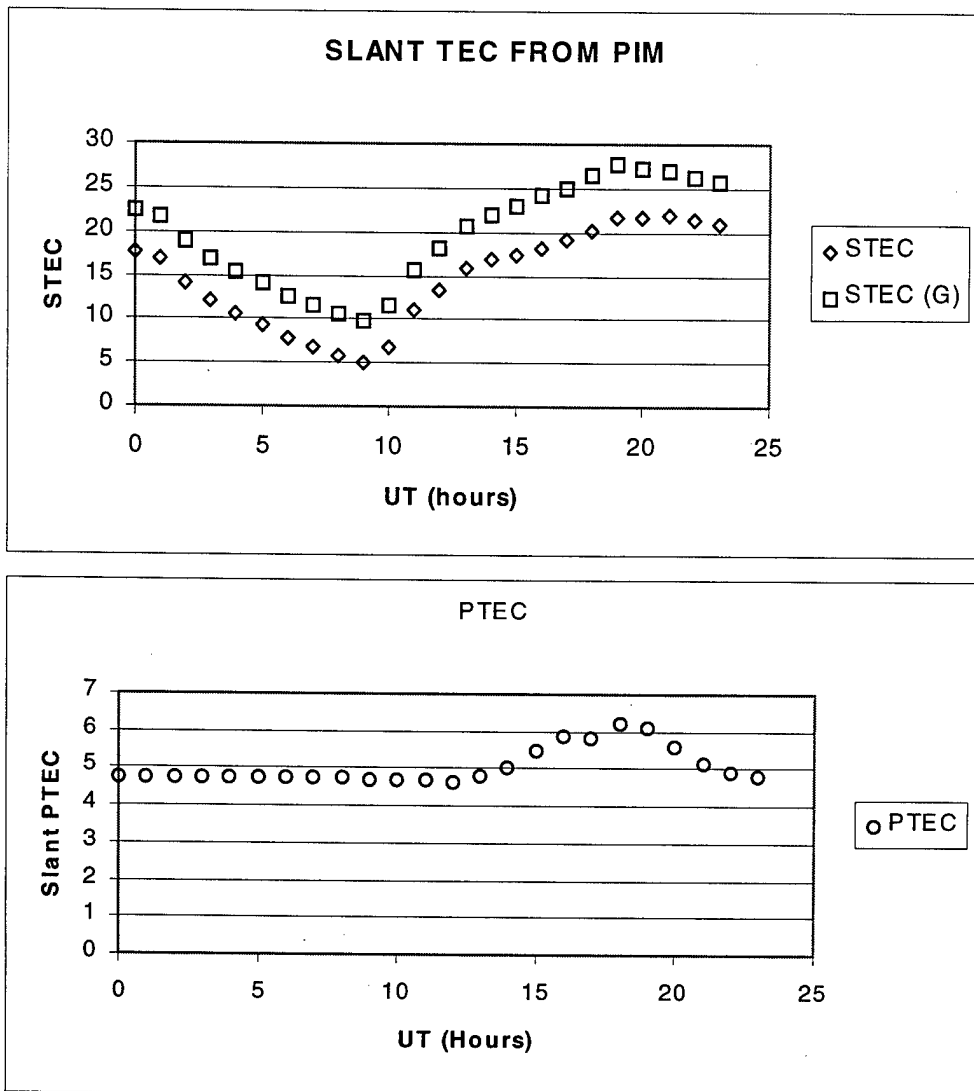


Figure 18c. Example of PIMPTEC Calculation. PIT STEC is calculated in PIM, with and without the Gallagher model. The difference is the PIMPTEC plotted in the lower graph.

## **4. Data Description and Analysis**

### **4.1 Scope**

#### **4.1.1 Planned Scope**

With an aim to compare MPTEC against PIMPTEC, which is at best an average, it was decided to select a week of GPS data from each 1997 season and average the MPTEC results. Geomagnetically quiet to unsettled days were desired, as the Gallagher model was not designed to model storm activity. The dates were initially chosen around equinox (March/September) and solstice (June/December) with the intent to initially verify that the incorporation of the Gallagher model into PIM did not create daily or seasonal PTEC variations the Gallagher model was not designed to capture. The data set was purposefully limited in size to alleviate both the Continuous Observing Reference System (CORS) archived data request procedures and the extensive processing times required for the GPS data.

#### **4.1.2 Resultant Scope**

The scope became necessarily limited due to data loss problems (discussed in this section), associated with receiver site operations and errors, signal loss, geomagnetic storms, multi-path errors, “orphans,” and calibration failures.

First, approximately 15 days were discarded because the Pittsburgh site was not functioning on those days.

Next, some days were discarded since the Pittsburgh site, while functioning, lacked several hourly files in the data due to receiver malfunctions [Drosdak, Private Communication, 1998].



Then, in an attempt to explore how the dual station technique recorded storm conditions (without comparison against Gallagher), the winter period was changed to incorporate a severe geomagnetic storm in late November. The hope was to explore post-storm changes in the MPTEC. However, accuracy problems arose with the Charleston site, probably caused by calibration break down due to unknown causes, forcing the elimination of the winter data set for study.

A different difficulty arose with the fall data. The Pittsburgh receiver seemed to be experiencing a problem and did not consistently receive GPS signals [Doyle, Private Communication, 1998]. Initially this problem was overlooked, as the file format had become one daily file as opposed to 24 hourly files that could formerly be inventoried prior to processing. Even though missing some header information and hourly data, it could be processed. Yet, the number of data points recovered for each day was reduced by over 90%. While bias calibration was successful, the data was so sparse as to provide only a handful of hourly averaged data points during the day. As a result, no more than 4 or 5 MPTEC points could be calculated for a 24 hour period, even when all steps to increase retrieval rates, such as lowering the decimation rate to 3, were taken.

Finally, other days eliminated from the data set had either failed calibration or contained too many orphans.

Therefore, the data set was reduced from approximately 30 days to 11, once all passes were examined for usability.

#### **4.1.3 Groundtruth Data Set**

Refer to Table 2, page 53, for a list of the data used in this research. This table lists the Julian day of the GPS data, the satellite almanac file used in the processing,

calibration and orphan status, as well as indicating if the data could be used in comparison. Total points refer to the number of measurements retrieved and processed for each site for each day. Hourly Points refer to the number of averaged data points within +/- 1800 seconds of the hour. PTEC Points refers to the usable number of comparable, hourly protonospheric TEC points obtained from that day's raw data.

1997	ALM				All	Bias			
DATE	USED	SITE	Calibrated	Total Points	Hourly Points	Orphans	USED	NOT USED	PTEC POINTS
74	55	PIT1	✓	1878	15	2	✓		13
		CHA1	✓	1805	24	3	✓		
75	55	PIT1	✓	1444	11	0	✓		11
		CHA1	✓	1908	24	0	✓		
76	76	PIT1	✓	1080	12	0	✓		11
		CHA1	✓	1795	24	2	✓		
77	76	PIT1	✓	1835	16	0	✓		12
		CHA1	✓	1725	21	5	✓		
78	76	PIT1	✓	1178	12	0	✓		10
		CHA1	✓	1838	23	2	✓		
80	80	PIT1				8		✓	
		CHA1						✓	
172	168	PIT1	✓	1699	15	0	✓		12
		CHA1	✓	1934	20	0	✓		
173	168	PIT1	✓	1931	17	0	✓		13
		CHA1	✓	1646	20	3	✓		
174	168	PIT1	✓	1375	11	0	✓		8
		CHA1	✓	1691	21	2	✓		
175	175	PIT1	✓	1279	11	2	✓		9
		CHA1	✓	1644	22	3	✓		
176	175	PIT1	✓	1990	15	0	✓		11
		CHA1	✓	1780	19	1	✓		
177	175	PIT1	✓	1975	16	0	✓		13
		CHA1	✓	1897	22	2	✓		
264	264	PIT1	✓	144	8	1		✓	4
		CHA1	✓	1891	20	1		✓	
265	264	PIT1	✓	131	9	0		✓	5
		CHA1	✓	2049	22	0		✓	
270	264	PIT1	✓	154	6	0		✓	5
		CHA1	✓	1945	23	0		✓	
326	324	PIT1	✓	154	7	0		✓	6
		CHA1	✓	2236	25	0		✓	
334	330	PIT1	✓	367	15	0		✓	13
		CHA1	✓	1725	22	0		✓	
335	330	PIT1	✓	343	15	0		✓	14
		CHA1	✓	2306	24	0		✓	
336	336	PIT1	✓	351	16	0		✓	14
		CHA1	✓	2205	23	0		✓	
339	336	PIT1	FAIL					✓	
		CHA1						✓	
340	336	PIT1	✓	198	12	0		✓	10
		CHA1	✓	1974	23	0		✓	
341	336	PIT1	✓	168	16	0		✓	14
		CHA1	✓	2059	24	1		✓	

Table 2. Data Inventory.

## **4.2 Examinations**

Two main examinations were conducted. The first examination was designed to confirm that the incorporation of the Gallagher model into PIM 1.7 did not alter the influence of various parameters on the resultant PIMPTEC. The second was to explore, using various statistics and plots, how the ground truth MPTEC compared to PIMPTEC.

### **4.2.1 Initial Gallagher Examination**

#### **4.2.1.1 Expectations for the Gallagher Model**

Of the several parameters that can be altered when running PIM with Gallagher to isolate PIMPTEC, only one is expected to produce any significant variation in PIMPTEC [Gallagher, 1988]: only variations in Magnetic Local Time (MLT) should produce significant changes in PIMPTEC. A test was devised to verify that this is the case and that PIM's incorporation of Gallagher did not produce unexpected results. (Note that for the sites in question MLT and Local Time (LT) differ by only 15 minutes.) Changes in season, solar flux (F10.7 cm flux), planetary magnetic indices ( $K_p$ ), and latitude should not alter PIMPTEC [Gallagher, Private Communication, 1998].

#### **4.2.1.2 Devised Tests for the Gallagher Model**

Although unrealistic in terms of pairing geophysical and solar parameters, a test was performed wherein only a single variable was altered in the input stream files that instruct PIM what conditions to use. Four tests were performed, one each for varying  $K_p$ , F10.7 flux, date, and MLT. The results of MLT variations are evident in every PIMPTEC calculation, as the files automatically produce 24 hour output.

All tests were run using, as closely as possible, the same slant TEC configuration that was used for PIMPTEC/MPTEC comparisons. A 100-point altitude grid, as specified by CPI, was used in each run to provide the most representative STEC results possible [Daniell, Private Communication, 1998]. With the exception of the date test, all other tests involved variations of the geophysical and solar parameters for day 7176. 7176 refers to year and Julian date: 1997 Day 176, 25 June 97. The tests were performed with a slant TEC configuration for Pittsburgh, at an azimuth of  $180^\circ$  (looking southward) and elevation of  $26^\circ$ . See the input stream file, Figure 4 on page 19.

Although day 7176 indicated an interplanetary magnetic field (IMF) configuration in which  $B_z$  (north/south magnetic component of the IMF) was north oriented (designated as + in the input stream file), it was necessary to change that parameter to a south orientation (designated -) value in order for PIM to acknowledge changes in  $K_p$ . (If  $B_z$  is positive or zero (north or neutral), PIM automatically adjusts  $K_p$  to one, regardless of input stream  $K_p$  [CPI, 1998].) A test was run for day 7176 to examine how PTEC and TEC change with the change in  $B_z$ . PTEC Results were exactly the same. Therefore, for all subsequent variable parameter tests,  $B_z$  was set to negative (south orientation).

Another consequence of the PIM configuration was that input parameters for SSN were ignored. CPI recommended deselecting the International Union of Radio Science (URSI-88) model normalization option when seeking daily changes in output [Daniell, Private Communication, 1998]. Because the URSI-88 ionospheric model coefficient set is based on monthly averages, it suppresses the impact of daily

geophysical and solar parameters [Daniell et al., 1995]. Without the URSI-88 normalization, PIM ignores the SSN and uses the 10.7-cm flux instead.

As in the comparison tests for PIMPTEC vs. MPTEC, PIM was run twice for each configuration with only the Gallagher setting changed between the executions. Pittsburgh Slant TEC was calculated and the difference was taken to be slant PTEC as seen from Pittsburgh. This PIMPTEC was then graphed separately and examined for changes with variables such as  $K_p$ , flux, etc.

A latitude test to confirm that PIMPTEC experiences no change was not performed, as the focus of this thesis is limited to the given Pittsburgh/Charleston configuration at an assumed IPP of  $35^\circ$  N geographic latitude. As discussed in section 2.3.2.2 The Gallagher Density Profile Equations, the 1981-86 data that was reduced to produce the model displayed no significant latitudinal PTEC variation along constant L-shells [Gallagher, Private Communication, 1998].

#### **4.2.1.3 Gallagher Results**

Refer to Figures 19 through 21, which show slant protonospheric TEC calculated for Pittsburgh (PIMPTEC) at an IPP of  $35^\circ$  N geographic latitude plotted over time for a variety of conditions.

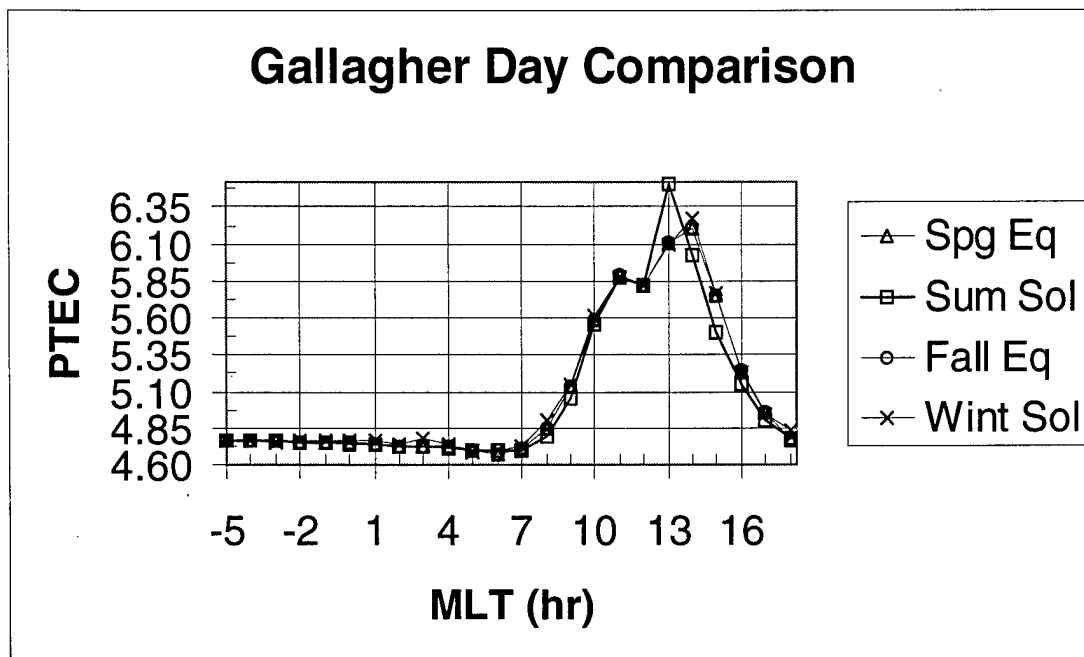


Figure 19. Comparison of PIMPTEC for four different days representing seasonal equinox and solstices.

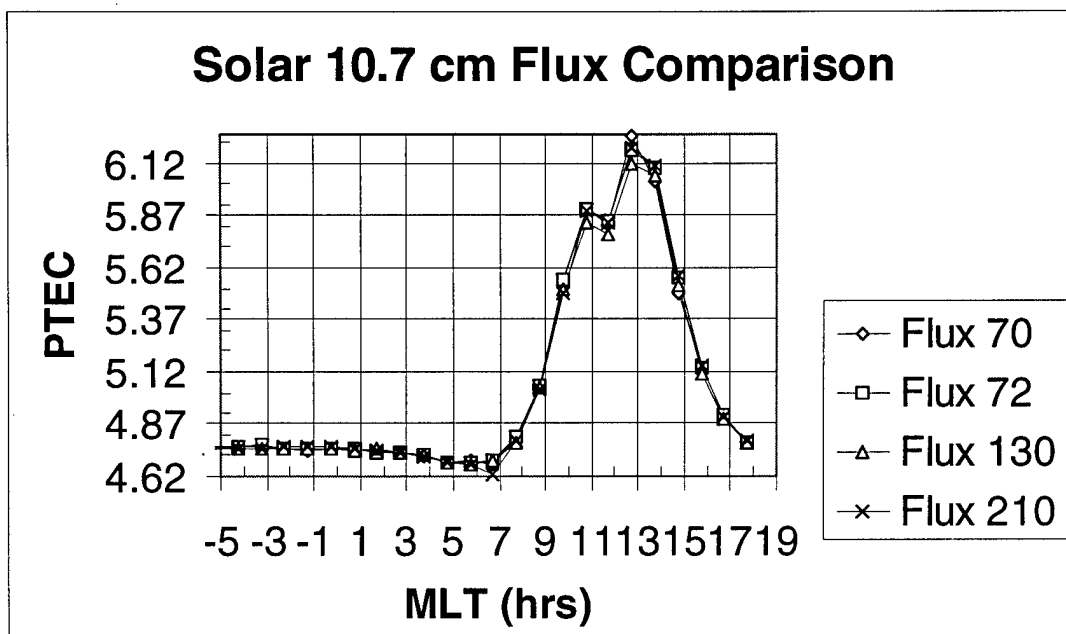


Figure 20. Comparison of PIMPTEC for different Solar Flux values.

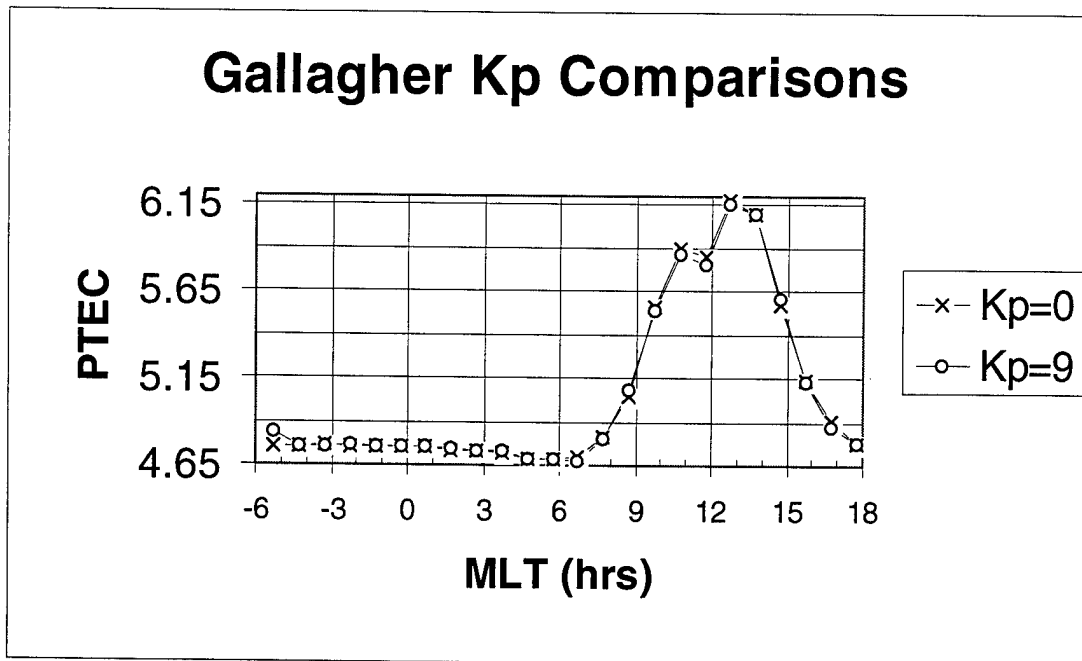


Figure 21. PIMPTEC for minimum and maximum  $K_p$  values.

The results confirmed that the Gallagher model is significantly affected only by changes in magnetic local time, but not by changes in the other tested parameters. Changes in time were compared for day 7176 with as realistic geophysical parameters as could be entered for that day. All PIMPTEC results were nearly identical in how they varied with time. While seasonal results were not expected, there was a minute yet noticeable change between summer solstice and winter solstice between the hours of 18 to 20 UT (13 to 15 MLT). The differences range from 0.41 TEC at 18 UT to 0.02 TEC at 20 UT. It is unclear at this time precisely why this discrepancy happens. Simple round-off or other numerical errors were ruled out, since 0.41 is significantly larger than what one would expect for computational “round-off” errors. Evidence that PIM’s parameterization of geophysical input has corrupted the PIMPTEC results is weak. For one, if summer solstice geophysical parameters were somehow altering the PIMPTEC,

it should be uniformly seen at all hours. Further, it would be a consistent influence. As seen in the plot, Summer PIMPTEC is higher than winter at 13 MLT (~18 UT) but lower after 13 MLT. Even with these errors taken into consideration, the standard deviations of the hourly PIMPTEC values are extremely small. The hourly variation and values of PIMPTEC can be taken as constant regardless of season or date. From -5 to 7 MLT (~0 to 12 UT), results were nearly constant at about 4.7 TEC units before increasing to the highest values at 13 – 14 MLT (~18 - 19 UT) of roughly 6.2 TEC.

When examining the PIMPTEC results, one must keep in mind that the model best represents the protonosphere from 00 to 10 MLT. Peak PIMPTEC occurred at 1300 MLT, with smallest PTEC at 0700 MLT. The plots show a double peak in PIMPTEC, the first near 5.9 TEC at 1100 MLT and the second near 6.2 TEC at 1300 MLT. The double peak may be a slight indication of the Gallagher model's best protonospheric representation (00-10 MLT (00:15-10:15 LT)). The first peak (within the prime time 00-10 MLT) is more representative than the second, which falls outside the 00-10 MLT period.

Likewise,  $K_p$  and Solar Flux produced no significant changes in PIMPTEC, as seen in Figures 19 through 21.

#### **4.2.2 MPTEC vs. PIMPTEC Comparisons and Results**

While the Gallagher model will consistently produce the same diurnal PIMPTEC pattern regardless of the Julian day, we are comparing PIMPTEC to a groundtruth resulting from several days of MPTEC data. Recall that the values we seek to compare would be slant PTEC as seen from Pittsburgh looking south at an elevation



angle of  $26^\circ$  through an IPP at approximately  $35^\circ$  North,  $79^\circ$  West at an altitude of 350 km. Comparisons were made as follows.

The hourly MPTEC points are averaged for all 11 days in the data set and compared, hour by hour, to PIMPTEC. These comparisons will look at the hourly averages, standard deviation, hourly model residuals, and hourly reduced chi-squared measurements. See Appendix A for statistical definitions.

Refer to Figure 22 for the MPTEC to PIMPTEC comparison over time.

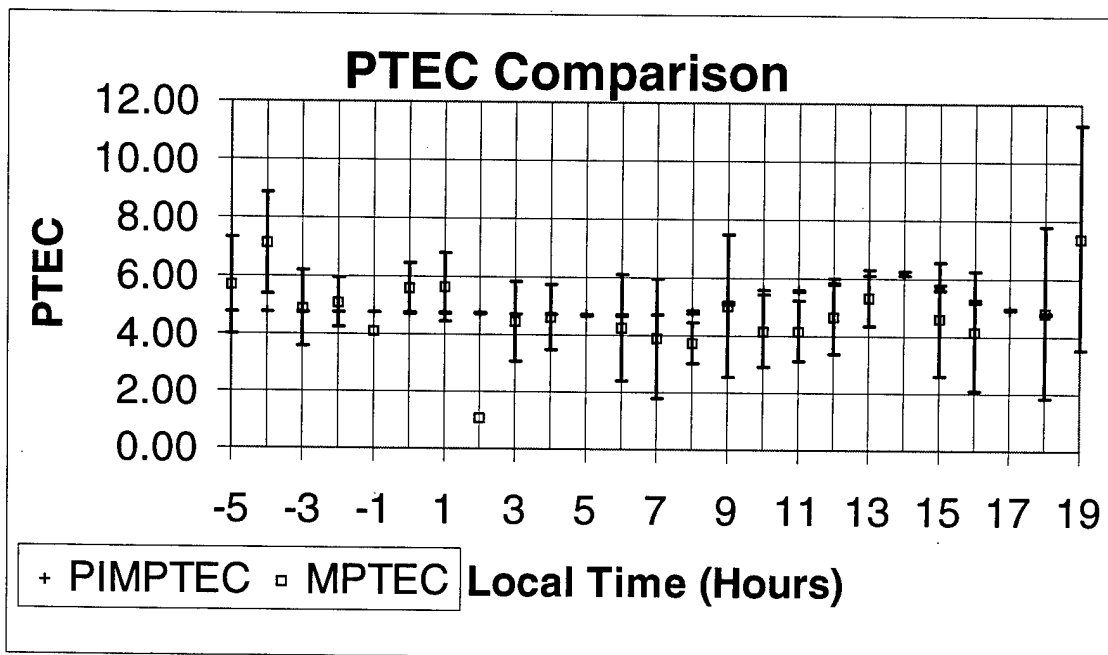


Figure 22. Gallagher model compared to groundtruth measurements over time.

The two MPTEC data points without error bars are solitary points. For  $-1$  and  $2$  LT, only one MPTEC point was recovered for all eleven days. While the low value of the  $2$  LT point seems to suggest it may be a wild point, the calibration and orphan sweep did not indicate conclusively that that was a bad point and so it was kept. Three

other hours (5, 14, and 17 LT) contained no MPTEC data. The MPTEC error bars are the hourly standard deviations calculated for 11 days worth of data. The PIMPTEC error bars are the hourly standard deviations from the seasonal tests over 4 days. They reflect minor influences, possibly from Gallagher model incorporation into PIM, rather than deliberate modulation within the Gallagher model itself. Since PIMPTEC was calculated on a 24-hour time scale as opposed to the 25-hour MPTEC range, the 19 LT hour does not have a PIMPTEC point although this would have the same value as the -5 LT point.

Ignoring the solitary points (-1 and 2 LT) and the empty hours (5,14,17,19), the PIMPTEC error bars do not overlap with those of MPTEC at -4, 8, 10, and 11 LT. Therefore, of the 19 possible hours for comparison, 15 hours have MPTEC values that overlap PIMPTEC values. Therefore, a promising initial correlation between PIMPTEC hourly-average values and those of MPTEC is evident. Table 3, pages 62-64, provides hourly TEC values and standard deviations for both MPTEC and PIMPTEC results. The table is broken up into three sections, spring MPTEC data, summer MPTEC data, and PIMPTEC data.

To get a better idea of the variability of hourly MPTEC values, see Figure 23. This plot includes every MPTEC point used in calculating the hourly averages. It allows the reader to gain an instant sense of how many data points made up each hourly average MPTEC point and their range of values. Included in this plot is PIMPTEC. Of note is the great variation in all the MPTEC data. All hours display a wide range of values. This suggests the MPTEC measurements may be detecting variability in the protonosphere that the Gallagher model is not designed to replicate. Hours -2 and

	A	B	C	D	E	F	G	H
1	HOUR	HOUR	HOUR	MPTEC	MPTEC	MPTEC	MPTEC	MPTEC
2	UT	LT	Seconds	7074	7075	7076	7077	7078
3	0	-5	0	#N/A	7.79	4.57	4.12	6.24
4	1	-4	3600	9.13	#N/A	6.16	6.11	#N/A
5	2	-3	7200	#N/A	#N/A	#N/A	#N/A	#N/A
6	3	-2	10800	5.27	6.33	5.07	4.01	4.77
7	4	-1	14400	4.11	#N/A	#N/A	#N/A	#N/A
8	5	0	18000	#N/A	#N/A	#N/A	#N/A	#N/A
9	6	1	21600	6.92	5.88	6.60	3.69	6.17
10	7	2	25200	#N/A	#N/A	#N/A	#N/A	#N/A
11	8	3	28800	#N/A	#N/A	#N/A	3.20	6.50
12	9	4	32400	4.84	#N/A	6.71	#N/A	#N/A
13	10	5	36000	#N/A	#N/A	#N/A	#N/A	#N/A
14	11	6	39600	#N/A	#N/A	#N/A	0.87	4.26
15	12	7	43200	5.44	5.77	5.77	1.19	#N/A
16	13	8	46800	#N/A	#N/A	#N/A	#N/A	#N/A
17	14	9	50400	7.42	7.45	8.28	3.24	5.73
18	15	10	54000	4.74	3.10	4.51	2.71	5.79
19	16	11	57600	5.49	4.47	3.42	2.87	4.61
20	17	12	61200	#N/A	#N/A	#N/A	#N/A	#N/A
21	18	13	64800	6.23	4.62	5.69	4.15	5.37
22	19	14	68400	#N/A	#N/A	#N/A	#N/A	#N/A
23	20	15	72000	#N/A	#N/A	#N/A	3.68	#N/A
24	21	16	75600	8.14	2.42	3.10	#N/A	4.83
25	22	17	79200	#N/A	#N/A	#N/A	#N/A	#N/A
26	23	18	82800	8.96	6.96	#N/A	#N/A	#N/A
27	24	19	86400	10.15	#N/A	#N/A	#N/A	#N/A

Table 3a. Spreadsheet of spring MPTEC data. (Averages, and standard deviations (Columns P,Q,R) by the hour are in Table 3b).

	I	J	K	L	M	N	O	P	Q	R
1	HOUR	MPTEC	MPTEC	MPTEC	MPTEC	MPTEC	MPTEC	Hourly	Hourly	Hourly
2	UT	7172	7173	7174	7175	7176	7177	Average	Median	STD
3	0	#N/A	#N/A	#N/A	#N/A	#N/A	#N/A	5.68	5.41	1.68
4	1	#N/A	#N/A	#N/A	#N/A	#N/A	#N/A	7.13	6.16	1.73
5	2	4.12	5.10	5.74	6.82	4.65	2.96	4.90	4.87	1.33
6	3	#N/A	#N/A	#N/A	#N/A	#N/A	#N/A	5.09	5.07	0.84
7	4	#N/A	#N/A	#N/A	#N/A	#N/A	#N/A	4.11	4.11	
8	5	5.18	4.66	#N/A	6.97	5.32	5.73	5.57	5.32	0.87
9	6	5.84	4.30	#N/A	#N/A	#N/A	#N/A	5.68	5.88	1.19
10	7	#N/A	#N/A	#N/A	#N/A	#N/A	1.06	1.06	1.06	
11	8	#N/A	4.50	2.94	6.13	4.25	3.61	4.45	4.25	1.39
12	9	4.86	4.17	4.17	5.53	3.28	3.47	4.63	4.50	1.12
13	10	#N/A	#N/A	#N/A	#N/A	#N/A	#N/A			
14	11	6.31	5.90	4.93	4.80	4.85	2.14	4.26	4.85	2.84
15	12	3.44	1.72	#N/A	#N/A	#N/A	#N/A	3.89	4.44	2.08
16	13	#N/A	4.44	3.98	#N/A	3.87	2.74	3.76	3.93	0.72
17	14	#N/A	3.32	#N/A	0.76	5.35	3.69	5.03	5.35	2.47
18	15	#N/A	#N/A	#N/A	#N/A	#N/A	#N/A	4.17	4.51	1.26
19	16	#N/A	#N/A	#N/A	#N/A	#N/A	#N/A	4.17	4.47	1.03
20	17	5.70	3.27	4.95	#N/A	6.13	3.41	4.69	4.95	1.31
21	18	5.85	3.85	6.08	#N/A	6.89	4.83	5.36	5.53	3.92
22	19	#N/A	#N/A	#N/A	#N/A	#N/A	#N/A			
23	20	6.92	5.52	5.17	1.72	#N/A	#N/A	4.60	5.17	1.98
24	21	3.59	#N/A	#N/A	2.10	5.02	#N/A	4.17	3.59	2.07
25	22	#N/A	#N/A	#N/A	#N/A	#N/A	#N/A			
26	23	4.26	#N/A	#N/A	0.88	5.51	2.36	4.82	4.89	2.97
27	24	4.66	#N/A	#N/A	#N/A	#N/A	#N/A	7.41	7.41	3.88

Table 3b. . Spreadsheet of summer MPTEC data. (Averages and Standard Deviations include the spring data from Table 3a.)

	A	B	C	D	E	F	G	H	I
29	<b>TIME</b>		<b>PIMPTEC</b>	<b>PIMPTEC</b>	<b>PIMPTEC</b>	<b>PIMPTEC</b>			
30	<b>UT</b>	<b>LT</b>	<b>7079</b>	<b>7172</b>	<b>7265</b>	<b>7355</b>	<b>AVERAGE</b>	<b>MEDIAN</b>	<b>STD</b>
31	0	-5	4.77	4.76	4.76	4.77	4.77	4.77	0.01
32	1	-4	4.76	4.77	4.76	4.76	4.76	4.76	0.01
33	2	-3	4.76	4.77	4.75	4.75	4.76	4.76	0.01
34	3	-2	4.75	4.76	4.77	4.74	4.76	4.76	0.01
35	4	-1	4.75	4.75	4.76	4.75	4.75	4.75	0.00
36	5	0	4.74	4.75	4.76	4.74	4.75	4.75	0.01
37	6	1	4.74	4.74	4.75	4.76	4.75	4.75	0.01
38	7	2	4.73	4.74	4.74	4.74	4.74	4.74	0.01
39	8	3	4.72	4.73	4.73	4.73	4.73	4.73	0.01
40	9	4	4.71	4.71	4.71	4.70	4.71	4.71	0.00
41	10	5	4.68	4.69	4.71	4.72	4.70	4.70	0.02
42	11	6	4.67	4.69	4.70	4.75	4.70	4.70	0.03
43	12	7	4.71	4.69	4.70	4.72	4.71	4.71	0.01
44	13	8	4.84	4.78	4.83	4.87	4.83	4.84	0.04
45	14	9	5.14	5.04	5.11	5.16	5.11	5.13	0.05
46	15	10	5.60	5.57	5.58	5.60	5.59	5.59	0.02
47	16	11	5.88	5.89	5.85	5.91	5.88	5.89	0.03
48	17	12	5.83	5.82	5.80	5.81	5.82	5.82	0.01
49	18	13	6.10	6.12	6.09	6.08	6.10	6.10	0.02
50	19	14	6.21	6.04	6.19	6.22	6.17	6.20	0.08
51	20	15	5.76	5.51	5.72	5.75	5.69	5.74	0.12
52	21	16	5.26	5.14	5.24	5.24	5.22	5.24	0.05
53	22	17	4.96	4.90	4.94	4.96	4.94	4.95	0.03
54	23	18	4.79	4.78	4.81	4.82	4.80	4.80	0.02

Table 3c. Spreadsheet of seasonal (4 days) PIMPTEC output, average, and standard deviations by the hour. Spring (7079), summer (7172), fall (7265), and winter (7355) are represented.

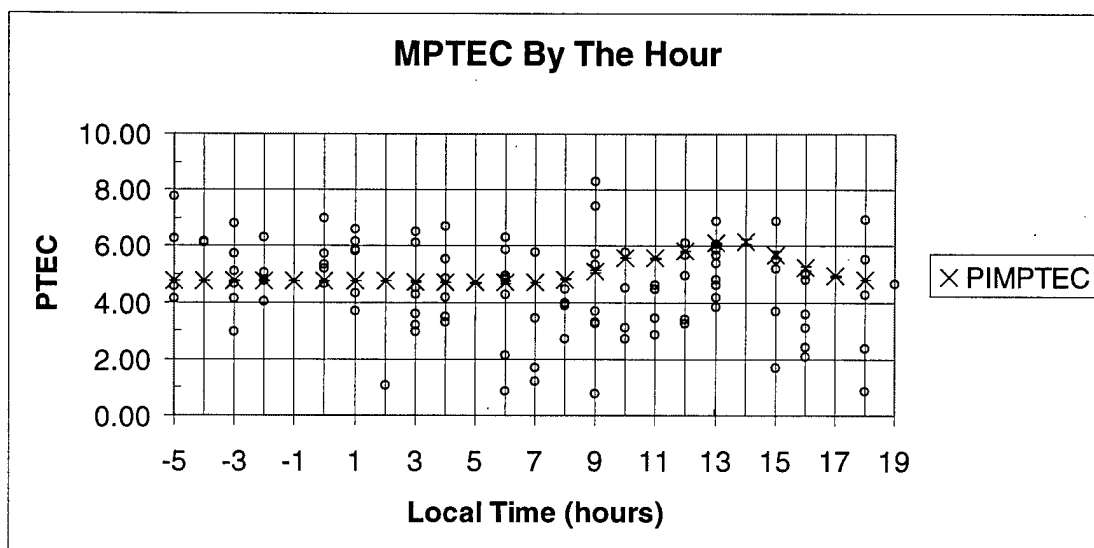


Figure 23. All MPTEC data points plotted against PIMPTEC. X is PIMPTEC from Gallagher and O is MPTEC.

13 LT show the tightest grouping among the MPTEC points, and the standard deviations and reduced Chi squared values for these hours are lower as well.

Another display of this large MPTEC variability against PIMPTEC is Figure 24, "Point By Point Comparison." As seen in the nearly vertical features, MPTEC varies a great deal whereas the PIMPTEC changes only slightly. This plot highlights the fact that while PIMPTEC varies only a few TEC units over the 24 hours, MPTEC varies nearly 8 TEC units. The greatest contrast is seen in the vertical feature when PIMPTEC is approximately 4.7 TEC. 4 TEC units is the average value of PIMPTEC during the late evening and morning hours, before the diurnal increase after 8 LT. Yet during this period, MPTEC was measured with values ranging from just under 1 TEC to nearly 9 TEC units.

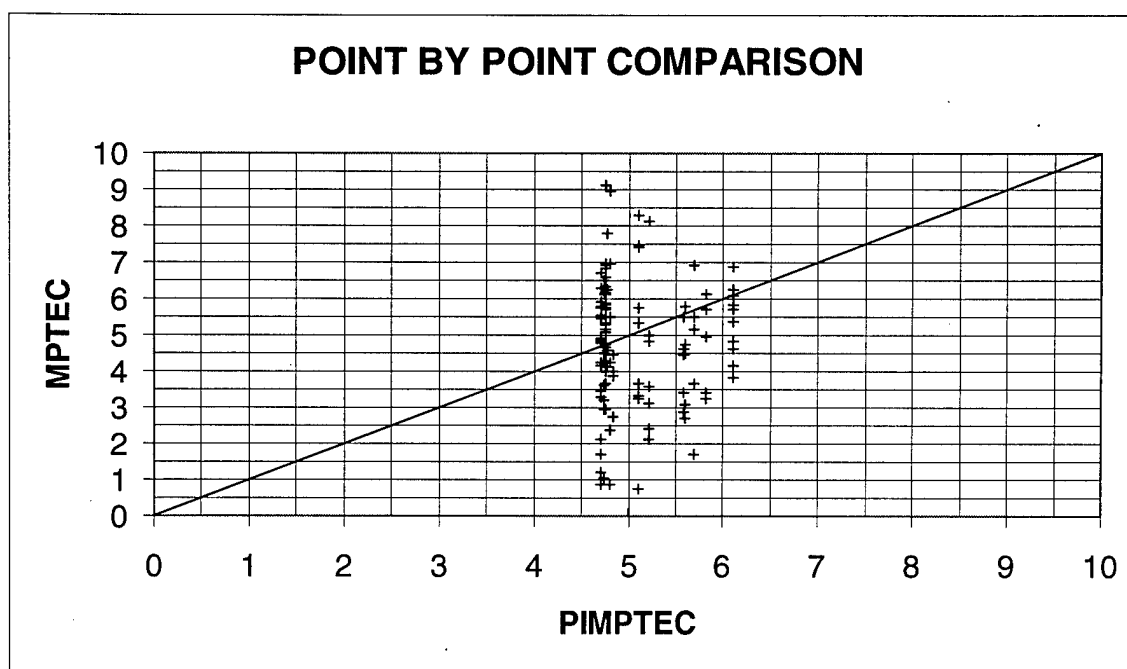


Figure 24. Point by point comparison. PIMPTEC varies only a few TEC units in a day, whereas MPTEC measurements vary greatly in the same period.

#### 4.2.2.1 MPTEC Standard Deviation

Refer to Table 3b, page 63, for MPTEC standard deviation data.

Values for standard deviation of MPTEC by the hour ranged from 0.72 TEC at 8 LT to 3.87 TEC at 19 LT with an average standard deviation of approximately 1.6 TEC. The large 3.87 standard deviation came from only 2 points for the 19 LT hour over all 11 days. The 1.6 standard deviation value at 8 LT resulted from four points, but they were tightly grouped. The range of MPTEC corresponds roughly to a day to day protonospheric hourly variability of 25 %. 00 LT experienced the least variability, changing on average 11% from day to day, while 18 LT had the greatest percent change at 48 % day to day.

#### 4.2.2.2 Reduced Chi-Squared (RCS)

Refer to Table 4 and Figure 25, below, for Reduced Chi-Squared results.

	A	B	C	D	E	F	G	H
1	HOURL	HOURL	HOURL	AVG	AVG	MPTEC	Residual	Hourly Reduced
2	UT	LT	Seconds	PIMPTEC	MPTEC	STD	ei=AvgMPTEC-PIMPTEC	Chi-Squared
3	0	-5	0	4.77	5.68	1.68	-0.91	0.54
4	1	-4	3600	4.76	7.13	1.73	-2.37	1.35
5	2	-3	7200	4.76	4.90	1.33	-0.14	0.40
6	3	-2	10800	4.76	5.09	0.84	-0.33	0.15
7	4	-1	14400	4.75	4.11	0.00	0.64	
8	5	0	18000	4.75	5.57	0.87	-0.82	0.24
9	6	1	21600	4.75	5.63	1.19	-0.88	0.38
10	7	2	25200	4.74	1.06	0.00	3.68	
11	8	3	28800	4.73	4.45	1.39	0.28	0.51
12	9	4	32400	4.71	4.63	1.12	0.08	0.28
13	10	5	36000	4.70	0.00	0.00	0.00	
14	11	6	39600	4.70	4.26	1.85	0.44	2.95
15	12	7	43200	4.71	3.89	2.08	0.82	3.31
16	13	8	46800	4.83	3.76	0.72	1.07	0.69
17	14	9	50400	5.11	5.03	2.47	0.08	3.76
18	15	10	54000	5.59	4.17	1.26	1.42	1.37
19	16	11	57600	5.58	4.17	1.03	1.41	1.10
20	17	12	61200	5.82	4.69	1.31	1.13	0.97
21	18	13	64800	6.10	5.36	0.97	0.74	0.36
22	19	14	68400	6.17	0.00	0.00	0.00	
23	20	15	72000	5.69	4.60	1.98	1.09	2.63
24	21	16	75600	5.22	4.17	2.07	1.05	1.85
25	22	17	79200	4.94	0.00	0.00	0.00	
26	23	18	82800	4.80	4.82	2.97	-0.02	4.57
27	24	19	86400		7.41	3.88	0.00	

Table 4. Reduced Chi-Squared results.

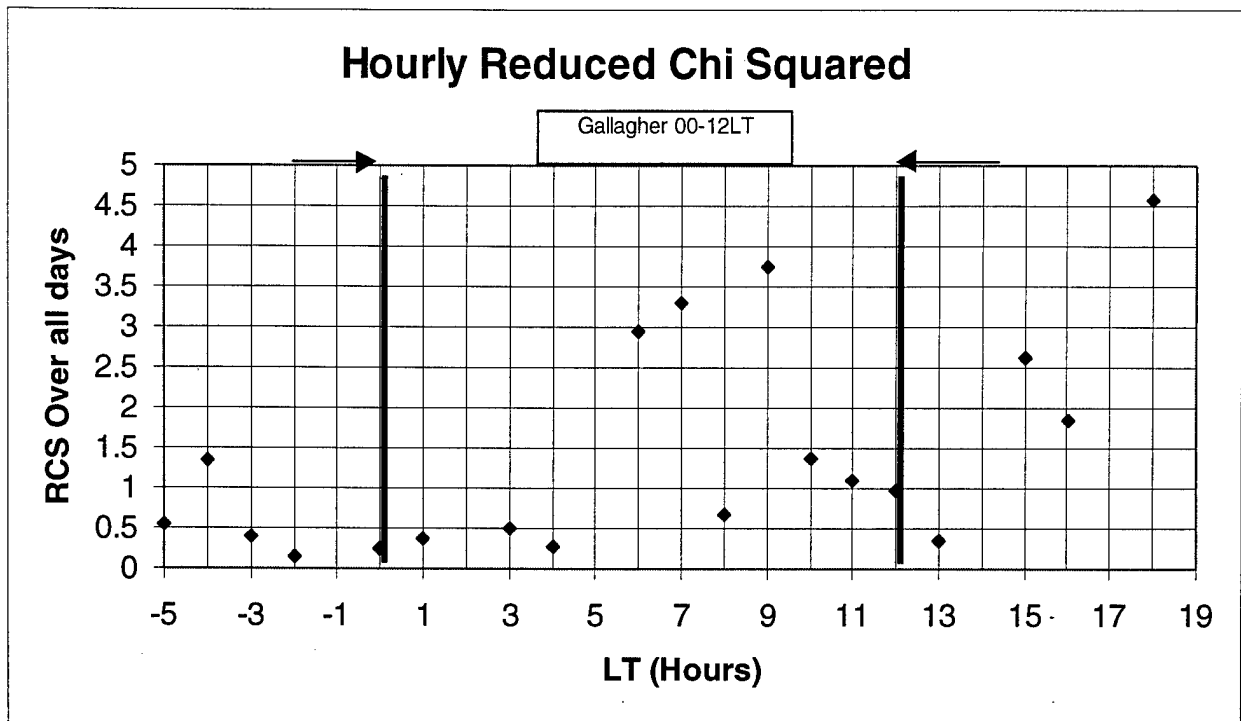


Figure 25. Reduced Chi-Squared by the hour. 00 and 12 LT (nearly 00 and 12 MLT) are marked to highlight the time period for which the paper claimed the Gallagher model should best represent the protonosphere. Actually, 00–10 LT is a better representative claim.

Theoretically, a value of zero for RCS represents perfect agreement between model and observation; realistically, a one indicates statistically likely agreement between the model and the measured MPTEC values. Values near zero indicate good agreement, and values much above one indicate little or no agreement.

The best agreement between PIMPTEC and MPTEC occurs in the late evening and early hours of the morning. During these hours (-5 to 5 LT) both PIMPTEC and MPTEC experienced the least variability, accounting for the decent agreement. Some of the MPTEC variability can be attributed to ionospheric diurnal variation. During late evening and early morning hours, ionospheric TEC values for March and December are typically less variable than during the afternoon and early evening hours. Since MPTEC is calculated using the ionospheric TEC measurement from Charleston, this



ITEC can influence the MPTEC measurements [Handbook of Geophysics]. The RCS trend for low values, ranging from 0.15 to 0.54, occurred between -5 and 5 LT. During this period, an outlier at hour -4 LT with an RCS of 1.35 is evident.

The weakest agreement occurred from 6 LT through 18 LT, with RCS values as high as 4.57: both PIMPTEC and MPTEC show greater variation during this period. Typical ionospheric TEC values vary greatly during the afternoon and evening hours and could be influencing the MPTEC variability. A greater number of measurements, spanning all seasons, would need to be taken to isolate the true causes of the variability. The hours with RCS values above 2 TEC (6, 7, 9, 15, and 18 LT) all had large MPTEC spreads for each hour.

#### **4.2.2.3 Positive and Negative Bias (Model Residual)**

Refer to Figure 26, "Model Residuals." Ignoring hours -1, 2, 5, 14, 17, and 19 LT, calculation of model residual (PIMPTEC - MPTEC) over time shows that the Gallagher model underestimates PTEC from -5 to 1 LT and overestimates PTEC after 2 LT. The marked positive trend beginning at 7 LT reflects the PIMPTEC diurnal increase that MPTEC does not indicate. The positive and negative biases are not surprising when one considers that we are comparing a diurnal model (PIMPTEC) with measurements that have no apparent diurnal trend.

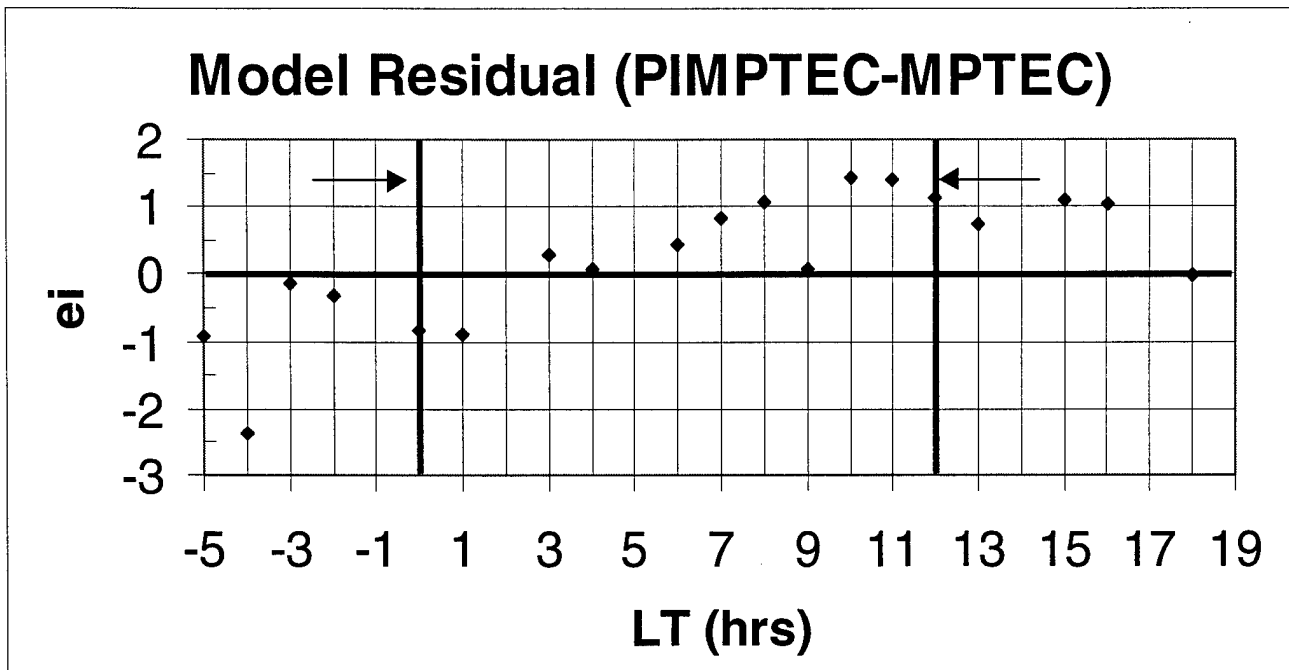


Figure 26. Model Residuals. The claimed “Optimum” Gallagher time period 00-12 LT is marked. As discussed in section 2.3.2.2, The Gallagher Electron Density Profile Equations, 00-10 LT is a more appropriate time period to use.

#### 4.2.2.4 Optimum Gallagher Time Period

Neither the RCS values nor the mean residuals showed trends corresponding to the optimum 00-10 MLT (23:45 –10:45 LT) time period, when the Gallagher model is thought to adequately represent the protonosphere. A conclusive statement should not be made as to the validity of the model outside this time.

#### 4.2.3 MPTEC Errors and Inaccuracies

It was hoped that MPTEC would give some indication of the diurnal variation evident in PIMPTEC. Refer to Figure 22 on page 60. However, the MPTEC results displayed no definitive diurnal tendencies. There can be several explanations for this, treated below, that fall into essentially two categories. First, perhaps the MPTEC data are in fact accurately reflecting variations in the protonosphere, and there is no measurable diurnal trend. However, similar research in England, using three years of

data, did indicate a diurnal variation [Lunt et al., 1998 d]. Second, perhaps the MPTEC is inaccurate to such an extent that it masks the small diurnal variations of the protonosphere. In determining which of these two explanations is correct, we need to examine the possible error sources in the MPTEC data.

MPTEC inaccuracies were estimated at approximately 2 to 3.5 TEC. See Appendix B for MPTEC error estimate.

#### **4.2.3.1 Orphans and Wild Points**

A significant portion of the processing dealt with the elimination of bad pass files and data points. Haphazard elimination of data could miss particularly bad data that can strongly influence the calibration. Retaining pass information with abnormal values can skew the rest of the calibration for an entire day. The opportunity to manually examine the pass files prevented this likelihood.

Not all sites and days experienced orphans (defined previously as satellites that fail to produce proper bias calculations) or wild points (calibrated data that is far outside the realm of ordinary values). Frequently, the appearance of an orphan satellite in the bias calibration tables is accompanied by an abnormally high TEC value for that pass period that is "influenced" by non-calibrations for those satellites. Occasionally, although orphans appear, the TEC values do not seem unusual. Therefore, a careful screening was done to remove unusual TEC values associated with orphans and wild points. A study was conducted to find any trends in the odd data points.

No trend involving specific azimuths, elevations, or orientations was evident. While odd data values from a specific satellite pass naturally shared a common time period and range of azimuths, elevations, latitudes, and longitudes, data that was in

calibration also had those ranges. Rather, the satellites themselves, regardless of their position in the sky, seemed to be the prevalent factor in accounting for orphan and wild data points. See Table 5. GPS satellites 14 and 18 produced orphans on 5 days out of the 11 days, satellite 5 on 4 days, and satellites 6 and 9 on 3 days.

<u>SAT</u>	<u>PIT1</u> <u>ORPHANS</u>	<u>CHA1</u> <u>ORPHANS</u>	<u>SAT</u>	<u>PIT1</u> <u>ORPHANS</u>	<u>CHA1</u> <u>ORPHANS</u>
1	0	0	17	1	1
2	2	0	18	0	5
3	0	1	19	0	0
4	0	0	21	0	0
5	2	4	22	0	0
6	0	3	23	0	0
7	0	0	24	0	0
9	0	3	25	0	0
10	0	0	26	0	2
14	1	5	27	0	0
15	0	1	29	0	0
16	0	1	30	0	0
			31	0	0

Table 5. Satellites and Site Orphans.

The highest TEC values for Charleston (typically >25 TEC) frequently occurred between 22 and 23 UT (17-18 LT) in the spring and between 23 and 24 UT (18-19 LT) in the summer. Such large VTEC values are attributed to orphans, although no concrete daily or hourly trend was identified. A study to find any correlation between a specific satellite pass during 17 – 19 LT and the high TEC at Charleston was not conducted. Comparison of those hours with winter and fall dates was also not possible, as those seasons were discarded in the data set. Pittsburgh showed a similar trend in the summer between 23 and 24 UT. In several instances in which one site reported high TEC values at those hours, corresponding data from the other site was unavailable. For example, if Pittsburgh values for one hour had to be discarded as a result of this corruption, there wasn't any Charleston data at the same time. MPTEC could not have been calculated in any case.

Most of the orphan and wild point data elimination removed one or two points at most from the resulting MPTEC hourly values. On a few occasions, removal of errant data prior to averaging into the hourly bins reduced the variability in the MPTEC values. Since proper elimination was conducted, it is unlikely wild points were retained that could have corrupted the calibration process and skewed the PTEC values.

#### **4.2.3.2 Common IPP Window**

Refer to Figures 27 and 28.

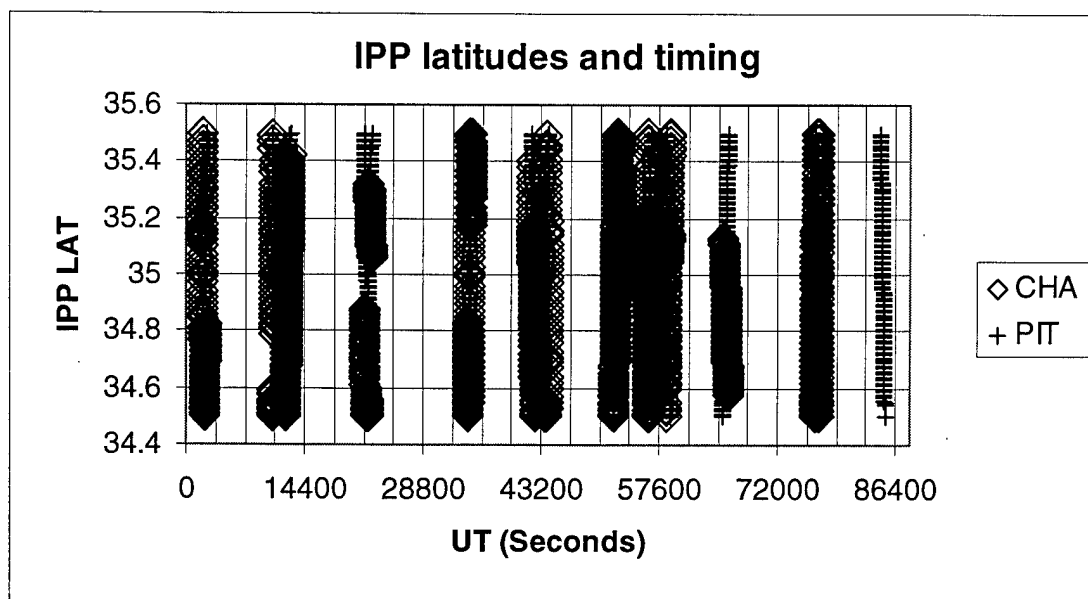


Figure 27. Raw, unaveraged data points recovered from GPS. This shows that both sites have raypaths through essentially the same IPP latitude at the same time.

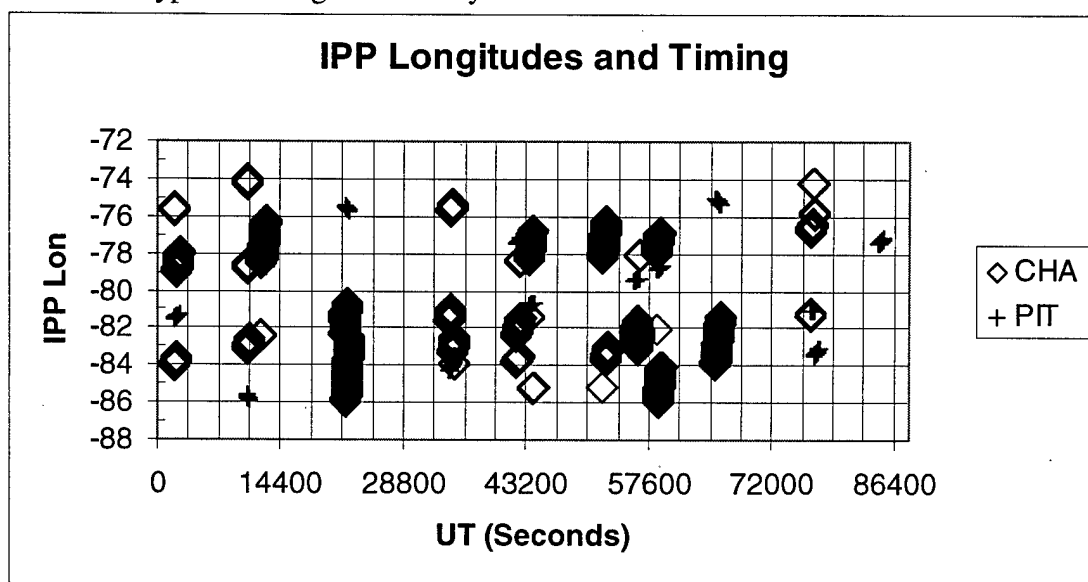


Figure 28. Raw, unaveraged data points from GPS. This shows that both sites have raypaths nearly the same IPP longitude, differing at most a few degrees, at the same time.

Of great concern in choosing the sites for the MPTEC measurements was whether they could be treated as viewing the same ionosphere below 350 km. Since restricting the GPS data to a point in the sky through which both raypaths had to travel

was unreasonable, an Ionospheric Penetration “Window” was examined. As Figure 17, on page 45, showed, any TEC data retrieved on passes within that window would be treated as if Pittsburgh and Charleston shared a common Ionospheric Penetration “Point”.

The IPP Window ranged from 34.5 to 35.5 ° N geographic latitude and from 74 to 86 ° W geographic longitude. This forms a 1 degree by 12 degree “box” on a spherical surface 350 km above the surface of the earth. While it might be possible for Charleston and Pittsburgh to view opposite corners of the box (approximately 12 degrees apart) simultaneously, possibly invalidating the common ionosphere assumption, that did not occur. It was not possible to statistically analyze the raw data to compare the exact distances between Pittsburgh and Charleston raypaths at the IPP. The processing spreadsheets were configured to compare averaged hourly values from the raw 5-second Pittsburgh and 30-second Charleston tables and were not conducive to a second-by-second analysis. Instead, examining the IPP latitudes and longitudes for each site over time demonstrated that such in depth statistics aren’t necessary. See Figures 27 and 28. Also, the average IPP latitude and longitude for each site for each day varied little. While the plots in Figures 27 and 28 suggest a few degrees of separation are possible between the raypaths, Table 6 shows that, on average, Pittsburgh and Charleston raypaths at the IPP were not more than a degree in separation. See Tables 6a and 6b.

	A	B	C	D	E	F	G
1		<b>DAY</b>	<b>7074</b>	<b>7075</b>	<b>7076</b>	<b>7077</b>	<b>7078</b>
2	<b>AVG LAT</b>	<b>PIT</b>	35.03	35.06	35.10	35.01	35.09
3	<b>AVG LON</b>		-79.73	-80.18	-79.38	-79.83	-80.56
4							
5	<b>AVG LAT</b>	<b>CHA</b>	34.91	34.91	34.91	34.91	34.91
6	<b>AVG LON</b>		-80.15	-79.98	-79.85	-79.91	-79.89
7							
8	<b>PIT LAT - CHA LAT</b>	<b>ABS Value</b>	0.12	0.16	0.19	0.09	0.18
9	<b>PIT LON - CHA LON</b>	<b>ABS Value</b>	0.43	0.20	0.46	0.08	0.67
10							
11	<b>DISTANCE</b>		0.44	0.25	0.50	0.12	0.69
12	<b>between CHA/PIT</b>						

Table 6a. For spring MPTEC data. The shaded cells represent the average distance, in degrees, between Pittsburgh and Charleston raypaths at the IPP for each given day.

	A	B	C	D	E	F	G	H
17		<b>DAY</b>	<b>7172</b>	<b>7173</b>	<b>7174</b>	<b>7175</b>	<b>7176</b>	<b>7177</b>
18	<b>AVG LAT</b>	<b>PIT</b>	35.05	35.03	35.04	35.03	35.04	35.03
19	<b>AVG LON</b>		-80.84	-80.00	-80.09	-78.73	-79.52	-80.04
20								
21	<b>AVG LAT</b>	<b>CHA</b>	34.95	34.96	34.93	34.91	34.96	34.96
22	<b>AVG LON</b>		-79.98	-79.75	-79.86	-79.54	-79.85	-80.10
23								
24	<b>PIT LAT-CHA LAT</b>	<b>ABS Value</b>	0.10	0.07	0.11	0.13	0.09	0.07
25	<b>PIT LON-CHA LON</b>	<b>ABS Value</b>	0.86	0.25	0.23	0.81	0.32	0.06
26								
27	<b>DISTANCE</b>		0.86	0.25	0.26	0.82	0.34	0.09
28	<b>between CHA/PIT</b>							

Table 6b. For summer MPTEC data. The shaded cells represent the average distance, in degrees, between Pittsburgh and Charleston raypaths at the IPP for each given day.

The “sky-view” of both locations, looking at the IPP, remains the same. The satellite tracks across that sky view change slightly over time, but the IPP window as seen in the plots from day 7173 is essentially identical for all days in the data set. Since for mid-latitudes, the ionosphere varies little over a degree or two of latitude, our raypaths are traveling through the same ionosphere in our IPP window [Tascione].



Therefore, the IPP window is not considered a significant error source in the MPTEC results.

#### **4.2.3.3 Geomagnetic Storm Influence**

Since SCORE's accuracy depends in part on the assumption of a static, thin shell ionosphere, it calibrates data best outside of geomagnetic storm periods. The data set was screened for potential geomagnetic storm influence to eliminate days when the geomagnetic activity was unsettled to storming. All days used to measure MPTEC had planetary geomagnetic activity indices ( $K_p$ ) of less than 5, indicating non-storming conditions.

An additional concern is raised when one considers how the ionosphere and protonosphere interact during geomagnetic storms. During storm periods, the protonosphere is depleted, draining into the ionosphere. Following the storm period, over approximately two weeks, the protonosphere is replenished from the ionosphere, providing there are no additional storms causing further depletion [Lunt et al., 1998 a]. If measurements were taken before full replenishment could occur, the MPTEC would be abnormally lessened.

The data set was reexamined to search for possible storm influence up to 14 days prior to any measurements. There were two geomagnetic storming days (7058-7059) just over 14 days prior to the spring data set (7074 – 7078). Since replenishment had sufficient time to occur, this did not contribute to MPTEC error. There was one day (7160) with  $K_p$  values greater than 5, twelve days prior to the winter data set (7172 – 7177). Its influence is considered weak, as the storm produced peak  $K_p$  values of 6 on a scale where strong storm conditions have  $K_p$  of 9. As it was not a severe geomagnetic

storm, and had 12 days to recover, this was also ruled out as a major cause of MPTEC error.

#### **4.2.3.4 Protonosphere Influence / Poor Low-latitude Cutoffs**

Another potential error source could be the low-latitude cutoffs chosen to increase the accuracy of the SCORE calibration. The intent of using the low-latitude cutoff was to ensure the protonosphere was excluded from the calibration while still allowing the use of the full range of data later in comparison. Pittsburgh and Charleston retrieve data from an unrestricted (outside of horizon influences) IPP latitude range from  $-90^{\circ}$  to  $90^{\circ}$ ; yet, the calibration is based solely on the region defined by the cutoff. If the cutoffs are legitimate, the calibration is based purely on ionospheric data and the MPTEC is accurate. Unfortunately, choosing inappropriate cutoffs could inadvertently include protonospheric data in the calibration. For example, if the low latitude cutoff for Charleston covered a region of the protonosphere (i.e., the cutoff is too far south), the resulting TEC data that would be considered purely ionospheric would actually contain a protonospheric component and would therefore be abnormally increased. Using a protonosphere-contaminated ITEC value in the PTEC calculations would lead to a decreased value for MPTEC. To complicate matters further, both sites could potentially suffer from protonospheric contamination in the calibration. Another consideration is that the region within which the protonosphere begins to influence measurements is probably not static but moving. If the boundary moves from day to day, this could account for the high degree of variation in the hourly PTEC values if sites were being influenced by varying amounts of the protonosphere not accounted for by the chosen cutoffs.

The cutoffs were found by exploring just one day of data, which was checked to ensure it was preceded by a geomagnetically quiet period. Further searches to seek out daily, seasonal, or monthly changes in the low-latitude cutoffs were not done since similar research covering a period of two to three years had used a single cutoff, with favorable results [Lunt et al., 1998 c].

Based on the one-day search results, Charleston VTEC changed by 2.2 TEC units for every degree change in low-latitude cutoff. See Figure 13a on page 38. Since MPTEC depends directly on the difference between Charleston and Pittsburgh VTEC, a low-latitude cutoff error would directly affect the accuracy of MPTEC. Any diurnal variation in PTEC for the mid-latitude Western Hemisphere is expected to be quite small, on the order of one or two TEC units [Lunt et al., 1998 b]. Even a slight miscalculation of the Charleston low latitude cutoff could alter resultant MPTEC enough to mask diurnal variations.

Pittsburgh VTEC has a smaller rate of change with latitude than Charleston as Figure 13b, on page 38, indicates: on average, TEC decreased 0.13 TEC units for every degree increase in low-latitude cutoff. However, the rate of change is not linear. For Pittsburgh low-latitude cutoffs between 32 and 38 degrees, the rate of change is roughly -0.03 TEC/degree. For cutoffs above 38 degrees, the rate of change becomes roughly -0.29 TEC/degree.

Another possible explanation of the exhibited MPTEC variations is the ionosphere itself. We know that the ionosphere is not a static medium, and the electron densities are not exclusively located in a thin shell at 350 km. Yet the calibration process depends on this assumption. The temporal changes in the ionosphere, the

altitude of the IPP, and a host of other ionospheric factors can influence the results. They have yet to be quantified in any sense but, given the range of MPTEC each hour, it is possible that the highly varying ionosphere is influencing the Dual Station Technique calibration process but not to the full extent as seen in the MPTEC variability.

#### **4.2.3.5 Multipath Impacts**

A candidate for systematic (non-random) error in MPTEC is multipath. While atmospheric and ionospheric impacts on GPS data accuracy can be overcome with differential GPS techniques, multipath is more difficult to isolate and correct. Multipath occurs when signals from the satellite are reflected from other surfaces before entering the site receiver [AIAA].

The impact of multipath on GPS accuracy can be significant in the extreme with estimates of 15 meter range error [AIAA]. In this data set, the worst cases of multipath occurred at the CHA1 site for the winter months, and that set had to be discarded. Some minor multipath was observed in spring and summer processing but not to such an extent to warrant data set elimination. A study by Andreasen on multipath impacts estimated that the greatest TEC error for a site from multipath was 4 TEC units [Andreasen et al.,1996]. See Appendix B for MPTEC Error estimate calculations.

#### **4.2.3.6 Low Elevation Angle at Pittsburgh (Slant Factor Function Assumptions)**

As mentioned in section 2.2.2.3 General Steps, the accuracy of the conversion of STEC to VTEC in the calculation of MPTEC depends on having a small zenith angle (a high elevation angle) so that a “flat-slab” geometry applies to the slant-to-vertical TEC calculation for which the Secant  $\chi$  conversion factor in Equation 3 (page 12) is accurate.

Selected Charleston raypaths, on average, had an elevation angle of  $52^\circ$  and a zenith angle of  $38^\circ$ . Charleston site geometry meets the desired zenith angle of less than or equal to  $40^\circ$ . When CHA1 STEC is converted to CHA1 VTEC, it is fair to say this is an acceptable conversion.

Pittsburgh, on average, had an elevation angle of approximately  $26^\circ$  and a zenith angle of  $64^\circ$ . Pittsburgh zenith angle is  $24^\circ$  too large and jeopardizes the assumption that for zenith angles less than or equal to  $40^\circ$ , we can treat the conversion as a matter of flat slab geometry. In essence, Cosine  $\chi$ , from flat slab geometry, is approximately equal to the Slant Factor Function derived using spherical Earth geometry. The impact of the low elevation angle for Pittsburgh is estimated in Appendix B, MPTEC Error Estimate.

## **5. Summary, Conclusions, and Recommendations**

### **5.1 Summary**

The goal of this research was to validate the Gallagher protonospheric model against groundtruth GPS TEC measurements obtained using the Dual Station Technique. The Gallagher model was tested within the platform program of the Parameterized Ionospheric Model 1.7 (PIM 1.7) to calculate slant protonospheric TEC (PIMPTEC) as seen by Pittsburgh, looking south at an elevation angle of  $26^\circ$ . The Dual Station Technique required extensive preparation and construction in order to obtain groundtruth GPS protonospheric TEC (MPTEC).

### **5.2 Conclusions**

#### **5.2.1 MPTEC Measurements Using Dual Station Technique**

The research demonstrated that, while the dual station technique can provide an estimate of PTEC, the accuracy of MPTEC cannot be conclusively stated beyond 2 – 3.5 TEC for the data set examined. The MPTEC variability was larger than the PIMPTEC variability. This was expected since the Gallagher model (which represents average conditions and changes with MLT only) was compared against groundtruth PTEC values affected by many more factors than just MLT. Several factors could be producing errors in the Dual Station Technique, as were discussed in the previous chapter: poor site location, non-coincident IPP viewpoints, improper low latitude cutoffs, protonospheric and ionospheric variability, low elevation angle, geomagnetic storm influence, and multipath effects could influence the accuracy of the measurements.

The “groundtruth” MPTEC data showed no definitive indications of a PTEC diurnal variation. It could be that for the North American sites chosen, the dual station technique is unable to detect a PTEC diurnal trend or that the trend itself is concealed by the variability of the data. Therefore, no conclusions can be made about the accuracy of the PIMPTEC diurnal trend. If the groundtruth measurements are accepted as accurate and unbiased by preceding periods of geomagnetic activity, the data indicates a highly variable protonosphere that the Gallagher model cannot replicate.

### **5.2.2 PIMPTEC Output Using Gallagher Model**

The Gallagher model proved to be an empirically based average with limited temporal and spatial variability. It did indicate an increase of PTEC on the order of 1 or 2 TEC units through the late morning and afternoon hours. Although this is a reasonable time period to expect an increase as the protonosphere fills, no statement about the accuracy of the Gallagher model during this time period can be made since the groundtruth lacked a diurnal pattern. More extensive measurements using the Dual Station Technique, over the globe for a period of years, might be averaged to extract a diurnal trend, but 11 days is too small a data set from which to extract such a trend. In fact, 3 years of analyzed data were just sufficient to reveal the hint of a diurnal pattern from the research conducted in England [Lunt et al., 1998 d].

For this study (North America, IPP Latitude 35 ° N geographic, Spring and Summer seasons), the Gallagher model did not represent the highly variable protonosphere as measured by the Dual Station Technique.

## **5.3 Recommendations**

### **5.3.1 The Gallagher Model**

Researchers and space environment forecasters intending to use the Gallagher model within the context of PIM 1.7 need to be aware of the applicability and limitations of the model.

The model is essentially a limited representation of the protonosphere. While the model does produce hourly changes, the accuracy of the temporal variation could not be confirmed by this study. The model, developed from time periods of quiet to unsettled activity with  $K_p$  ranging from 2.5 to 4.5, should not be used in geomagnetic storm conditions. Within PIM 1.7, the altitude grid for the slant TEC configuration should use the stated 100 point altitude grid for best representation.

Along with more expansive validation research into the Gallagher model within PIM 1.7, a new version, currently unpublished, should be examined separately. The next version, a conglomeration of several regional models as well as empirical data, is expected to fully reproduce a three dimensional model of electron densities as a function of year, date, hour, solar flux, average annual sunspot number,  $K_p$ , and location [Gallagher, Private Communication, 1998].

### **5.3.2 The Dual Station Technique**

Using the latitudinal asymmetry of the protonosphere and GPS to measure PTEC shows merit. As this effort was limited in scope, it is essential that more research be conducted into the accuracy of the Dual Station technique in the Western Hemisphere: an extensive data set covering one to two years should be reviewed and researched to answer the following questions/concerns:



Are the low-latitude cutoffs in fact increasing SCORE accuracy for our hemisphere?

For a given site, how often must the low-latitude cutoff be empirically determined? Seasonally? Monthly?

How well can SCORE be applied using successful calibrations on geomagnetically quiet days to force calibration for geomagnetically stormy days?

Can it be used to detect protonospheric plasma filling and depletion?

Can it be used to detect protonospheric plasma diurnal variation?

How can the equation for MPTEC be modified to offset low elevation angle impacts?

How does the depletion and refilling of the protonosphere affect the low-latitude cutoff location?

In order to explore these questions, the calibration processing would need further automation, although not all labor intensive steps can be eliminated. Incorporating an automatic data retrieval and quality control check utilizing the University NAVSTAR Consortium's (UNAVCO) TEQC program might help eliminate poor data prior to calibration and help resolve some questions on the causes of bad passfiles [Doyle, Private Communication, 1998]. Other data scans would be needed to remove undesirable geophysical days from the set.

Finally, how did the Gallagher protonospheric model fare against real protonospheric measurement using the Dual Station Technique? The Gallagher model did not represent the protonosphere as measured. As an empirical model, it is not

capable of emulating the day to day variability of the protonosphere. Its placement within PIM 1.7, a theoretical climatological model, should not be construed to imply that the Gallagher model shares the same capabilities as PIM 1.7. It is a good initial step toward protonospheric incorporation into ionospheric modeling, but should be used with care.

## APPENDIX A

### Statistical Definitions

#### 1) Standard Deviation

Standard Deviation is a measure of the dispersion of a data set and is defined as the square root of the variance. This helps characterize the variability or the uncertainty of the data set. The equation for standard deviation is:

$$\sigma \equiv \sqrt{\left[ \frac{1}{n} (\sum x_i^2) - \mu^2 \right]} \quad [A1]$$

Where  $x_i$  are the measured values ( $i$  from 1 through  $n$ ) and  $\mu$  is the mean [Bevington, 1992].

#### 2) Model Bias (Model Residual)

The difference between the model output ( $\text{PIMPTEC} = m_i$ ) and measured values ( $\text{MPTEC} = o_i$ ), given by  $e_i$  ( $e_i = m_i - o_i$ ) [Bevington].

#### 3) Reduced Chi Squared (RCS)

Reduced  $\chi^2$  will be defined as:

$$\chi_v^2 = \frac{\chi^2}{v} \quad [A2]$$

$$\chi^2 = \sum_{i=1}^n \frac{e_i^2}{o_i} \quad [A3]$$

Where  $v = n$  and is equal to the number of pairings of MPTEC and PIMPTEC on a given day [Bevington]. The error or difference between MPTEC and PIMPTEC is  $e_i$ . MPTEC is the observed value or  $o_i$ .

$\chi^2$  is a statistical descriptor giving the theoretical probability distribution that MPTEC and PIMPTEC agree. It is a measure of the dispersion of the model output from the measured output. If MPTEC and PIMPTEC were in perfect agreement, CHI SQUARED would have a value of zero. In reality, a value other than zero is to be expected and a value of one or less is considered to be an indicator of good agreement.

## Appendix B

### MPTEC Error Estimate

General sources of error were discussed in Chapter 4, Data Description and Analysis. Errors due to orphans and wild points, common IPP window geometry, and geomagnetic storm depletion of the protonosphere were not considered significant. However, multipath errors, protonospheric corruption of SCORE due to poor low-latitude cutoffs, and the impact of low elevation angles need to be estimated.

From Lunt et al. [1998 b], we have an intrinsic SCORE accuracy for protonospheric TEC measurements of approximately 1 TEC. This value comes from a study conducted in England. Computer simulations from the Sheffield University Plasmasphere Ionosphere Model (SUPIM) were used as groundtruth against TEC calculated from SCORE. SCORE calibrations were accurate to within a fraction of a TEC when SUPIM concentrated all the plasma into the ionosphere below an arbitrary altitude of 1100 km. When SUPIM was modified to include plasma out to GPS orbits, SCORE estimated TEC values 2 TEC higher than the model. However, if SCORE was adjusted using low-latitude cutoffs to exclude protonospheric influence, it regained accuracy of about 1 TEC [Lunt et al., 1998 b]. It is this value, 1 TEC, that we will use for SCORE accuracy, assuming low-latitude cutoffs are correct. If anything, this value should be slightly less than 1 TEC when applied to the North American sites due to the lesser influence of the protonosphere. Refer again to Figure 3. For this error estimate, we will use 1 TEC. Call this intrinsic SCORE error.

Unfortunately, if the low-latitude cutoffs are incorrect and actually allow for protonospheric influence in the bias calibration process, then SCORE could have an additional inaccuracy of 1 TEC. Again, for the sites used in this study, we would expect a slightly lower value but, for purposes of the estimate here, we will call 1 TEC our Protonosphere Corruption Error.

While previous studies [Andreasen et al.,1996] suggested multipath could contribute as much as 4 TEC of error, multipath error was estimated using phase delay and group delay tables produced during the bias calibrations. See tables A1 through A3, pages 90-92. In the first two tables, Passfile identifies the date, hour, and satellite for a particular pass. For example, 70780001.004 would be Day 078 in 1997 at 0001 UT as measured by GPS satellite 4. NSAMP is the number of samples from that pass file, where “sample” is an individual TEC measurement. PhAvAdj is the Phase Average Adjustment (PAA) in TEC units, the difference between the phase and group delay averages of all the samples. StdDev is the standard deviation of all the sample PAAs, and error is the StdDev over the Square root of NSAMP. CumuPhAv Adj is the Cumulative Phase Average Adjustment (CAA) in TEC units, indicative of how the effective PAA changes as the satellite pass progresses [Mazzella, Private Communication, 1998].

The multipath error estimate (MP), in TEC units, was made by taking the absolute value of the difference between PAA and CAA and adding that to the error standard deviation from each satellite. This value was then averaged for each site. The average MP value for Pittsburgh was 1, and the average MP value for Charleston was just over 1. Both sites had maximum MP values between 2.3 and 3.04 TEC units. This

estimate provides a more conservative MP error estimate than the Andreassen study found. Call the MP error value 1 TEC unit, the average of all MP errors.

	A	B	C	D	E	F	G
1	Passfile	NSAMP	PhAvAdj	StdDev	Error	CumuPhAv Adj	Multipath Error
2	70780004.004	1316	35.597	2.337	0.064	35.602	0.069
3	70780004.005	1969	41.950	3.468	0.078	42.968	1.096
4	70780004.007	1013	43.991	5.189	0.163	44.880	1.052
5	70780004.010	3304	56.682	2.641	0.046	55.797	0.931
6	70780004.016	765	49.506	4.592	0.166	49.271	0.401
7	70780004.018	1685	51.245	9.106	0.222	50.446	1.021
8	70780004.024	3207	46.227	3.376	0.060	46.850	0.683
9	70780004.030	2313	41.690	5.367	0.112	42.817	1.239
10	70780127.006	3162	43.932	3.291	0.059	44.851	0.978
11	70780233.026	2719	44.455	2.494	0.048	43.384	1.119
12	70780318.017	3019	48.371	2.503	0.046	48.548	0.223
13	70780409.027	525	45.779	9.997	0.436	43.702	2.513
14	70780414.023	3593	46.990	2.622	0.044	47.433	0.487
15	70780520.009	2862	45.049	3.349	0.063	44.014	1.098
16	70780553.021	2629	45.154	2.027	0.040	45.506	0.392
17	70780603.003	1317	36.022	10.531	0.290	36.684	0.952
18	70780649.001	3573	45.485	2.442	0.041	45.452	0.074
19	70780812.005	2201	46.958	6.060	0.129	45.359	1.728
20	70780842.030	2442	40.299	4.316	0.087	39.419	0.967
21	70780853.025	4198	39.451	3.531	0.054	39.532	0.135
22	70780917.015	1840	37.242	7.277	0.170	37.729	0.657
23	70781045.029	3316	31.979	3.493	0.061	32.967	1.049
24	70781108.014	2180	36.284	3.162	0.068	36.986	0.770
25	70781116.022	3028	46.887	2.455	0.045	46.391	0.541
26	70781204.006	1416	50.497	9.508	0.253	49.695	1.055
27	70781224.016	2118	46.457	5.088	0.111	47.187	0.840
28	70781342.003	2669	57.418	3.070	0.059	56.678	0.799
29	70781352.018	2613	44.347	3.803	0.074	45.718	1.445
30	70781443.031	3225	59.361	3.216	0.057	58.558	0.860
31	70781444.019	2879	54.695	2.513	0.047	55.032	0.384
32	70781624.027	2635	53.876	2.785	0.054	54.855	1.033
33	70781727.015	2305	70.396	3.200	0.067	68.979	1.484
34	70781844.007	3308	70.248	2.503	0.044	69.589	0.703
35	70782026.014	2322	63.831	6.149	0.128	60.913	3.046
36	70782043.004	2022	59.315	2.538	0.056	59.065	0.306
37	70782057.016	1697	68.405	3.300	0.080	67.130	1.355
38	70782119.009	1733	50.272	7.280	0.175	50.923	0.826
39	70782206.024	1263	66.031	4.002	0.113	63.978	2.166
40	70782248.005	642	52.131	4.052	0.160	52.353	0.382
41							
42						MIN	0.069
43						MAX	3.046
44						AVG	0.941

Table A1. Example: Pittsburgh Multipath Estimate Table for Day 7078.

	A	B	C	D	E	F	G
1	Passfile	NSAMP	PhAvAdj	StdDev	Error	CumuPhAv Adj	Multipath Error
2	70780001.004	394	47.163	7.910	0.399	48.472	1.708
3	70780001.005	409	58.202	6.892	0.341	58.393	0.532
4	70780001.007	215	55.467	10.056	0.686	54.639	1.514
5	70780001.010	692	66.536	6.782	0.258	67.974	1.696
6	70780001.016	112	61.698	9.055	0.856	60.897	1.657
7	70780001.018	268	64.556	9.960	0.608	66.775	2.827
8	70780001.024	610	57.157	7.845	0.318	59.492	2.653
9	70780045.030	382	53.358	9.750	0.499	52.424	1.433
10	70780141.006	522	56.092	5.669	0.248	56.059	0.281
11	70780215.026	658	53.088	7.834	0.305	52.576	0.817
12	70780331.017	677	58.122	8.758	0.337	58.244	0.459
13	70780400.023	844	60.964	7.947	0.274	61.412	0.722
14	70780555.021	750	59.017	7.654	0.280	59.243	0.505
15	70780633.001	851	59.200	7.100	0.243	60.249	1.292
16	70780633.003	165	47.981	11.692	0.910	48.234	1.163
17	70780755.005	400	57.003	9.199	0.460	56.488	0.975
18	70780821.030	497	51.186	10.382	0.466	51.319	0.599
19	70780832.025	777	51.795	5.851	0.210	52.456	0.871
20	70781051.029	712	49.629	8.188	0.307	50.243	0.921
21	70781058.022	712	56.071	6.929	0.260	57.292	1.481
22	70781205.006	193	60.327	9.862	0.710	60.339	0.722
23	70781319.003	612	70.013	9.027	0.365	71.918	2.270
24	70781425.031	667	71.690	7.155	0.277	71.804	0.391
25	70781426.014	150	64.058	7.044	0.575	64.476	0.993
26	70781439.018	502	45.228	6.740	0.301	46.237	1.310
27	70781452.019	715	68.765	8.355	0.313	69.295	0.843
28	70781640.027	628	68.317	8.308	0.332	68.023	0.625
29	70781706.015	514	89.402	9.012	0.398	89.473	0.468
30	70781735.002	754	83.382	7.702	0.281	83.199	0.464
31	70781826.007	637	89.856	6.453	0.256	90.940	1.340
32	70782010.014	401	78.883	9.673	0.483	77.282	2.084
33	70782024.004	424	81.454	4.994	0.243	81.403	0.293
34	70782037.016	398	87.482	10.429	0.523	86.603	1.402
35	70782146.024	262	84.040	6.407	0.396	83.288	1.148
36	70782149.009	261	63.384	9.543	0.591	63.155	0.820
37							
38						MIN	0.281
39						MAX	2.827
40						AVG	1.098

Table A2. Example: Charleston Multipath Estimate Table for Day 7078.



	A	B	C	D
2	<b>SITE DAY</b>	<b>AVG MP</b>	<b>MAX MP</b>	<b>MIN MP</b>
3	PIT 7173	1.1138175	2.82787	0.1305
4				
5	PIT 7174	0.856779565	2.4647	0.08475
6				
7	PIT 7177	0.998832391	2.35666	0.12893
8				
9	PIT 7078	0.941045263	3.0456	0.06942
10	CHA 7078	1.097594118	2.8274	0.2811

Table A3. Final results from multipath error estimates. Tables for days 7173,7174,7177 are not shown.

Pittsburgh zenith angle is approximately 64 °, 24 degrees higher than the 40-degree value for which we can treat the slant to vertical conversion with simple slab geometry, since the earth's curvature cannot be ignored in such cases. For slant TEC measurements at such high zenith angles, calculated vertical TEC values are approximately 24% lower than if converted using a zenith angle of 40 °. For example, the MPTEC error of 3 TEC (SCORE + Corruption + Multipath) would be increased to 3.75 by this zenith angle effect. Call the error from the low Pittsburgh elevation angle approximately 1 TEC.

Although the elevation angle, multipath, and corruption errors are systematic biases, they are treated as if they were random errors in order to estimate a root sum squared error.

### MPTEC Error

Intrinsic SCORE Error:	1
Protonospheric Corruption Error:	1
MP Error:	1 (worst case 3)
Low Elevation Angle	~1

**MPTEC Error Range**

$$\text{SQRT}[1^2+1^2+1^2+1^2] - \text{SQRT}[1^2+1^2+3^2+1^2]$$

$$= 2-3.5$$

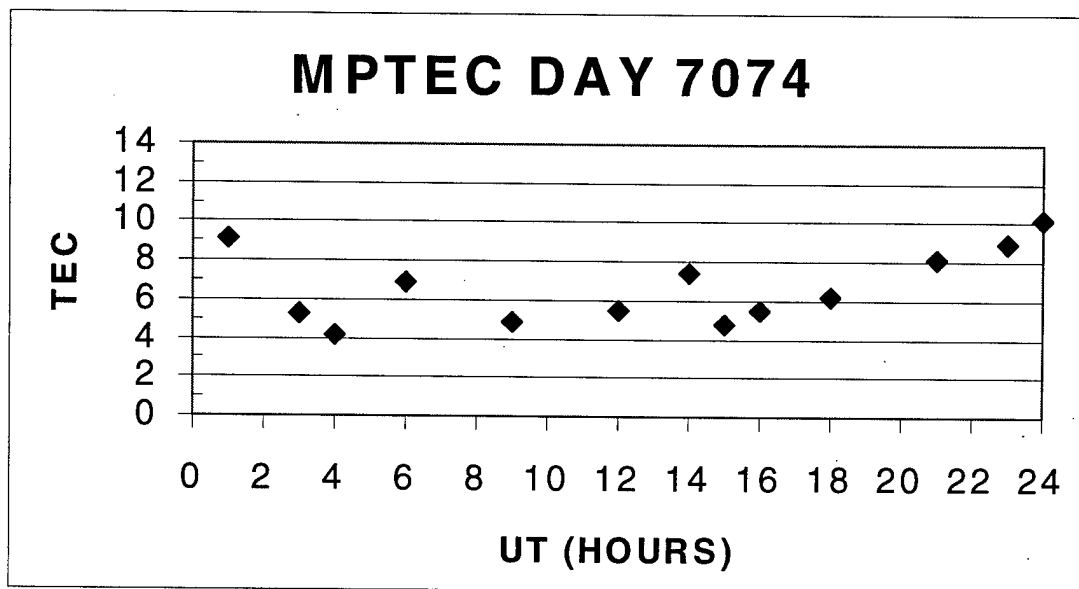
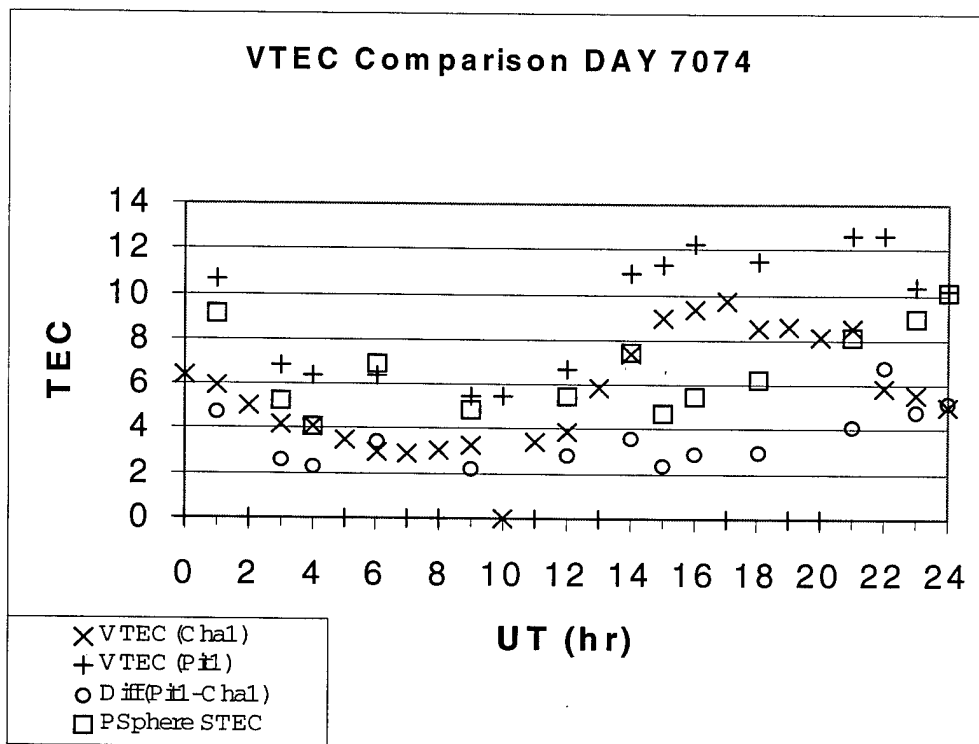
Appendix C

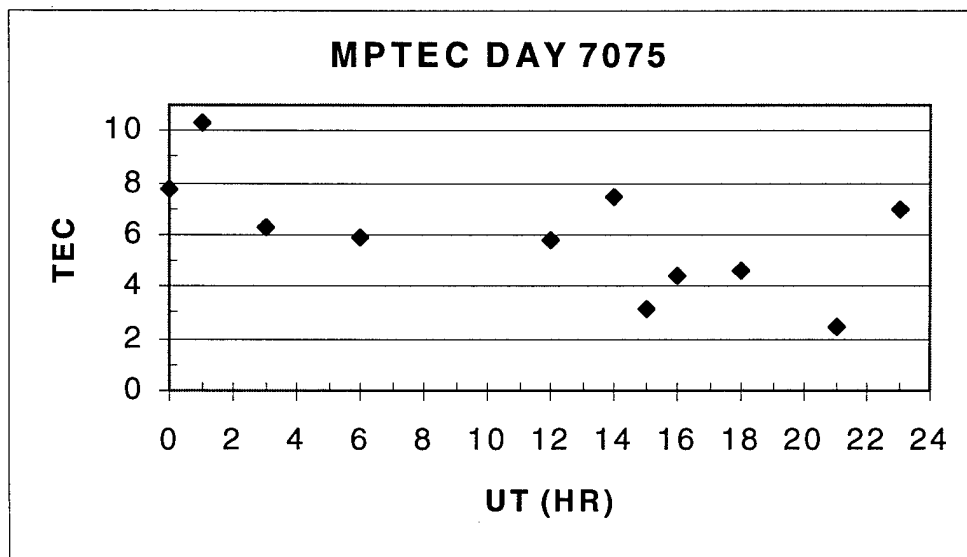
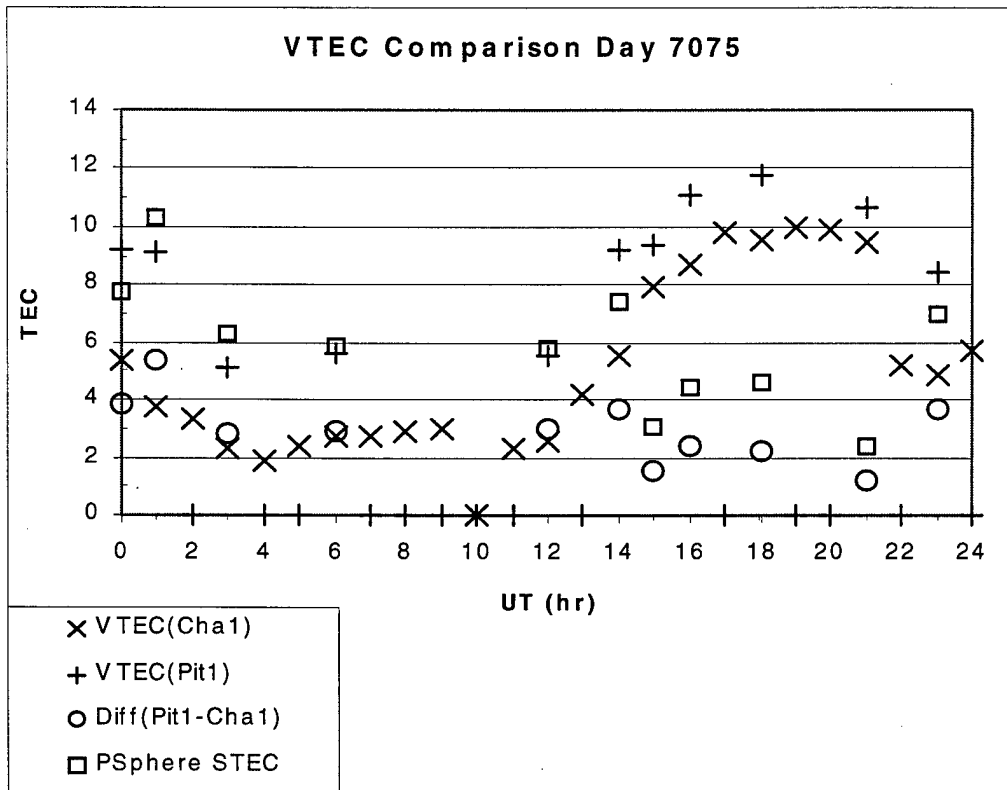
MPTEC Plots: Days 7074-7079, 7172-7177

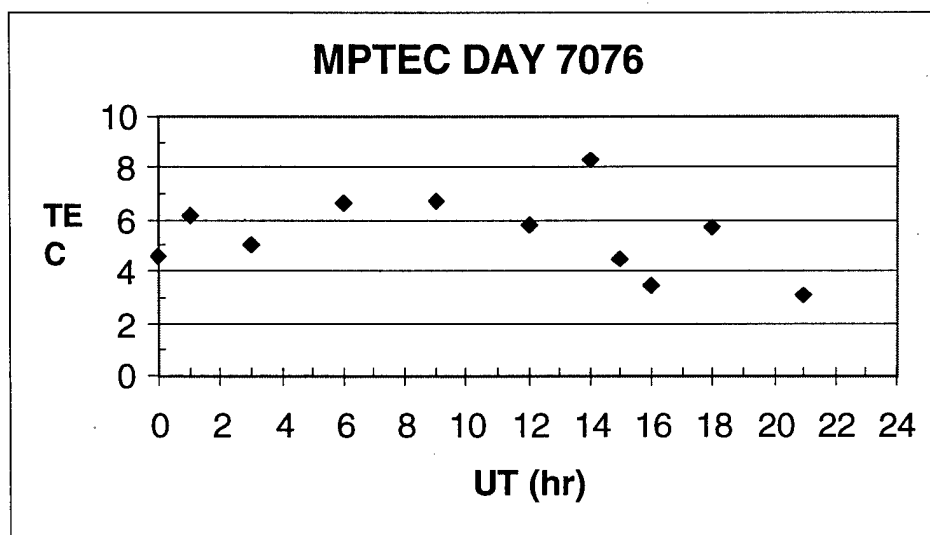
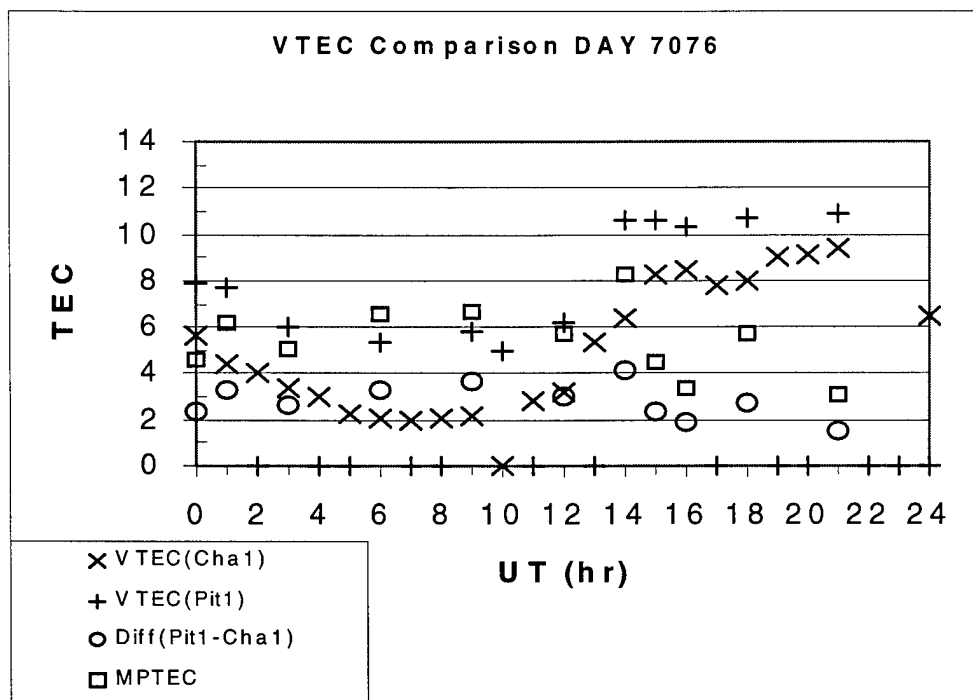
Presented by day where, for example, day 7074 is day 74 of 1997:

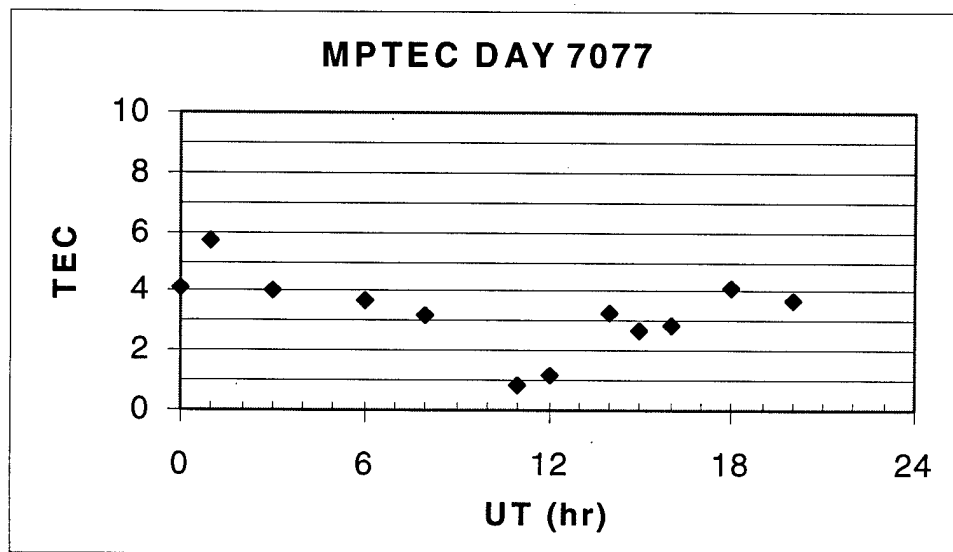
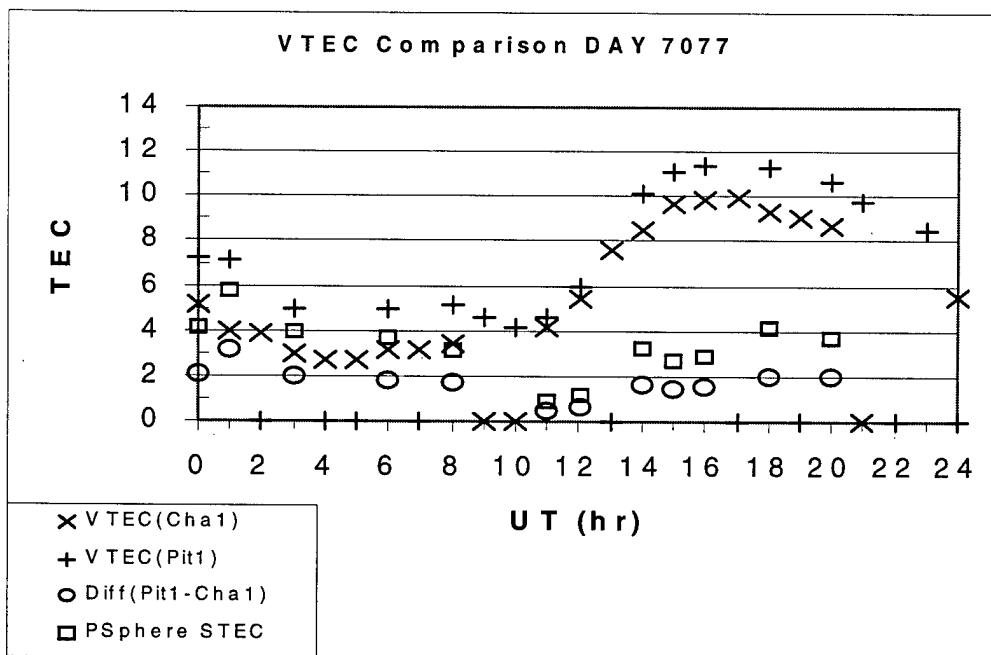
YDDD (Julian Day)	Date
7074	15 March 97
7075	16 March 97
7076	17 March 97
7077	18 March 97
7078	19 March 97
7172	21 June 97
7173	22 June 97
7174	23 June 97
7175	24 June 97
7176	25 June 97
7177	26 June 97

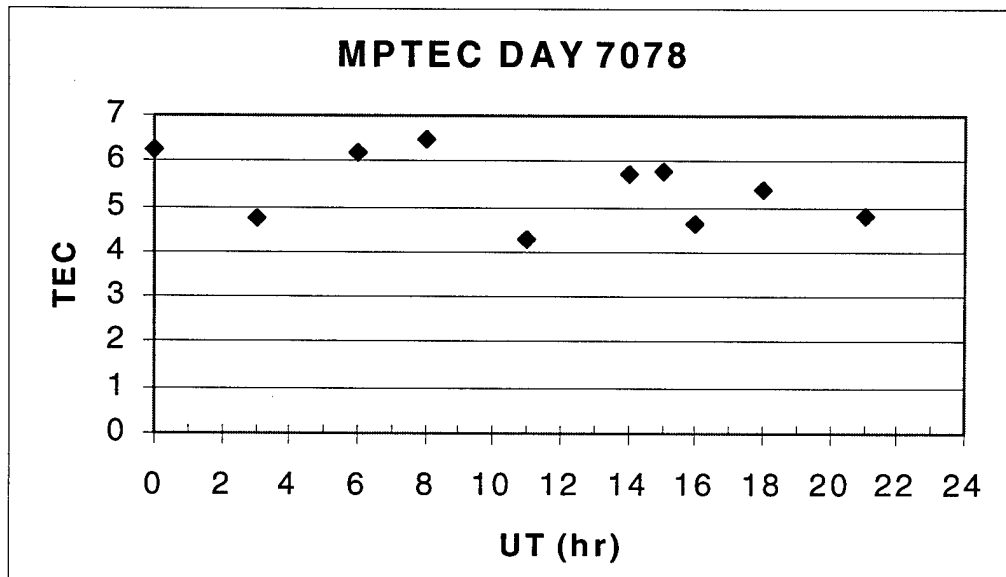
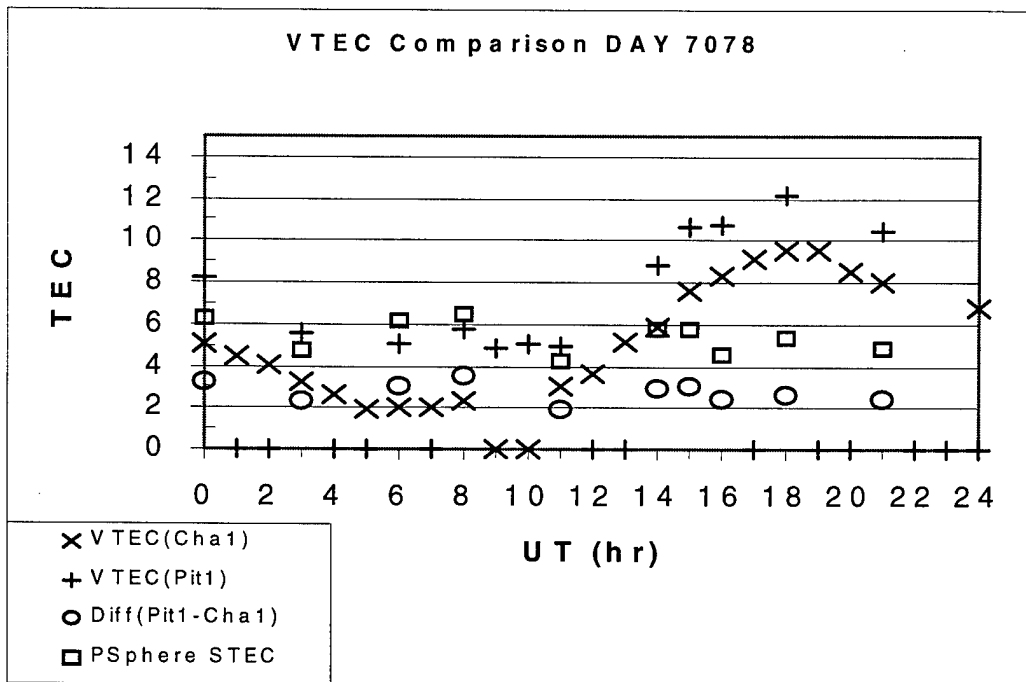
Table C1. Date Conversion.



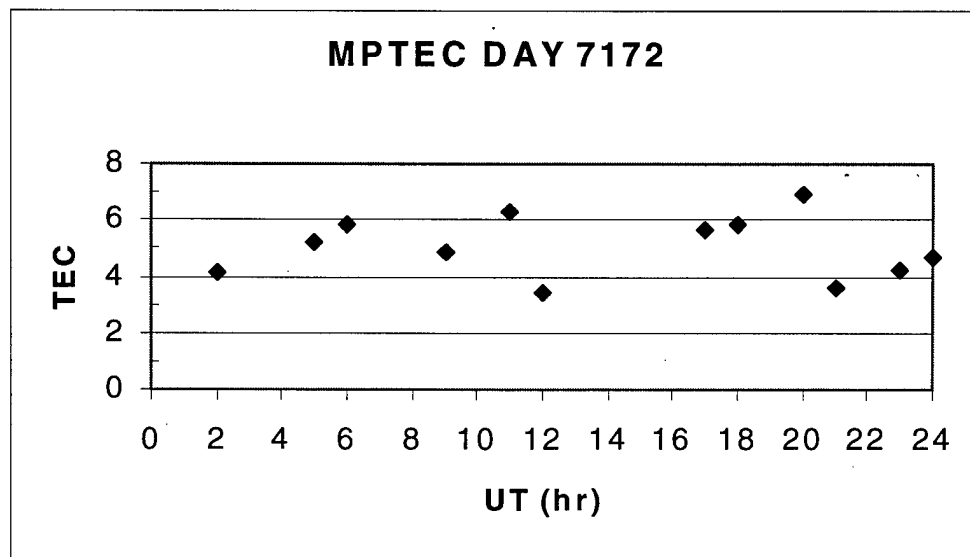
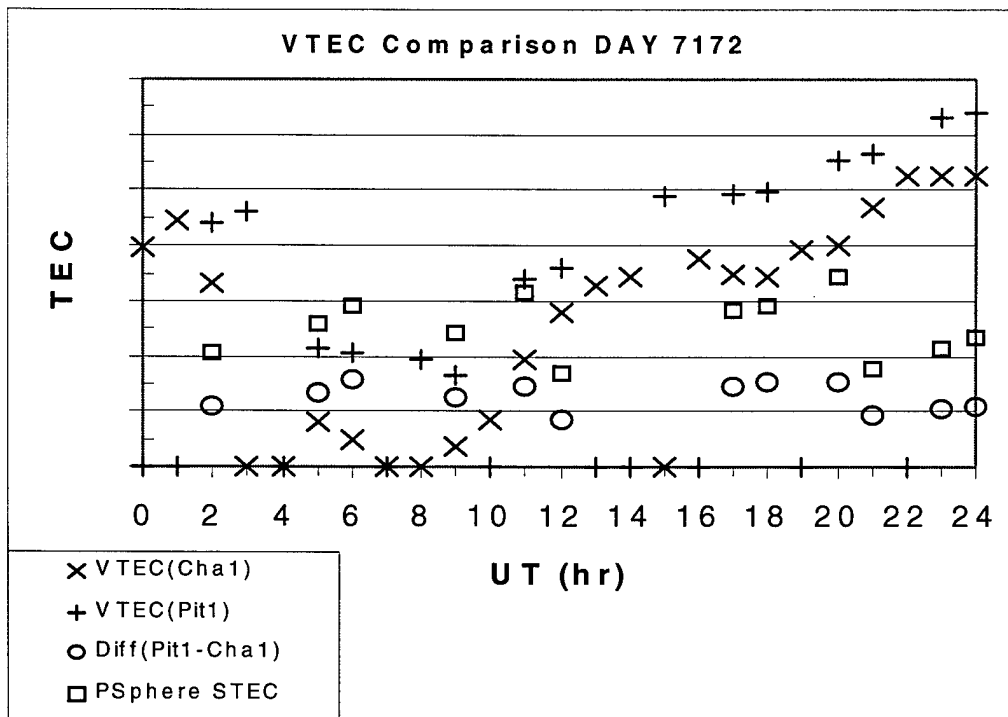


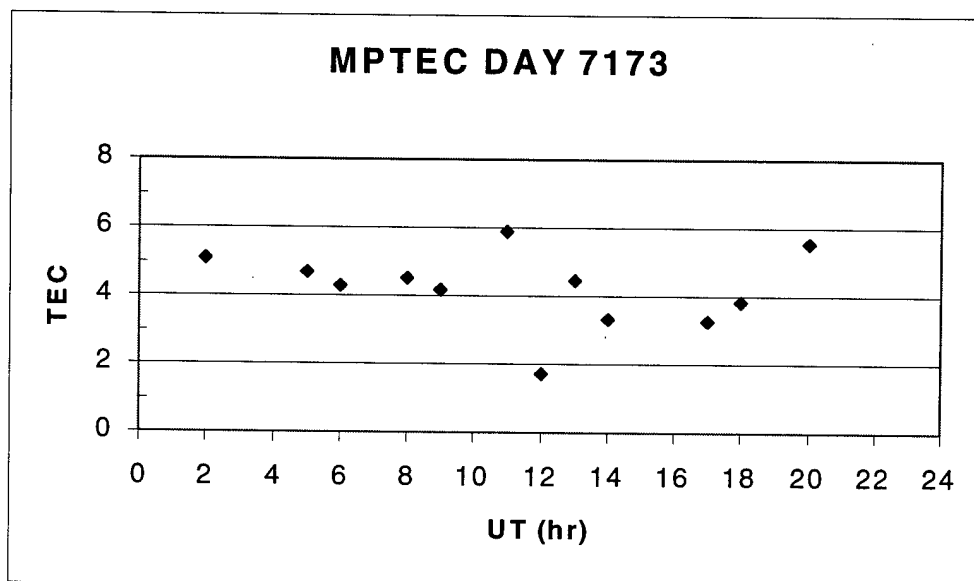
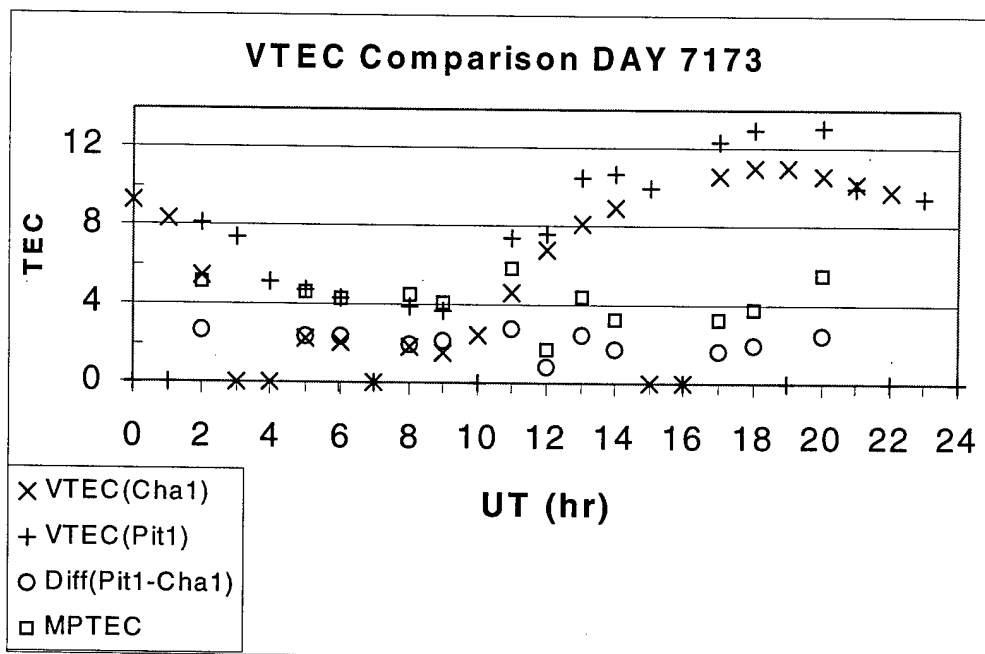


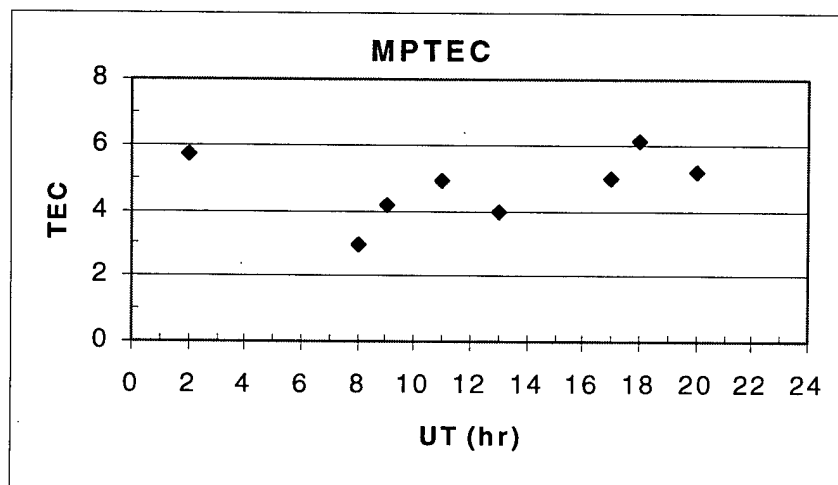
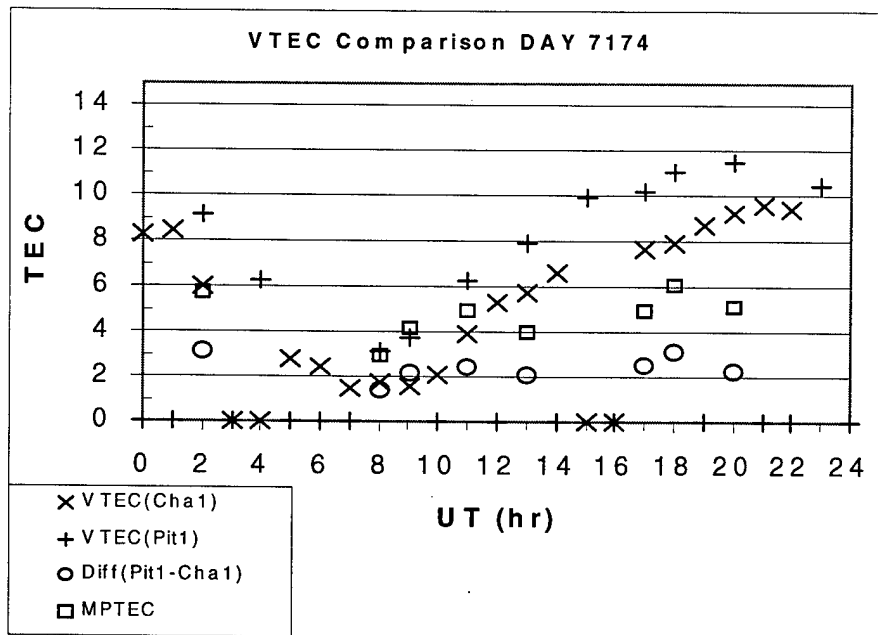




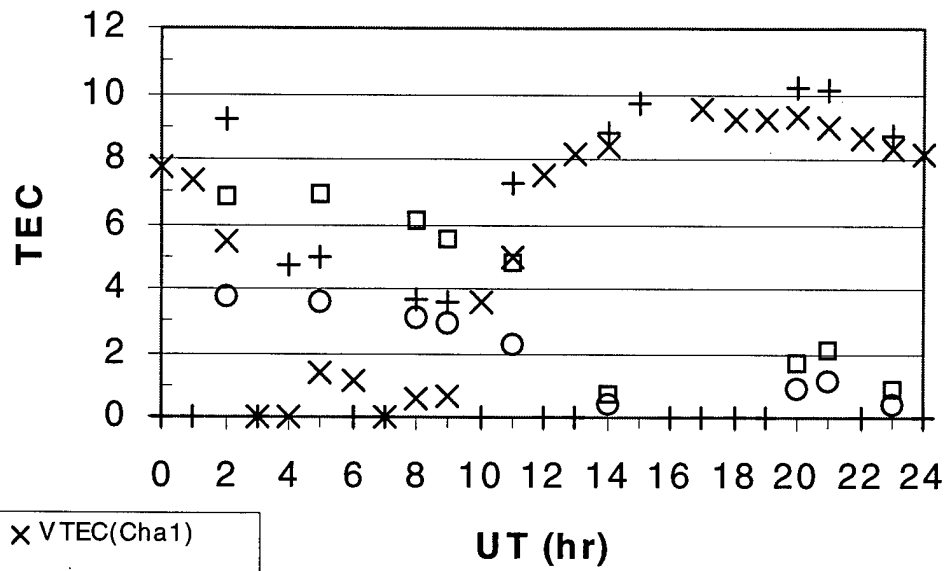




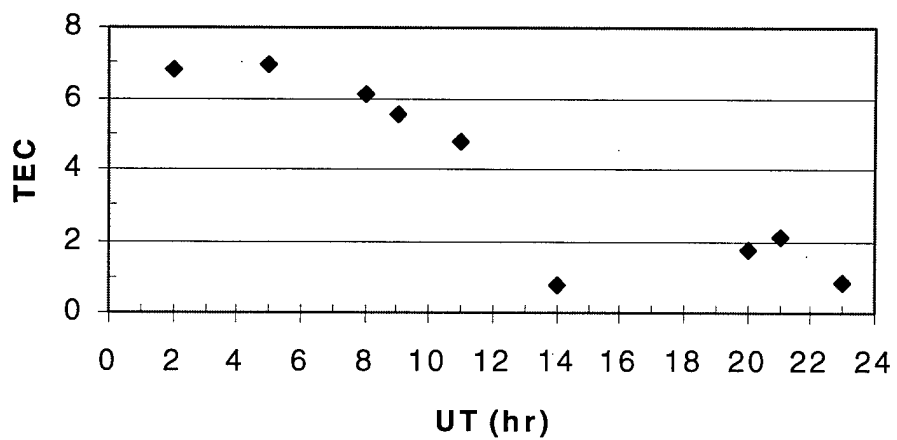


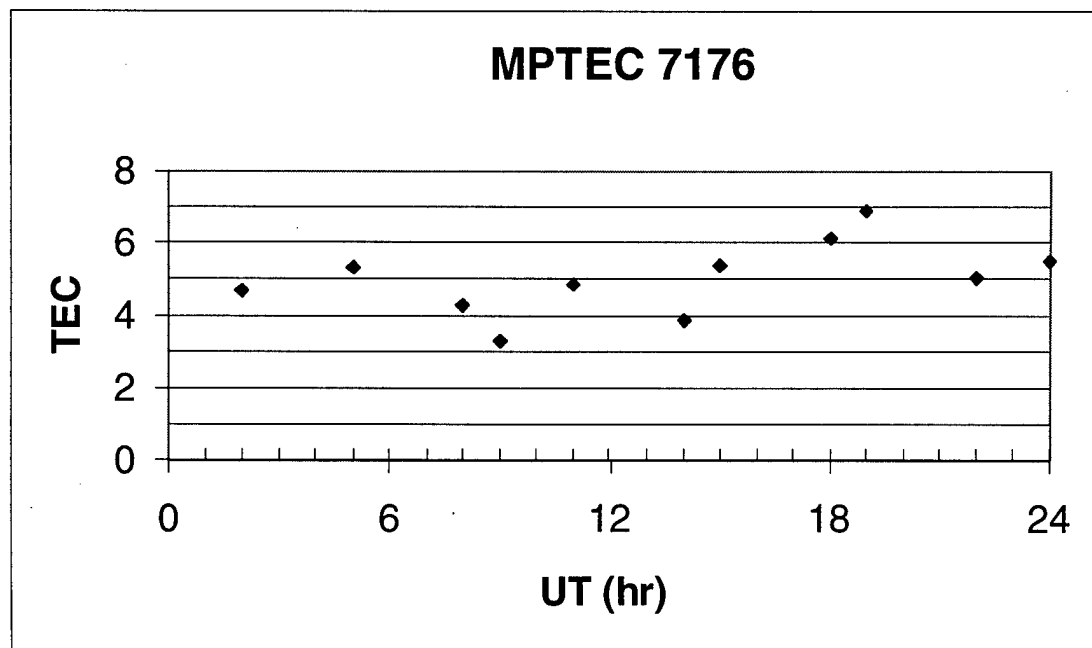
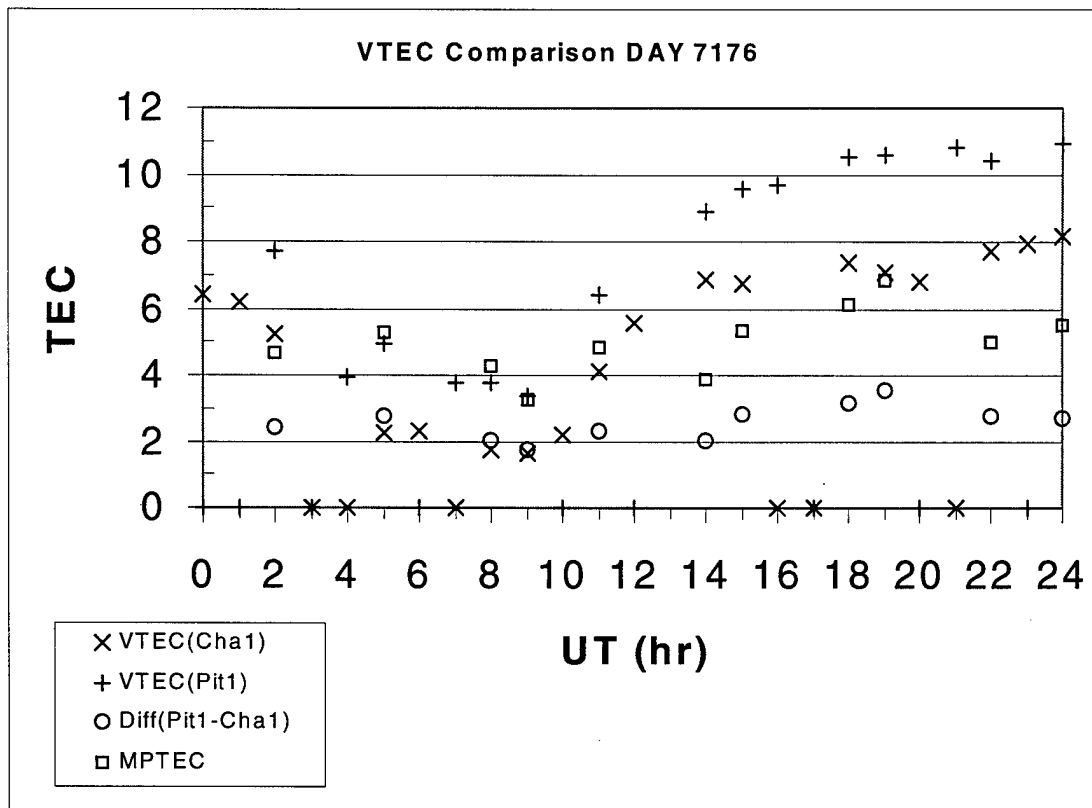


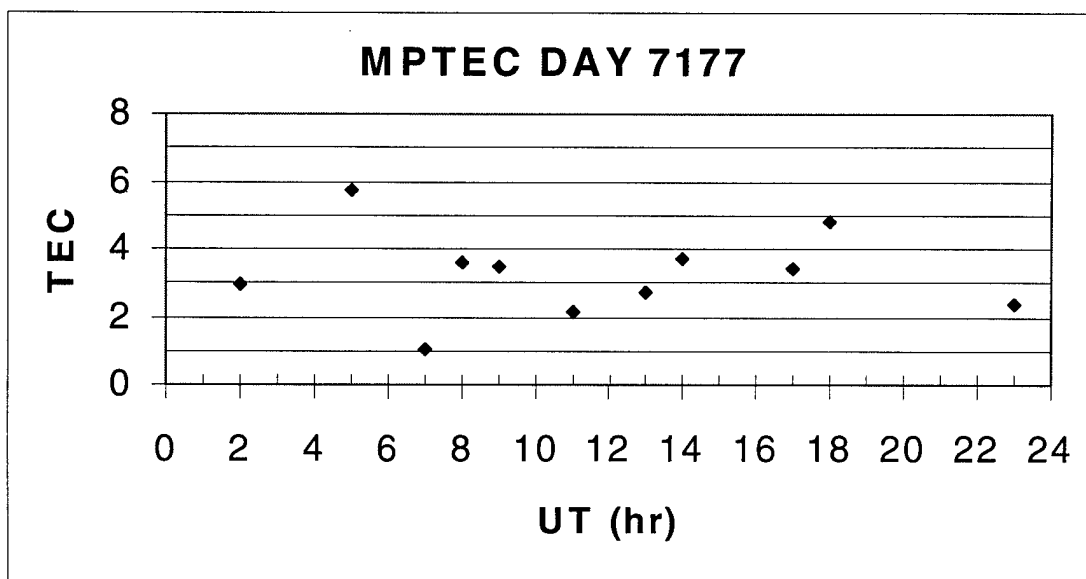
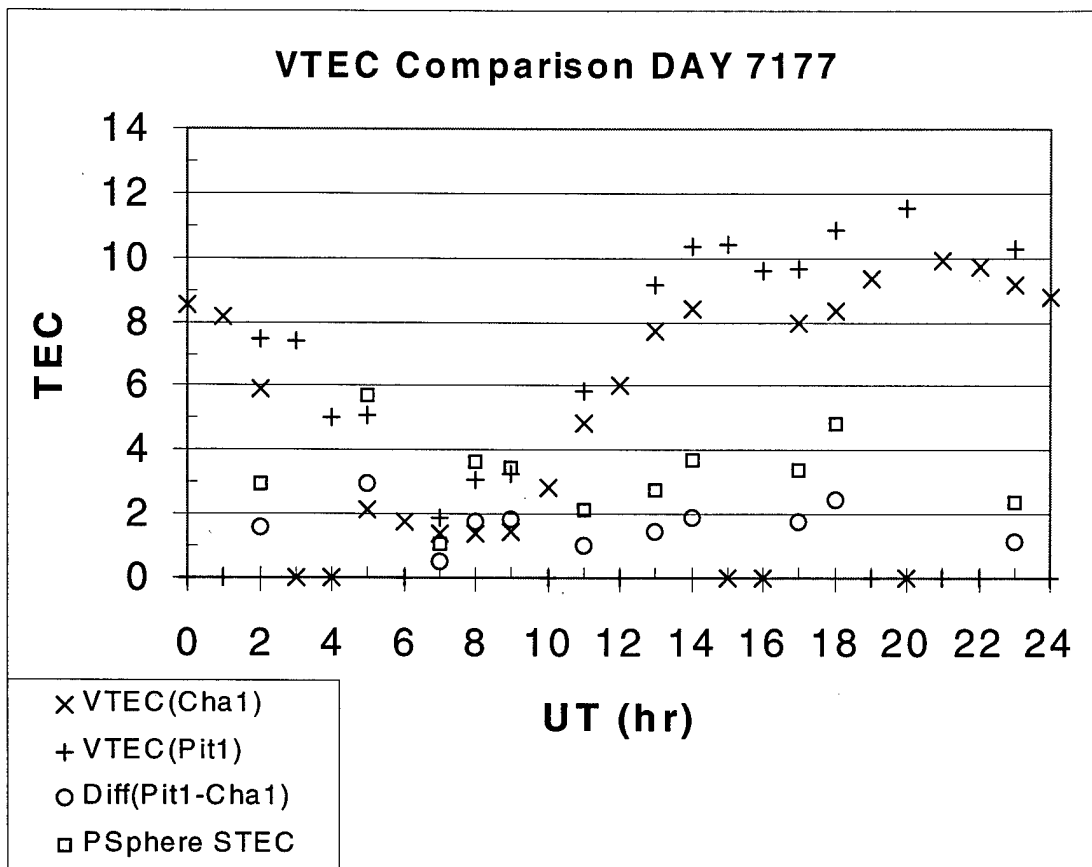
VTEC Comparison DAY 7175



MPTEC DAY 7175







## Bibliography

American Institute of Aeronautics and Astronautics. Global Positioning System: Theory and Applications Volume I: Ed. Bradford T. Parkinson. Progress in Astronautics and Aeronautics, Volume 163, 1996.

Andreasen, C.C., Fremouw, E.J., Holland, E.A., Mazzella, A.J., Rao, G.S., Secan, J.A., "Observation, Analysis, and Modeling of Ionospheric Total Electron Content (TEC) and Scintillation Effects," Phillips Laboratory, Air Force Systems Command, 1996. (PL-TR-96-2227).

Bevington, P.R., Robinson, D.K., Data Reduction and Error Analysis for the Physical Sciences. Massachusetts: McGraw-Hill, 1992.

Bishop, G. J., Mazzella, A.J., Holland, E. A., Rao, S., "An Overview of Ionospheric Effects and Mitigation in RF Communication, Navigation and Surveillance," Ionospheric Effects Symposium, 1996.

Bishop, G.J., Coco, D.S., Lunt, N., Coker, C., Mazzella, A.J. and Kersley, L., "New methods of monitoring the protonosphere, Space Weather Workshop: Effects on Propagation of Navigation and Communications Signals", COMSAT, Bethesda, MD, USA, October, 1997.

Bishop G.J., Mazzella, A.J. "Project Meeting", Interviews, October, 1998.

Bishop G.J., "Protonospheric TEC Impacts", Meeting, February, 1999.

Daniell, R.E. Jr., Brown, L.D., Anderson, D.N., Fox, M.W., Doherty, P.H., Decker, D.T., Sojka, J.J., Schunk, R. W., "Parameterized Ionospheric Model: A Global Ionospheric Parameterization Based on First Principles Models," Radio Science, 30(5): 1499-1510, 1995.

Daniell, R.E. Jr, "PIM 1.7", Electronic Messages, 1998

Computational Physics, Inc. "PIM 1.7 User Guide" 13 Jan 98

Department of the Air Force. Handbook of Geophysics and the Space Environment: Ed. Adolph S. Jursa. Air Force Geophysics Laboratory, Air Force Systems Command, 1985. (AD-A167000).

Doyle, N. "CORS Data Loss Problems", Electronic Messages, December 1998.

Drosdak, J. "CORS Data Retrieval", Electronic Messages, November – December 1998.

Filby, S.D., A Validation of the Parameterized Real-Time Ionospheric Specification Model (PRISM) Version 1.7 B, MS Thesis, AFIT/ENP/GAP/97D. School of Engineering, Air Force Institute of Technology (AETC), Wright-Patterson AFB, OH, 1997.

Gallagher, D.L., Craven, P.D., Comfort, R.H., "An Empirical Model of the Earth's Plasmasphere," Advances in Space Research, 8(8): 15-24, 1988.

Gallagher, D.L., "Model Questions." Electronic Messages and Phone Communication, November 1998 through January 1999.

Gurtner, W., "RINEX: The Receiver Independent Exchange Format Version 2", CSTG BPS Bulletin, (Revised), 1995.

Johnson, F.S., The Satellite Environment Handbook. California: Stanford University Press, 1961.

Kersley, L., Hajeb-Hosseini, H., Edwards, K. J., "ATS-6 Observations of Ionospheric/Protonospheric Electron Content and Flux," Air Force Geophysics Laboratory, Air Force Systems Command, 1977. (AFGL-TR-77-0107).

Kivelson, M. G., Russell, C. T., Introduction to Space Physics. California: Cambridge University Press, 1995.

Lunt, N., Kersley, L., Bailey, G.J., "The influence of the protonosphere on GPS Observations: Simulations using the SUPIM Model," Radio Science, 1998a (Submitted).

Lunt, N., Kersley, L., Bishop, G.J., Mazella, A.J., Bailey, G.J., "The Effect of the Protonosphere on the estimation of GPS TEC: Validation Using the SUPIM Model," Radio Science, 1998b (Submitted).

Lunt, N., Kersley, L., Bishop, G.J., Mazella, A.J., "The Contribution of the Protonosphere to GPS Total Electron Content: Experimental Measurements," Radio Science, 1998c (Submitted).

Lunt, N., Kersley, L., Bishop, G.J., Mazella, A.J., Bailey, G.J., "The Protonospheric Contribution to GPS TEC: Two Station Measurements," Radio Science, 1998d (Submitted).

Mazella, A.J., "Dual Station Technique and SCORE." Electronic Messages, October 1998 through January 1999.

National Academy of Sciences. The Upper Atmosphere and Magnetosphere. Studies in Geophysics, 1977.



Tascione, T.F., Introduction to the Space Environment, Florida: Kriefer Publishing Company, 1994.

### Vita

Captain Kelly M. Law was born 1 September 1970 in Warwick, New York. She received a Bachelor of Science degree in Physics from Norwich University - The Military College of Vermont in 1992. On 15 May 1992 she was commissioned as a second lieutenant in the United States Air Force. She completed the Basic Meteorology Program at Pennsylvania State University, earning a Bachelor of Science degree in Meteorology in 1993 before being assigned overseas.

She enjoyed a variety of assignments including Osan Air Base, Republic Of Korea, Camp Red Cloud, Republic Of Korea, and Fort Stewart, Georgia before entering the School of Engineering, Air Force Institute of Technology, Wright-Patterson Air Force Base, Ohio in August 1997.

Permanent Address: 60 West Avenue  
Chester, NY 10918

REPORT DOCUMENTATION PAGE			Form Approved OMB No. 0704-0188	
Public reporting burden for this collection of information is estimated to average 1 hour per response, including the time for reviewing instructions, searching existing data sources, gathering and maintaining the data needed, and completing and reviewing the collection of information. Send comments regarding this burden estimate or any other aspect of this collection of information, including suggestions for reducing this burden, to Washington Headquarters Services, Directorate for Information Operations and Reports, 1215 Jefferson Davis Highway, Suite 1204, Arlington, VA 22202-4302, and to the Office of Management and Budget, Paperwork Reduction Project (0704-0188), Washington, DC 20503.				
1. AGENCY USE ONLY (Leave blank)		2. REPORT DATE March 99		3. REPORT TYPE AND DATES COVERED
4. TITLE AND SUBTITLE Validation of the Gallagher Protonospheric Model				5. FUNDING NUMBERS
6. AUTHOR(S) Kelly M. Law, Capt, USAF				
7. PERFORMING ORGANIZATION NAME(S) AND ADDRESS(ES) AFIT/ENP 2950 P. St. Wright-Patterson AFB, OH 45433 Advisor: Major Derrick T. Goldizen, COMM (937) 255-3636 Ext 4510				8. PERFORMING ORGANIZATION REPORT NUMBER  AFIT/GAP/ENP/99M-04
9. SPONSORING/MONITORING AGENCY NAME(S) AND ADDRESS(ES) AFRL/VS 29 Randolph Road Hanscom AFB, MA 01731 Sponsor: Mr. Gregory J. Bishop, COMM (617) 377-3036				10. SPONSORING/MONITORING AGENCY REPORT NUMBER
11. SUPPLEMENTARY NOTES				
12a. DISTRIBUTION AVAILABILITY STATEMENT Approved for public release; distribution unlimited				12b. DISTRIBUTION CODE
13. ABSTRACT (Maximum 200 words) Ionospheric models are used in many systems throughout the Department of Defense: for example, they are useful in correcting range errors in radio signals. However, correction models don't incorporate the protonosphere, the torus-shaped plasma volume above the ionosphere. The Gallagher Protonospheric Model, recently incorporated into the Parameterized Ionospheric Model 1.7 (PIM 1.7), was validated against protonospheric total electron content (PTEC) measurements made by the GPS system. Gallagher model calculations of slant PTEC for Pittsburgh ground station looking south with a raypath at an elevation of 26 degrees were compared against GPS PTEC measurements for the same configuration derived from the Dual Station Technique (DST). In the DST, 11 days of GPS TEC measurements were obtained from Charleston and Pittsburgh, taking advantage of the latitudinal asymmetry of the protonosphere to obtain PTEC. The Gallagher model results were in general agreement with measured PTEC, indicating a slight diurnal change in PTEC (<2 PTEC). Groundtruth PTEC accuracy was estimated at 2-3.5 PTEC, masking any trend measurement, yet good enough to validate the potential of Self Calibration Of Pseudo-range Errors (SCORE) and DST to measure PTEC using GPS. PIM 1.7 users should be aware of Gallagher's limits: empirical, limited to 00-10 Magnetic Local Time, and +/- 40 degrees geomagnetic latitude.				
14. SUBJECT TERMS Protonosphere, Ionosphere, Model Validation, Parameterized Ionospheric Model 1.7 (PIM 1.7), Gallagher, Global Positioning System (GPS), Total Electron Content (TEC), Self Calibration Of Pseudo-range Errors (SCORE), The Dual Station Technique (DST)				15. NUMBER OF PAGES 122
				16. PRICE CODE
17. SECURITY CLASSIFICATION OF REPORT UNCLASSIFIED		18. SECURITY CLASSIFICATION OF THIS PAGE UNCLASSIFIED		19. SECURITY CLASSIFICATION OF ABSTRACT UNCLASSIFIED
				20. LIMITATION OF ABSTRACT UL